

UNIVERSITY OF NAPLES FEDERICO II



**FACULTY OF MATHS, PHYSICS AND NATURAL
SCIENCES**

PHD IN CHEMISTRY

XXIII CICLE

Structure of macromolecules from Gram-negative bacteria
involved in elicitation of plant immune system

Maria Rosaria Leone

TUTOR
PROF. ssa ROSA LANZETTA
CO-TUTOR
Dr. Alba Silipo

SUPERVISOR
Prof. Piero Pucci

Papers related to PhD thesis:

1. Deciphering the structural and biological properties of the lipid A subcomponent of lipopolysaccharides from *Burkholderia cepacia* strain ASP B 2D, in *Arabidopsis thaliana* (*Glycobiology*. Accepted for publication)
2. An Unusual Galactofuranose Lipopolysaccharide That Ensures the Intracellular Survival of Toxin-Producing Bacteria in Their Fungal Host (*Angew. Chem.* 2010, **41**: 7476-80)
3. Bradirhizose, the unique Bicyclic monosaccharide is the O-antigen component of *Bradirhizobium* lipopolysaccharide and plays a key role symbiosis (submitted to *Angew. Chem.*).
4. Structural analysis of the lipid A of *Bradirhizobium* reveals a new carbohydrate and fatty acids arrangement that have pivotal consequences on symbiosis (manuscript in preparation).

Papers do not related to PhD thesis:

1. The lipid A of *Burkholderia multivorans* C1576 smooth-type lipopolysaccharide and its pro-inflammatory activity in a cystic fibrosis airways model (*Innate Immun.* 2009 Oct 30)
2. Structural study and conformational behavior of the two different lipopolysaccharide O-antigens produced by the cystic fibrosis pathogen *Burkholderia multivorans* (*Chemistry*, 2009 **15**: 7156-7166)
3. *Pseudomonas aeruginosa* Exploits Lipid A and Muropeptides Modification as a Strategy to Lower Innate Immunity during Cystic Fibrosis Lung Infection *PLoS One* **12**: 8439.

Index

Chapter 1: Gram-negative bacteria

1.1 The bacterial cell	2
1.2 Bacterial cell wall	4
1.3 Lipopolysaccharides	5
1.3.1 O-chain: structure and function	6
1.3.2 The core oligosaccharide: structure and function.....	7
1.3.3 Structure and biological properties of lipid A.....	8
1.4. Plant communication with different other living systems	9
1.5 The plant innate immune system	10
1.5.1 The hypersensitive response and localized induced resistance.....	12
1.5.2 Plant pathogens	13
1.5.3 Plant symbiont bacteria.....	14
1.5.4 LPS and symbiosis.....	17

Chapter 2: Structural investigation of lipopolysaccharides and lipooligosaccharides

2.1 Extraction and purification of Lipopolysaccharide (LPS) and Lipopoligosaccharide (LOS)	23
2.2 Structural characterization of LPS and LOS	24
2.2.1 Acid and alkaline degradation.....	24
2.2.2 Chemical analysis of LPS and LOS.....	25
2.2.3 Circular dichroism	26
2.2.4 Mass-spectrometry	28
2.2.5 NMR spectroscopy.....	29
2.2.6 Two-dimensional NMR.....	29
2.2.7 Lipid A structural investigation	30

Chapter 3: Structural elucidation of LPS from *Burkholderia rhizoxinica*

Section I

3.1 <i>Burkholderia rhizoxinica</i>	34
3.2 Structural characterization of LPS from <i>Burkholderia rhizoxinica</i> B1wt	35
3.2.1 LPS extraction and preliminary analysis	35
3.2.2 Full characterization of O-chain from LPS of <i>Burkholderia rhizoxinica</i>	

wild type	36
3.3 Full characterization of LOS from <i>Burkholderia rhizoxinica</i> WaaL mutant	38
3.3.1 NMR characterization of oligosaccharide fraction of LOS from <i>Burkholderia rhizoxinica waaL</i> mut.....	39
3.3.2 Structural characterization by MALDI mass spectrometry of the intact LOS from <i>Burkholderia rhizoxinica</i> B1 mut.....	43
3.4. Biological activity of <i>Burkholderia rhizoxinica</i> strain B1wt and WaaL mutant	44
Discussion	45
Section II	
3.5 Structural elucidation of LPS from <i>Burkholderia rhizoxinica</i> strain wt B4	47
3.5.1 LPS Extraction and preliminary analysis.....	47
3.5.2 Full characterization of the O-chain from LPS of <i>Burkholderia rhizoxinica</i> strain B4.....	47
3.6 Structural elucidation of lipid A from <i>B. rhizoxinica</i> strain B4	50
Discussion	54
Chapter 4: Structural elucidation of lipid A from <i>Burkholderia cepacia</i> strain ASP B 2D	
4.1 introduction	58
4.2 Chemical characterization of lipid A structure	58
4.2.1 NMR spectroscopy of lipid A.....	59
4.2.2 MS analysis on intact and selectively degraded lipid A.....	61
4.3 Biological activity of lipid A from <i>B. cepacia</i> ASP B2D	64
Discussion	66
Chapter 5: Structural elucidation of LPS from <i>Bradyrhizobium</i> bacteria	
5.1 Introduction	70
5.2 Isolation and structural characterization of LPS from <i>Bradyrhizobium</i> BTai1 and ORS278	71
5.2.1. NMR structural elucidation of O-chain fraction from <i>Bradyrhizobium</i> <i>sp.</i> BTai1 (Br1).....	72
5.2.2 Absolute configuration of the novel monosaccharide from the O-chain fraction of <i>Bradyrhizobium sp.</i> BTai1.	77

5.2.3 Full characterization of the O-chain fraction from <i>Bradyrhizobium</i> <i>sp.</i> ORS278	80
5.3 Structural characterization of Lipid A from <i>Bradyrhizobium sp.</i>	
BTAi1 and ORS278	84
5.3.1 MALDI/TOF analysis of Lipid A.....	84
5.3.2 NMR spectroscopy of Lipid A.....	89
5.4 Biological assay on LPS from <i>Bradyrhizobium sp.</i> BTAi1 and ORS278	95
Discussion	96

Chapter 6: Experimental methods

6.1 Bacterial growth	101
6.1.1 <i>Burkholderia rhizoxinica</i> B1 (wt and <i>waaL</i> mut) and B4	101
6.1.2 <i>Burkholderia cepacia</i> strain ASP B 2D	101
6.1.3 <i>Bradyrhizobium sp.</i> BTAi1 and ORS278.....	101
6.2 LPS and LOS extraction	102
6.3 Isolation of lipidA and oligo(OS)/polysaccharide(PO) fraction	102
6.3.1 Isolation of PO and OS from <i>Burkholderia rhizoxinica</i>	102
6.3.2 Isolation of polysaccharide and lipidA fractions from <i>Bradyrhizobium</i> <i>sp.</i> BTAi1 and ORS278.....	103
6.4 Compositional analysis	103
6.4.1 Absolute configuration of bradyrizose.....	104
6.5 Mass spectrometry	104
6.5.1 <i>Burkholderia rhizoxinica waaL</i> mutant	104
6.5.2 <i>Bradyrhizobium sp.</i> BTAi1 and ORS278.....	105
6.6 NMR analysis	105
6.7 Biological assays	106
6.7.1 Testing of LPS mutants for defects in bacterial-fungal interaction.....	106
6.7.2 Callose deposition.....	106
Conclusions	109

Chapter 1

Gram-negative bacteria

1.1 The bacterial cell

Bacteria are a group of prokaryotic unicellular microorganisms that differ from eukaryotes for their simple cellular organization. Most of them are single-celled but some are organized in multicellular forms consisting of numerous cells that constitute distinctive cell morphologies (coccus, bacillus, spirillum, filamentous) and create distinct colonies visible by light microscopy when grown on petri plates. These are among the first characteristics that suggest the identity of an unknown bacterial culture. The prokaryotic bacterial cells present a general architecture composed by the following important structural components (Fig. 1.1):

- **Nucleoid**: an irregularly-shaped region where is localized the genetic material of bacteria (circular double-stranded piece of DNA). Unlike eukaryotes, the bacterial chromosome is not enclosed in the nuclear membrane, but resides completely inside the cytoplasm. It means that all processes of translation, transcription and DNA replication occur in the same region of bacterial cell interacting also with other cytoplasmic structure like ribosomes.
- **Cytoplasmatic membrane**: composed, like in eukaryotic cells, by a phospholipid bilayer (at molecular level, a model known as “fluid mosaic” best explains the structure and composition of the cell membrane); it has all the general functions of a cell membrane such as acting as a permeability barrier for most molecules and serving as the location of several enzymes involved in the biosynthesis of membrane phospholipids, cell wall polymers and DNA. In addition to these functions, in the prokaryotic membrane are also located several proteins responsible of the transport of a variety of molecules into and outward the cell.
- **Cell wall**: indispensable for the bacterial growth and viability and localized outside the cell membrane, is responsible of guaranteeing the structural support and the strength of the bacterial cell, offers protection against the internal turgor pressure higher compared to the external environment. Moreover, it represents a defensive barrier which help the bacteria to resist to environmental stresses. Its structural composition depends on the different bacterial classes and will be extensively discussed in this chapter.
- **Capsule**: can be found in many bacteria and composed by homo and/or heteropolysaccharides. The capsular polysaccharides possess several biological functions; they can mediate the bacterial interactions with external environment and support the bacterial colonization and adhesion to the host tissue. Moreover, concerning pathogen bacteria, they are considered virulence factors because they are able to trigger the immune response in the host. A remarkable example is done by *Streptococcus pneumoniae*, one of the bacteria responsible for pneumonia. It was demonstrated that unencapsulated strains of this bacterium are not pathogenic and thus they are unable of causing disease^[1]. Moreover, the

bacterial capsule can mediate (allows) the adhesion between bacterial cells, and forms a thin biofilm that protects bacteria from the attack of phagocytes and bacteriophages.

- **Flagella:** used by bacteria for locomotion. An example of a flagellated bacterium is the ulcer-causing *Helicobacter pylori*, which uses multiple flagella to propel itself through the mucus lining to reach the stomach epithelium. The bacterial flagellum is mainly composed by the flagellin protein, a strong elicitor of innate immunity in both mammalian and plant organisms.

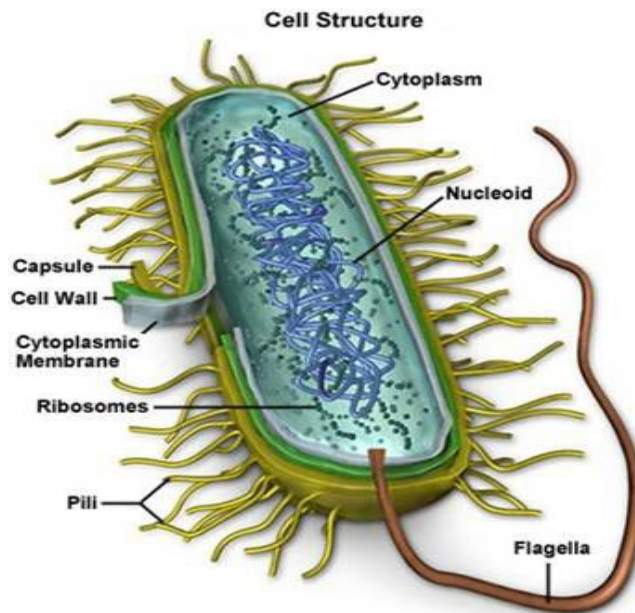


Fig.1.1 General structure of prokaryotic cell.

There are two main family of prokaryotes: *Archea* and *Eubacteria*, that differ for structural, functional and genetic characteristics^[2]. The first group involves many extremophiles able to live in extreme conditions of pH, temperature, pressure etc. and present characteristics that are similar to the eukaryotic system. The domain of *Eubacteria* involves a large group of bacteria that are in turn classified into other two families, namely Gram-positive and Gram-negative, based upon the cell reaction to the Gram staining. The differences between Gram-positive and Gram-negative bacteria are related to differences in the structure and chemical composition of their cell wall. Gram-positive bacteria reveal walls that are thick, nearly uniformly dense layers. Conversely, the cell walls of Gram-negative bacteria are more complex, and present a second “outer membrane”^[1] (Fig.1.2).

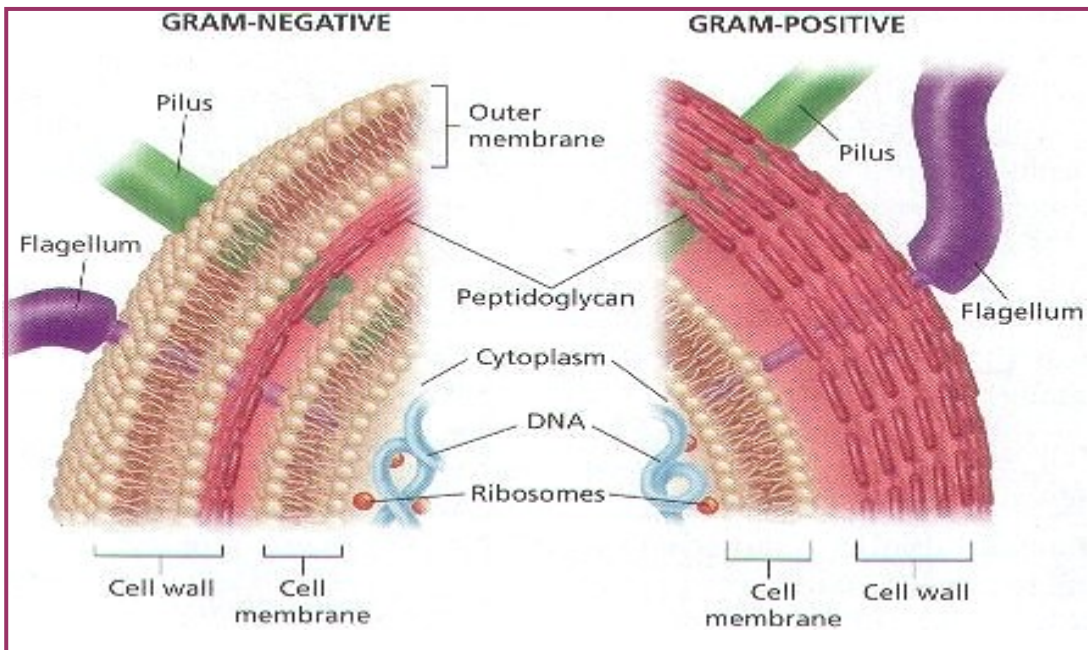


Fig. 1.2 Structural differences between Gram-negative and Gram-positive bacteria

1.2 Bacterial cell wall

The peptidoglycan polymer (murein or PGN) is an essential component of both Gram positive and negative bacteria that provides rigidity and structure to the bacterial cell wall although the amount, location and specific composition can vary. It is composed of carbohydrate chains of β -(1-4)-linked, alternating *N*-acetyl glucosamine and *N*-acetylmuramic acid monosaccharides cross linked by short peptide chains with alternating L and D-amino acids. These peptide chains contain unique amino acids such as *meso*-diaminopimelic acid (*m*-DAP) and D-glutamic acid that is connected by its lateral chain carboxyl group. The two major types of PGN are classified by the nature of the third residue of the stem peptide. In Gram-negative bacteria this residue is *m*-DAP (DAP-PGN) while in Gram-positive bacteria the third residue is commonly lysine (Lys-PGN). Unlike the Gram positive cell wall, where the PGN constitutes almost 95% of the cell wall, Gram-negative bacteria contain a thin peptidoglycan layer, almost 5-10% of the cell wall, adjacent to the cytoplasmic membrane. In addition to the PGN layer, the Gram-negative cell wall also contains an outer membrane composed by phospholipids and lipopolysaccharides (LPS), which face into the external environment (Fig1.2, Fig.1.3). As the LPS are highly-charged, the Gram-negative cell wall has an overall negative charge. The chemical structure of these macromolecules is unique to specific bacterial strain (e.g. sub-species) and is responsible for many of their biological properties.

1.3 Lipopolysaccharides

The lipopolysaccharides or LPSs are the major component of the outer membrane of Gram-negative bacteria, contributing greatly to the structural integrity of the bacteria and to the protection of the bacterial cell envelope. LPS also increases the negative charge of the cell membrane and helps to stabilize the overall membrane structure. They comprises about 10-15 % of the total molecules in outer membrane covering about 75% of bacterial surface area^[3,4]. Owing to their external location on outer bacterial membrane, the LPSs are responsible for many biological interactions of bacteria with the external environment. In particular, they are pivotal in many processes of host-bacteria interaction like adhesion, recognition, pathogenesis, symbiosis etc.^[5]. Moreover, LPSs are also called endotoxins because they are cell-bound and, once released, play a key role in the pathogenesis of Gram-negative infections owing to the ability to trigger the immune system in a wide range of eukaryotic organisms^[4]. In order to understand the molecular basis for bacterium–host interaction, it is important to elucidate the structure of LPS and to identify how bacterium modifies this structure in response to different environments. It has been already demonstrated that a correct structure of LPS is required to establish a disease (pathogens) or to produce a beneficial outcome (symbiont) in host-microbe interaction^[3].

From the chemical point of view, the LPSs are amphiphilic macromolecules consisting of three different fractions:

- a lipophilic domain called **Lipid A**
- a hetero-oligosaccharide denominated **Core**
- a hydrophilic hetero-polysaccharide called **O-polysaccharide chain** or **O-chain**

Bacteria can also synthesize LPS without O-chain, a Lipooligosaccharide, (LOS) also termed rough type-LPS (R-LPS) because confers a rough morphology to the bacterial colonies; conversely, the presence of a LPS provides a smooth aspect to the bacterial colonies (S-LPS) (Fig.1.3).

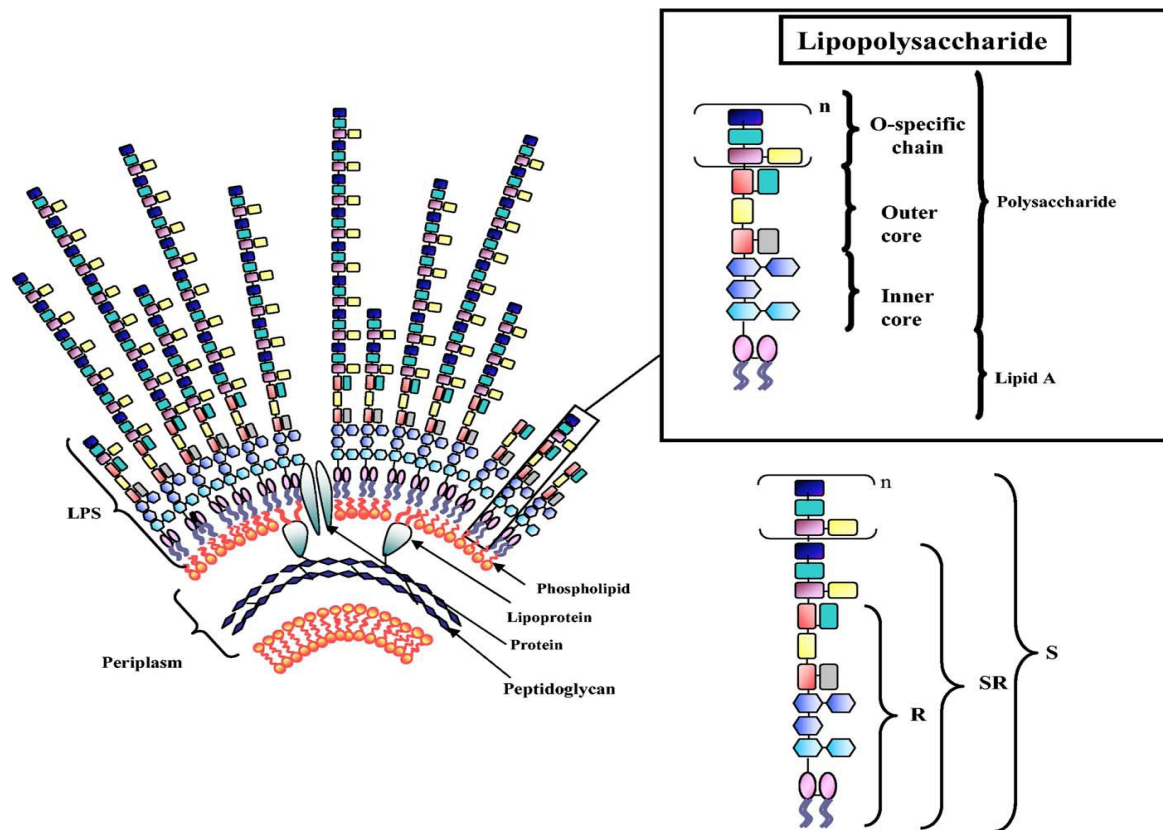


Fig1.3 General architecture of Lipopolysaccharides (LPSs). The R, SR and S structures indicate the rough, semi-rough and smooth LPS type respectively.

1.3.1 O-chain: structure and function

The O-polysaccharide chain^[6], the hydrophilic component of LPS, is the most variable portion in the LPS also within bacteria belonging to the same genus. It is usually composed by a regular polysaccharide, homopolymeric or heteropolymeric, linear or branched, with subunits consisting of up to eight different sugars^[5] and there may be up to 50 identical repeating units. During the biosynthesis of LPS the O-chain is formed by the polymerization of blocks of different length and added to the core. It means that the LPS results as a mixture of species that differ for molecular weight responsible of the typical ladder-pattern of LPS molecules on SDS electroforesis gel.

The monosaccharides can also have a very peculiar structure. A remarkable example is a carbocyclic sugar named caryose (Fig.1.4), founded in the O-polysaccharide from *Burkholderia caryophilli*, a phytopathogenic bacterium responsible for the wilting of carnations^[7,8].

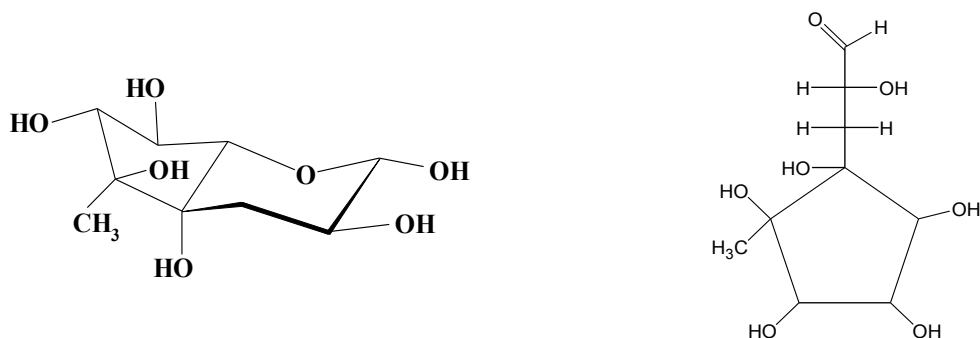


Fig.1.4 The structure of caryose

The structural variability of the O-chain is ascribable to the great number of monosaccharides that can constitute the repeating units as well as to the glycosidic sequence and to the presence of non-carbohydrate substituents like phosphate, amino acids, sulphate, acetyl or formamide groups, often present in non stoichiometric amount and that can mask the repeating oligosaccharide unit^[9,10]. The significance of these substituents is frequently unknown although bacteria can often modify their LPS to mask themselves to the host and escape the detection from the immune system^[9,11]. For instance, the O-chain fraction from *Helicobacter pylori*, that express Lewis antigenic epitopes (mainly Le^x and Le^y), seems to be essential for bacterium to survive in the acidic environment of human stomach and rough LPS mutant of *Helicobacter pylori* revealed a strong reduced colonizing ability^[3,12].

The O-chain also plays important roles as well as in plant-microbe interaction. In mammalian immune system, it represents the antigenic moiety of smooth LPS and can be pivotal for bacterial pathogenesis and survival^[13]. The O-chains from *Actinobacillus pleuropneumoniae* have been shown to be responsible for adhesion to mammalian tissue favoring the process of infection^[14]. Interestingly, these chains help the bacterium to avoid the attack from numerous antibiotics as shown by the relative sensitivity of rough type respect to smooth strain^[15,16].

1.3.2 The core oligosaccharide: structure and function

The core domain always contains a very complex oligosaccharide component that is directly attached to the lipid A. It includes approximately fifteen monosaccharide residues collected in two different domains: inner core and outer core. The inner core, which is proximal to the lipid A, is structurally less variable and contains peculiar monosaccharides like heptose (*L-glycero-D-manno*-heptose and *D-glycero-D-manno*-heptose) and Kdo (3-deoxy-*D-manno*-octulosonic acid), a monose marker for all Gram-negative bacteria that connects the core oligosaccharide to lipid A backbone. The composition of the outer core is usually characterized by a few glycosidic residues: neutral

sugars, uronic acids and aminosugars. The core fraction together with the lipid A is the structural motive common to all LPS; this suggests that these domains are indispensable for Gram-negative bacterial life. Some of the bacteria which are not possessing the O-polysaccharide chain are nasty microbes such as *N. meningitis* and *H. influenzae* that are both human pathogens responsible of meningitis. These two species are able to mimic the host cell surface glycoconjugates and escape, in a stealth strategy, the attack from the MAC (Membrane Attack Complex) of outer membrane (molecular mimicry)^[3,17,18].

1.3.3 Structure and biological properties of lipid A

The lipid A is a glycolipid and represents the hydrophobic domain of LPS, being responsible of the anchorage of the whole macromolecule on the outer membrane. Its general structure consists of a disaccharide backbone formed by a 2-amino-2-deoxy-D-glucopyranose (D-GlcN, glucosamine) disaccharide linked by a β -(1 \rightarrow 6) bond, phosphorylated at position 1 and 4' and acylated by 3-hydroxy fatty acid residues, called "primary" fatty acid, linked with ester bonds at positions 3 and 3' and with amide bonds at positions 2 and 2'. These fatty acids can be further acylated at hydroxyl position with secondary fatty acids, usually not hydroxylated and with different length. (Fig.1.5)

The first lipid A structure elucidation was achieved on from *E. coli* and *S. enterica* LPS in 1983^[19]. It resulted to be built up of a disaccharide backbone of phosphorylated GlcN [P \rightarrow 4- β -D-GlcN-(1 \rightarrow 6)- α -D-GlcN-1 \rightarrow P] acylated at position 2 and 3 of both GlcNs by four 14:0 (3-OH). The primary fatty acids located on the distal GlcN (GlcNII) were both esterified at their hydroxy group by two secondary fatty acids; the amine linked 14:0 (3-OH) was esterified by a 12:0; the ester linked 14:0 (3-OH) by a 14:0. This hexa-acylated lipid A has asymmetric (4+2) distribution of the acyl chains. The Lipid A is often composed by a mixture of glycoforms that differ for the acylation and phosphorylation pattern. These subtle chemical differences have been identified as responsible for variation of the virulence degree of bacteria in response to adaptation to the host environment. More recently, lipid A differing from the classical Lipid A of *E. coli* have been also identified. Actually, some lipid A isolated from *Rhizobiaceae* are constituted by mixture of glycoforms in which one or both GlcNs are replaced by 2,3-diamino-2,3-dideoxy-D-glucopyranose (GlcN3N). In particular, *Rhizobium etli*^[20] possesses a lipid A in which the non reducing GlcN is α -1-6 linked to a residue of 2-amino-2-deoxy-D-gluconate and in position 4 is substituted by a distal galacturonic acid residue. The *Rhizobium* bacterial genus is very characterised also by the presence of a long chain secondary fatty acid, such as like 28:0 (27OH), 30:0 (29OH).

The lipid A is the endotoxic principle of LPS and is able to trigger the mammalian and plant innate immune system. The toxicity of lipid A is strongly influenced by its primary structure whose changes strongly influence their capacity to interact and activate receptors of the immune system.

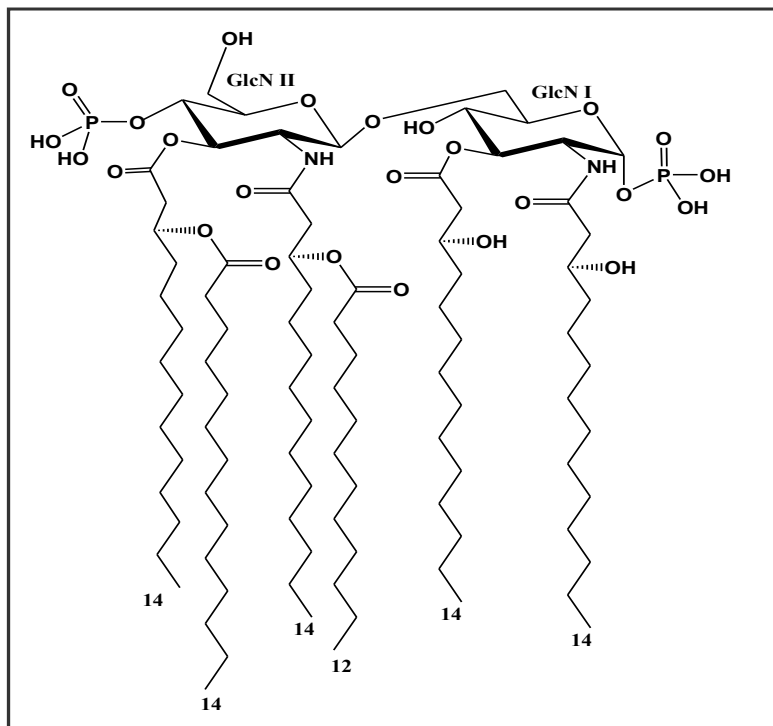


Fig.1.5 The lipid A structure from *E. coli* LPS.

1.4. Plant communication with different other living systems

Plant organisms have coexisted for millions of years in contact with other species and so have evolved the capacity to establish a wide number of relationships with prokaryotes and eukaryotes that live in rhizosphere. The chemical signals are usually polysaccharides, amino-acid, aromatic acid, fatty acid, sterols, enzymes, proteins and other secondary metabolites. Many evidences demonstrated that the plants use different chemical compounds and the choose depend on coupled microorganism^[21]. In Fig.1.6 there are shown some examples of chemical communications owing to various relationships of plants with a different kind of prokaryotes and eukaryotes.

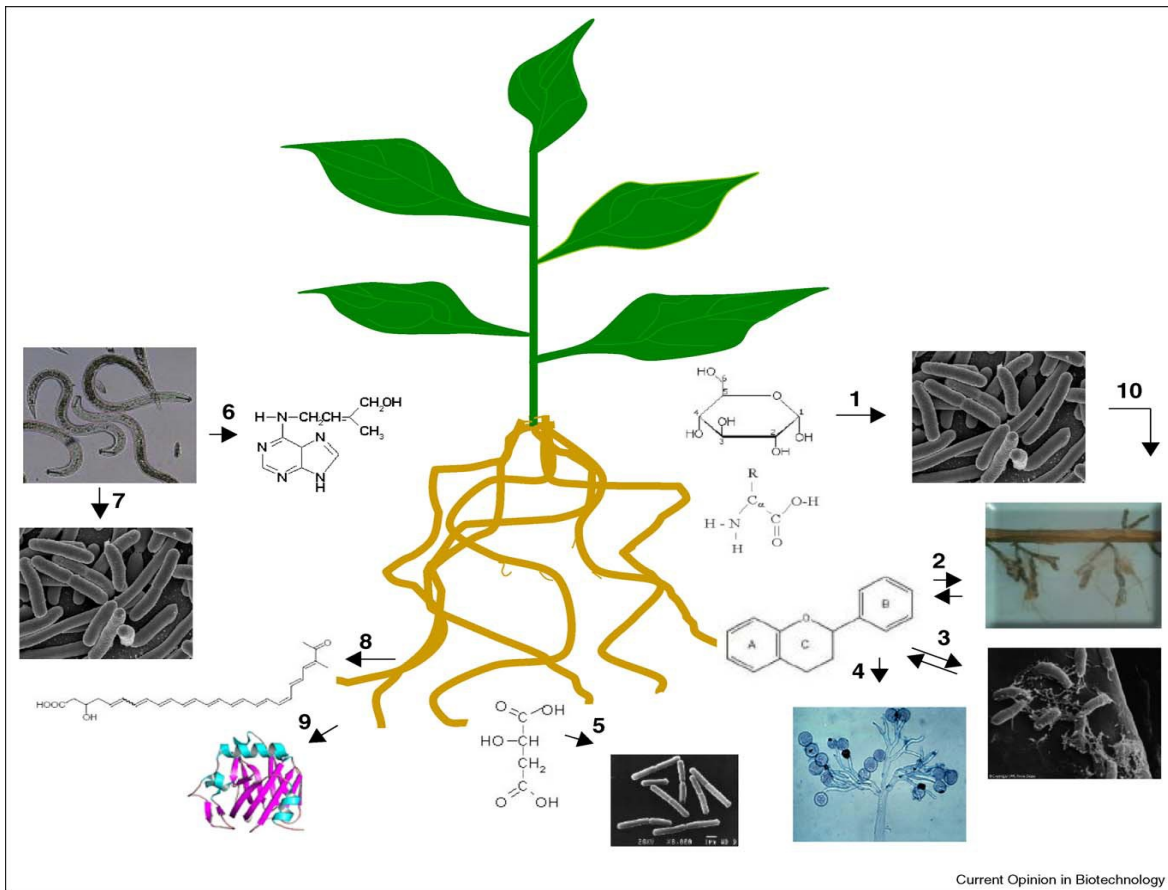


Fig1.6 Illustration of the chemical communication between plant roots and a complex group of microorganisms of rhizosphere.

As shown in Fig1.6, the plants release a wide range of compounds in order to attract microorganism and to establish both harmful (with pathogens) and beneficial (with mutualistic organisms) interactions.

1.5 The plant innate immune system

The innate immune system comprises the cells and mechanisms that defend the host from infection by other organisms, in a non-specific manner. It results to be the first line of defense against external pathogens and is a well described phenomenon in vertebrate and insects while results less studied in plant system^[22]. Like in mammals, the innate plant immunity has acquired the ability to recognize the molecular structure defined **MAMPs** (**M**icrobe **A**ssociated **M**olecular **P**atterns) that are absent in eukaryotic cells but are indispensable for microbial life and for biological activity of bacteria. These molecular patterns are recognized by a family of receptors called **PRRs** (**P**attern **R**ecognition **R**eceptors). There are many elicitors in plants that trigger the innate immune response

among which there are flagellin, elongation factor Ef-Tu, lipopolysaccharides and peptidoglycan. For most of these the PRRs have not been identified yet. In Fig. 1.7 a scheme with same known PRRs in plants has been reported.

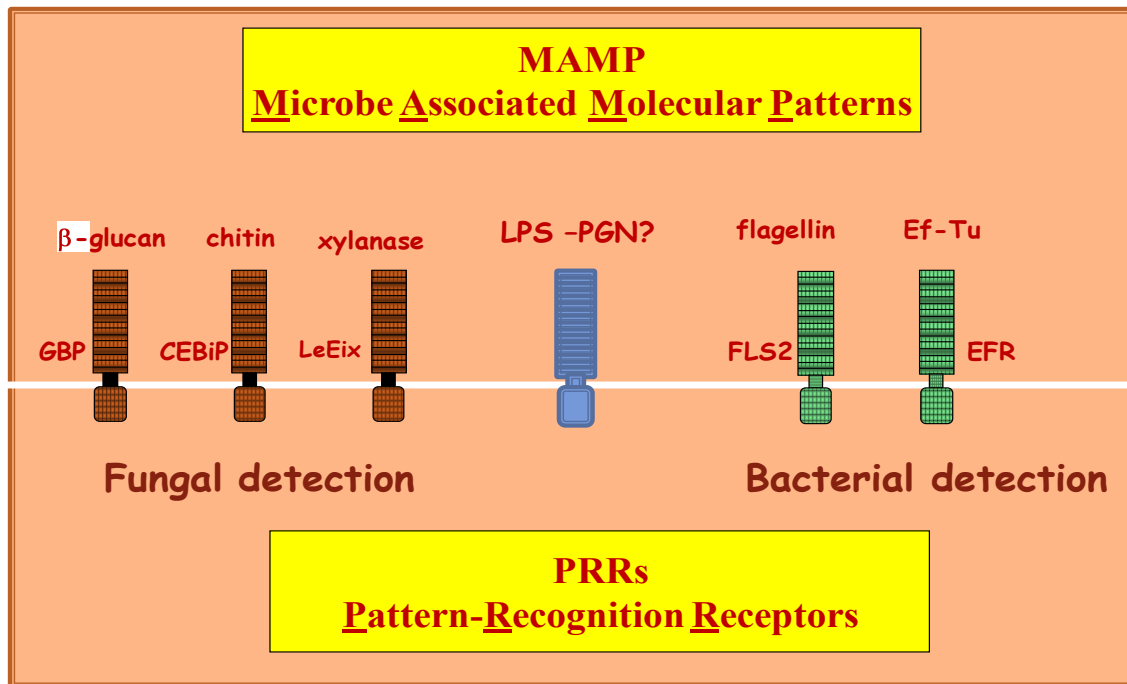


Fig.1.7 Elicitors recognition in plant innate immunity. No receptor for LPS and PGN has been identified so far.

The innate immune system in mammals perceives invading pathogens through Toll-like receptors (TLRs), that possess a structure analogue to the Toll receptor in *Drosophila*^[23,24]. *Drosophila* Toll and mammalian TLRs recognize the general elicitors by an extracellular leucine rich repeat domain (LRR) and transduce the signal through a TIR domain (*Drosophila* Toll and human IL1 receptor)^[25]. Several cytoplasmatic plant disease resistance genes (*R* genes) are found to be homologous in some modules to members of TLR family and it was shown that they mediate host defense against specific viral and fungal plant pathogens (Fig.1.8)^[26]. Examples of *R* proteins that present a Toll-interleukin 1 receptor (TIR) homology domain are the N protein from tobacco, the L6 protein from flax and the RPP5 protein from *Arabidopsis*. The presence of these *R* genes with TIR domain suggests that they are involved in transduction process but not in recognition of elicitors. Another key feature of MAMP recognition in plants appears to be the exclusive localization of their receptors in the plasma membrane. To date, there is no case reported on intracellular recognition of MAMPs in plants. This property is certainly another difference from animal cells, in which activation of innate immune responses may also result from intracellular MAMPs recognition by, for example, nucleotide-binding oligomerization domain (NOD) proteins^[22].

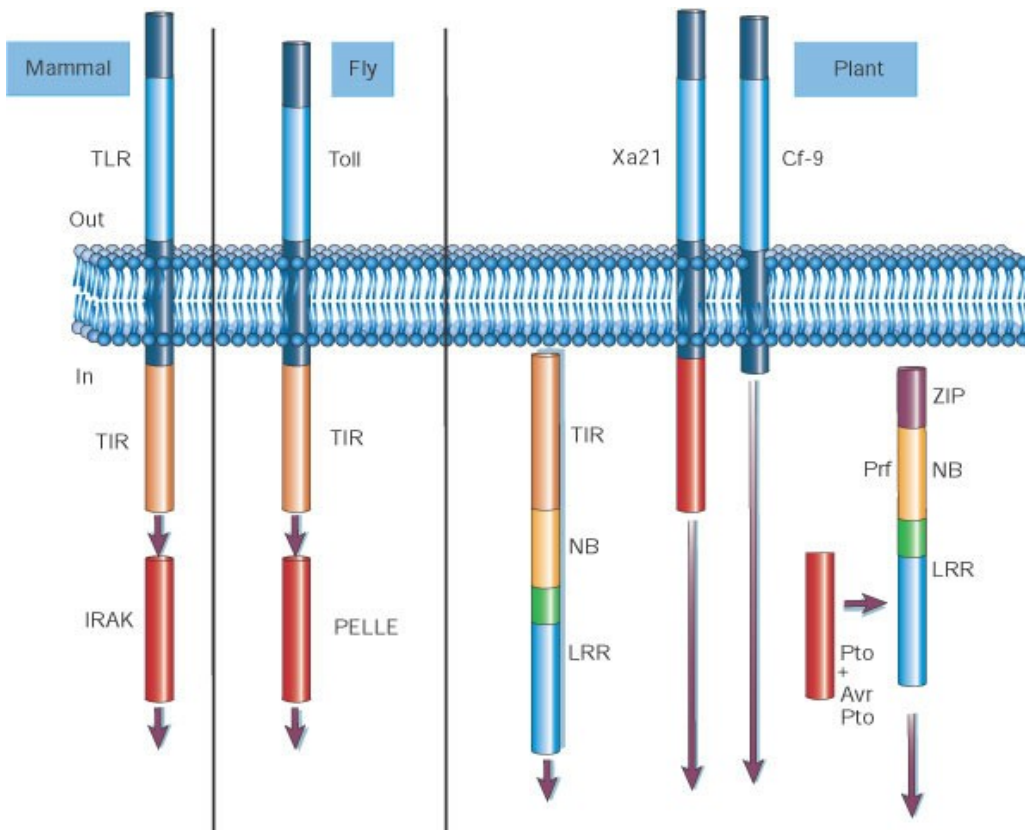


Fig.1.8 Comparison of R proteins with those involved in mammalian innate immunity

1.5.1 The hypersensitive response and localized induced resistance

Often the immune plant response is followed by a localized cell necrosis at the infection site known as Hypersensitive Response (HR). The HR is a strategy used by plants to confine the infection. Resistance (*R*) genes detect the pathogens and trigger the necrosis of plant tissue depositing compounds like callose, lignin, HGRP (Hydroxyproline-rich glycoproteins) and pathogen related (PR) proteins also including 1,3-glucanase and chitinases. During HR there is a rapid decline of bacterial proliferation and a suppression of the pathogen growth protecting in this way the plant from infection. The plant response is accompanied by rapid cell death in the site of the infection and is associated with a decline of the number of viable bacteria recovered in the tissue and follows a rapid necrosis of plant tissue representing the final stage of resistance, when stress signals request strong defensive responses.

The capacity of LPS to prevent the HR response induced in plants by avirulent bacteria has been widely demonstrated. The pre-inoculation of leaves with heat-killed bacterial cells delays or prevents the disease symptoms and the HR, when leaves are subsequently inoculated with living bacteria. The LPS was shown to be responsible for the activity of suppression. The effect of LPS in preventing the HR is phenomenon that has been termed by Sequeira and coworkers^[27] as “localized induced resistance” or LIR. The lipopolysaccharide has the ability to induce some non-specific defence related responses. Soluble peroxidase, cationic peptides and β -1-3-glucanase are compounds induced by the LPS interaction with plant receptors. The capacity to induce low-molecular weight antimicrobial compounds has been also reported. The hydrogen peroxide is believed to have a role in triggering the hypersensitive cell death and in the induction of antioxidant protective compounds. Interestingly, LPS can induce changes in the plant cell surface which accumulate granular material and cell thickening. LPS preparations of from *Xantomonas campestris* pv *campestris* can prevent the HR process in pepper cultivar; the source of LPS and the nature of bacteria appear to be irrelevant since LPS preparations from different Gram-negative bacteria, including *E. coli* or *P. aeruginosa*, are able to induce LIR. The LPS structural requirements to provoke LIR in plants have been investigated. Studies on LPS mutants lacking the O-chain and with progressive truncation of the core oligosaccharide have demonstrated that the minimal structural requirement to trigger LIR resides in the lipid A-core region^[28]. A parallel study performed on LPS from *Xantomonas campestris* pv *campestris* from Newmann and colleagues concluded that the O-chain is not responsible for preventive effect^[29], that the lipid A alone is also inactive and then the minimal structure required for HR prevention is the lipid A with a truncated core oligosaccharide. The inability of lipid A to prevent HR is explained with its insolubility in an aqueous environment owing to its hydrophobicity and so with its incapacity to trigger the immune system of plants. The LIR process is usually localized to the site of inoculation of LPS and requires several hours before to be visualized^[30]. The molecular basis of LIR induced by LPS still remains obscure and so difficult to explain. It is possible that the effects of LPS in HR prevention and in triggering basal defense may allow the plants to express resistance without catastrophic tissue collapse^[31].

1.5.2 Plant pathogens

There are many groups of plant pathogens and they include not only Gram negative bacteria, like *Agrobacterium tumefaciens* or *Burkholderia caryophilli*, but also organisms as fungi and nematodes. Like plants-mutualist association, pathogens also utilize chemical signaling to communicate and to establish the infection. In many cases the roles and mechanism of action of LPS in plant immune process are still to be investigated but there are many evidences that

demonstrate their involvement in the process of infection. The roles of LPS in bacterial pathogenesis in plants are investigated testing different LPS mutant for their virulence degree. The evidences demonstrate that LPS mutants of major genera of Gram-negative phytopathogens have reduced virulence^[32]. Furthermore, the contribute of LPSs to the resistance to plant derived antimicrobial compound has been widely demonstrated (barrier function)^[3]. In particular, the O-chain fraction may not have a specific role in plant pathogenesis suggested by finding of rough type LPS isolated from diseased plants. Conversely, mutants for biosynthesis of inner or outer core show a reduced virulence degree and they are no longer able to survive *in vivo* owing to chemical and physical stress (see par. 1.5.1).

Many experimental evidences suggest that there are suitable differences between symbiosis and pathogenicity; owing to that, probably, symbiont bacteria can evade or neutralize the plant defense system and so establish a beneficial symbiosis. In several cases the symbiotic organisms constitute a system able to be pathogen for plants. A remarkable example is constituted by a mutualistic relationships between *Rhizopus microspores*, a plant pathogenic fungus causing rice seedling blight, and *Burkholderia rhizoxinica*. This represent a unique system in which a fungus harbors endobacteria for the production of a phytotoxin and so to infect the plants^[33] (see chapter 3).

1.5.3 Plant symbiont bacteria

Symbiotic relationships include those associations in which one organism lives on another (ectosymbiosis), or where one partner lives inside the other (endosymbiosis). When both microorganisms involved in symbiosis take advantages from relationship, the process is defined as mutualistic symbiosis. There are many examples of mutualism interaction between plants and bacteria and the most described is leguminous/Rhizobia association.

The interaction of *Rhizobium* bacteria with plants leads to the formation of the specific organs on roots, the nodules, in which the bacteria are able to fix the atmospheric nitrogen in ammonia, used by plant for nitrogen source. In fact, the symbiosis process is established under conditions of nitrogen limitation, status that stimulates the plants to release the chemical signaling to attract a specific strain of *Rhizobium* and so to establish the symbiosis. *Rhizobia* play a key role in agriculture sustainability because of enhancing the ability of legumes to fix atmospheric nitrogen^[34]. Nitrogen is an essential nutrient for plants and is required to biosynthesize the basic building blocks, e.g. nucleotides for DNA and RNA and amino acids for proteins. Thus, the use of

these bacteria, defined biofertilizers, in agricultural system would decrease the need of chemical fertilizers which are not only cost effective but also may create environmental problems.

The genus of *Rhizobiaceae* are represented by 12 genera containing more than 70 species of α and β proteobacteria referred to as α and β -*Rhizobia*^[35]. In Fig. 1.9 are shown morphological variations due to a symbiosis between different couple of *Rhizobium*-legume. It is clear that there are many phenotypic variations regarding the localization, shape, anatomy of the nodules as well as the infection mode and differentiation status of endobionts. These observations suggest the existence of different genetic strategy used by *Rhizobia* to establish the symbiosis with plants.

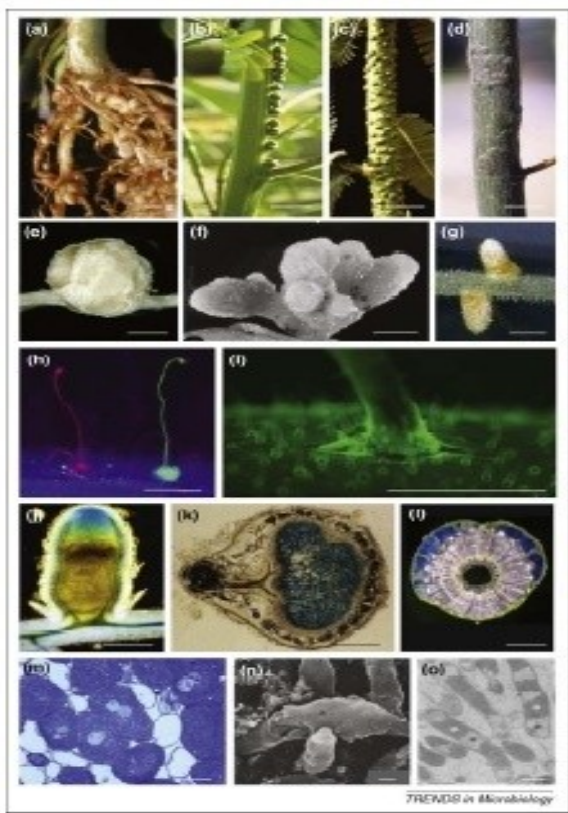


Fig.1.9 *Rhizobia* form nodules on roots (a) *Cupriavidus taiwanensis*–*Mimosa pudica*, (b) *Azorhizobium caulinodans*–*Sesbania rostrata*, (c) *Bradyrhizobium* sp. ORS322–*Aeschynomene afraspera*, (d) *Bradyrhizobium* sp. ORS278–*Aeschynomene sensitive*, (e) *Sinorhizobium fredii*–soybean, (f) *Methylobacterium nodulans*–*Crotalaria perrottetii*, (g) *Sinorhizobium meliloti*–*Medicago sativa*, (h) *S. meliloti*–*M. sativa*, (i) *Bradyrhizobium* sp. ORS285–*Aeschynomene indica*, (j) *M. sativa*, (k) *Lotus*, (l) *Bradyrhizobium* sp. ORS278–*A. sensitive*, (m) *C. taiwanensis*–*M. pudica*, (n) *caesalpinoid* legumes, (o) *S. meliloti* bacteroids in *M. sativa* nodule symbiosomes.

Conversely, up to ten years ago, there was a belief that the formation of nodules involved only a specific molecular signaling pathway constituted by lipochitooligosaccharides (simply called Nod factors, NF). In this scenario, secondary metabolites such as flavonoides or isoflavonoides, attract the specific *Rhizobia* and are recognized by NodD proteins responsible of activation of *nod* ABC genes for the biosynthesis of NF. Successively, the nodule formation is obtained by a specific binding between NF and a kinase-like receptor of plants that trigger the nodule organogenesis^[36] (Fig1.10 a). In this frame, the NF are indispensable to the formation of nodules and so to establish the symbiosis with plants.

Giraud et al.^[37] have recently shown, by complete genome sequencing of two symbiotic photosynthetic *Bradyrhizobium* strains, BTAi1 and ORS278, that canonical *nod* ABC genes are absent and thus the typical Nod factors are not required for symbiosis in some particular group of *Aeschynomene* plants among which are indicated *A. indica* and *A. sensitiva*. These data indicate that there is **NF-independent mechanism** that bacteria use to infect the plants and so that the NF-strategy is not universal. Further studies performed on strain of *Bradyrhizobium* genus confirm the existence of a alternative nodulation mechanism.

Bradyrhizobium sp. ORS275 is another photosynthetic strain isolated by *Aeschynomene* plants but that contains the canonical *nod* ABC genes. It is capable to establish the symbiosis with a broader host range that extend to all stem-nodulated *Aeschynomene* species^[38]. Interesting finding was obtained from a Nod deletion mutant of strain ORS285 that retains the ability to nodulate *A. indica* and *A. sensitiva* (the leguminosae specie colonized by *Bradyrhizobium* strains BTAi1 and ORS278) but not the other species^[39]. This suggest that this group of photosynthetic bradyrhizobia uses both NF-dependent and independent strategy to form the nodules and that the choose to use one or the other depends on the host plant. Some NF-dependent alternative process are just proposed. One of them is shown in Fig1.10 b, in which is postulated that a bacterial purine derivatives, the cytokinins, trigger the nodule organogenesis. This hypothesis is supported by the fact that several *Bradyrhizobium* strains were shown to produce cytokynins and by the implication of plant cytokinin receptor in nodule development in *Medicago truncatula* and *Lotus japonicas*^[40]. In this frame also a variety of bacterial surface polysaccharides, e.g., lipopolysaccharides, are of particular interest, since they could play a role as signaling compounds, presumably acting as suppressors of plant defense reactions in initial colonization. In fact, the genome sequences of BTAi1 and ORS278 have revealed a number of LPS and EPS biosynthesis genes involved during the symbiotic interaction with their host plants.

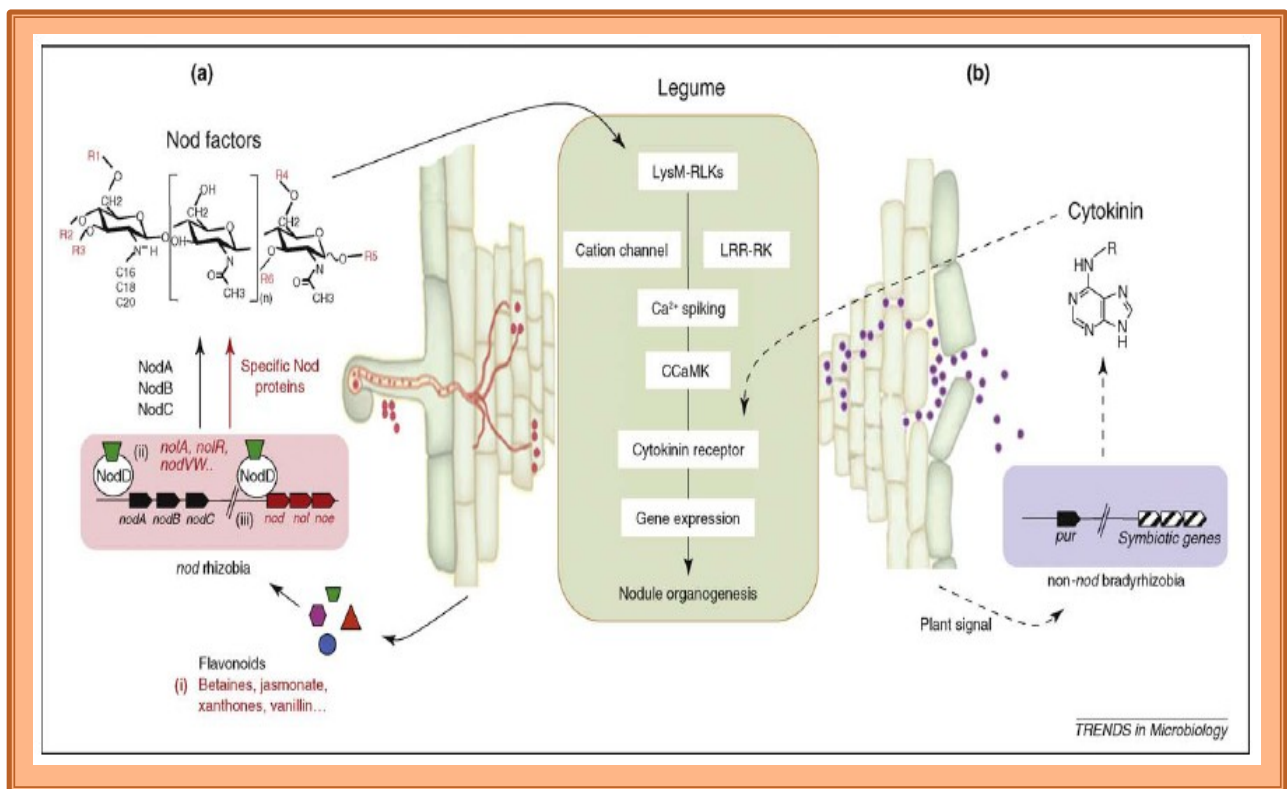


Fig.1.10 Nodulation strategies in *Rhizobia*. *Rhizobia* induce the formation of nodules on legumes using either a NF-dependent (a) or a NF-independent (b) process. In the NF strategy (a), plant signals of the flavonoid family are perceived by bacterial NodD regulatory proteins that induce the synthesis—through nodulation genes—of lipochitooligosaccharidic NFs that trigger nodule organogenesis. A hypothetical scheme is proposed for the NF-independent process (b). The need for one initial plant signal remains to be demonstrated. The bacteria enter in the plant via cracks in the epidermis which result from the emergence of lateral roots. Accumulation in these infection zones of cytokinin-like compounds synthesized by the bacteria might directly bypass the early NF signaling pathway and trigger nodule organogenesis.

1.5.4 LPS and symbiosis

The surface polysaccharides, including lipopolysaccharides (LPS), have been shown to play an important role in the symbiosis process since they are required to establish an effective symbiosis. It was demonstrated that a correct LPS structure is essential for root hair infection, nodule invasion, for avoiding the host defense responses and for physiological adaptation to the endophytic microenvironment. There are many observations that indicate the requirements of O-antigen in a successful plant-bacterium interaction in different stages of nodulation. For example, in *Rhizobium leguminosarum* bvs. *viciae* and *trifolii* the LPS resulted to be important in the very early recognition steps with plants^[41,42]. In particular, host-encoded lectins and interaction with LPS is very important to establish a correct root adhesion of bacteria on the plants. The presence of O-antigen fraction

revealed to be important also in infection thread initiation and elongation. In fact, use of Rhizobia strain with LPS mutant lacking the O-chain showed a premature of abortion of infection threads. Furthermore, the polysaccharide fraction is required to avoid the immune response in host plants owing to the O-chain covers compounds that trigger the immunity system like lipid A-core structure or outer membrane proteins.

The lipid A is endotoxic part of LPS and its roles in symbiosis process is still unknown. Rhizobial lipids A significantly differ from enterobacterial analogues and are usually less toxic or not toxic at all^[43]. The hexa-acylated lipid A from enteric *E. coli* results to have great structural differences with rhizobial lipid A, differences attributed once again to a strategy adopted by symbiont bacteria to avoid the host immune system. For example, the lipid A from *Rhizobium leguminosarum* and *Rhizobium etli* CE3 is constituted by two different types of glycoforms that report, in both cases, a residue of galacturonic acid attached on distal glucosamine while the proximal glucosamine is present in reducing form or replaced by a 2-amino-2-deoxygluconic acid residue. Other chemical variations concern phosphate content, the fatty acid acylation pattern and the structure of the carbohydrate backbone. As stated above, *Rhizobium* sp. Sin-1 presents a glucosamine backbone without phosphate groups and the proximal residue is oxidized to 2-aminogluconate^[44]. Instead, *Mesorhizobium huakuii* LPS possesses a lipid A blend with the 2,3-diamino-2,3-dideoxy-D-glucopyranose (Glc_pN₃N) as aminosugar (Fig.1.11). Other remarkable features of these lipid A structures concern the fatty acid composition and the the presence of a very long chain fatty acids like C28:0 (27-OH) or C30:0 (29-OH). In some cases, these secondary fatty acids are substituted with a tertiary 2-hydroxy-butirroyl moiety as ester at the (ω -1) hydroxy group (Fig.1.11). These structural modifications on LPS moiety are supposed to be an arrangement used to escape or attenuate the host recognition. This is an important condition by which bacteria can colonize the host plants and establish the symbiosis; bacteria modify structurally many molecular patterns in order to adapt themselves to the host environment.

A

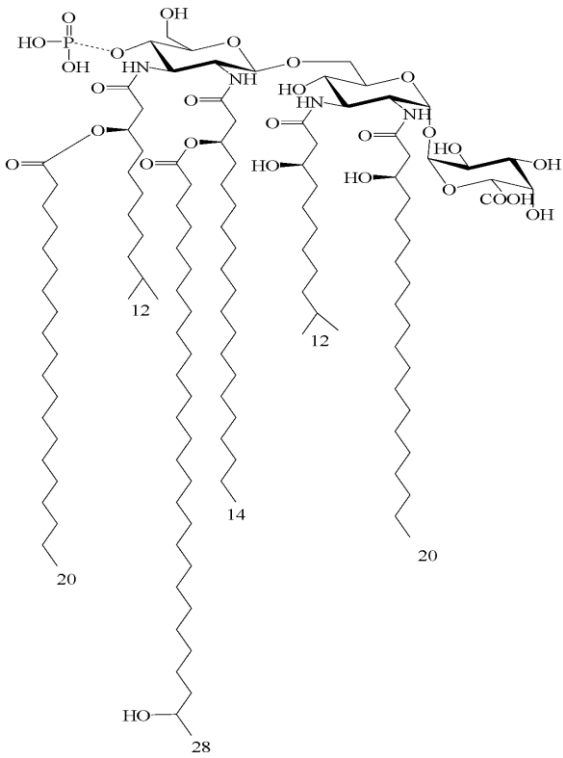
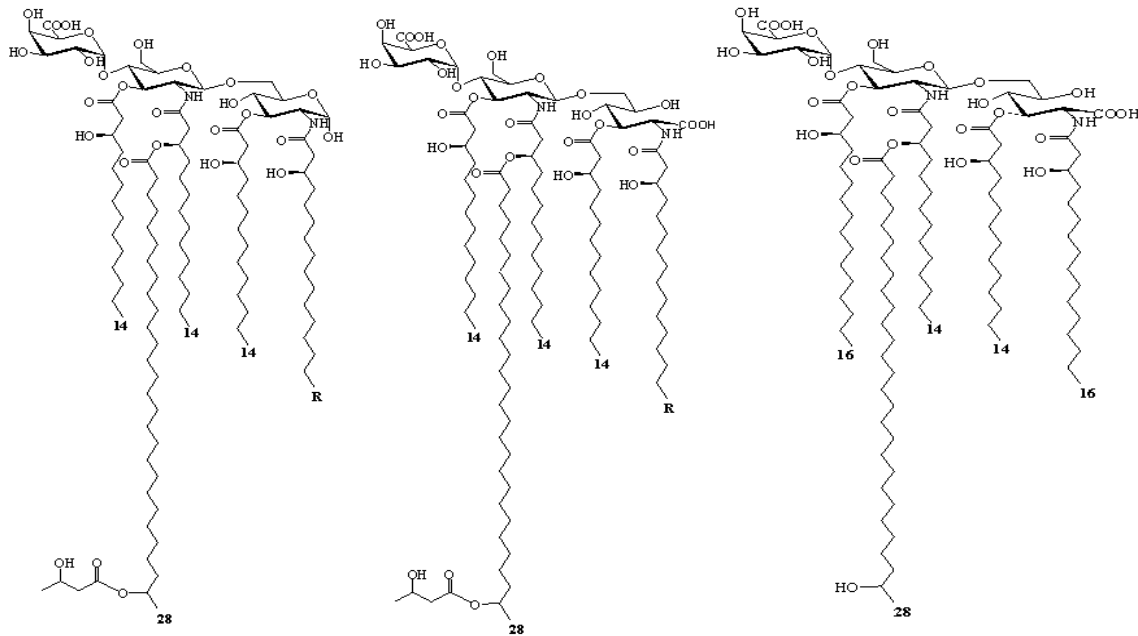


Fig.1.11 Structures of lipid A of *Mesorhizobium huakuii* IFO 15243 (A), and *Rhizobium etli* CE3, *Rhizobium leguminosarum* and *Rhizobium* species sin-1 (B). Dotted lines indicate non-stoichiometric substitution.



Rhizobium etli CE3 and *Rhizobium leguminosarum* pv. *viciae* 3841

Rhizobium Species Sin-1

B

References

1. Staley J T, Gunsalus R P, Lory S, Perry J J. *Microbial Life* (2007) second edition , chapter 4.
2. Madigan, M.; Artinko, M.A.; Parker J., *Biology of microorganism* (Ed.: T. Brock) Pearson education international, New York, **2003**.
3. Lerouge I, Vanderleyden J. *FEMS microbiology reviews*, (2001). **26**:17-47.
4. Alexander C, Rietschel ET. *J.endotoxin Res.* (2001). **7**:167-202.
5. Konig H, Herald C, Varma A, *Prokaryotic cell wall*, chapter 4 : 133-154
6. Raetz CRH, Whitfield C. *Annu.Rew.Biochem.* (2002) **71**:635-700.
7. Adinolfi M, Corsaro MM, De Castro C, Evidente A, Lanzetta R, Molinaro A, Parrilli M. *Carbohydrate Research* (1996) **284**: 111-118.
8. Adinolfi M, Corsaro MM, De Castro C, Evidente A, Lanzetta R, Molinaro A, Lavermicocca P, Parrilli M. *Carbohydrate Research* (1996) **284**: 119-133.
9. Jansson PE, Brade H, Morrison DC, Opal S, Vogel S. *Endotoxin in Health and Disease*, New York pp. (1999) 155-178.
10. Stenutz R, Weintraub A, Widmalm G *FEMS Microbiol Rev* (2006) **30**: 382–403.
11. Whitfield C. *Annu Rev Biochem* (2006) **75**:39-68.
12. Amano Y, Kanda T. *Trends in Glycoscience and Glycotechnology* (2002) **14**: 105-114.
13. Holst O, Brennan PJ, von Itzstein M. *Microbial Glycobiology* (2009) First edition, section I, chapter 4.
14. Caroff M, Karibian D. *Carbohydrate research* (2003) **338**:2431-2447.
15. Nikaido K, *Biochim, Biophys. Acta* (1976) **433**: 118-132.
16. Banemann A, Deppisch H, Gross R, *Infect.Immun.* (1998) **66**:5607-5612.
17. Preston A, Mamdrell RE, Gibson BW, Apicella MA, *Crit. Rew. Microbiol.* (1996) **22**:139-180
18. van Putten JP, *EMBO J* (1993) **12**:4043-4051.
19. Wollenweber HW, Schlecht S, Luderiz O, Rietschel ET, *Eur. J.Biochem.* (1983) **130**:167-171
20. Que NLS, Ribeiro AA, Raetz CRH, *J.biol.chem.* (2000) **275**:28006-28016
21. Badri DV, Weir TL, van der Lelie D, Vivanco JM. *Current Opinion in Biotechnology* (2009) **20**:642–650.
22. Nüßberger T, Brunner F, Kemmerling B, Piater L. *Immunological Reviews* (2004) **198**: 249–266
23. Hashimoto C, Hudson KL, Anderson KV. *Cell.* (1988) **52** :269-79.
24. Lemaitre B, Nicolas E, Michaut L, Reichhart JM, A Hoffmann J. *Cell* (1996) **88**: 973-983

25. Erbs G., Molinaro, A., Dow, MJ, Newman, M.A. Lipopolysaccharide and plant innate immunity in Endotoxins: structure, function and recognition, volume 53 of the Subcellular Biochemistry series, Springer, Heidelberg, 2010. pp. 387-403.
26. Hammond-Kosack KE, Jones JDG, *Annual Rew. Plant Physiol. Plant Mol. Biol.* (1997) **48**: 575-607
27. Sequeira L, Hill LM. *Physiol. Plant Pathol.* (1974) **4**:447-455
28. Dow MJ, Newman MA, von Roepenack E. *Annu. Rew, Phytopathol.* (2000) **38**: 241-261
29. Dow MJ, Osbourn AE, Wilson TJG, Daniels MJ. *Mol. Plant-Microbe Interact.* (1995) **8**:768-777
30. Newman MA, Daniels MJ, Dow MJ. *Mol. Plant-Microbe Interact* (1997) **10**: 926-928
31. Dow MJ, Molinaro A, Cooper RM, Newman MA. *In Microbial Glycobiology Structures, Relevance and Applications*
32. Newman MA, von Roepenack E, Daniels MJ, Dow MJ. *Plant Pathol.* (2000) **1**:25-31
33. Partina Martinez LP, Monajembashi S, Greulich KO, Hertweck C, *Current Biology* (2007) **17**:773-777.
34. Ogutcu H, Adiguzel A, Gulluce M, Karadayi M, Sahin F. *Romanian Biotechnological Letters*, (2009) **14**: 4294-4300
35. Masson-Boivin C. Giraud E, Perret X. and Batut J. *Trends in Microbiology* (2009) **17**: 458-466.
36. Oldroyd JED, Downie JM, *Annual Rew. Plant Biol.* (2008) **59**: 519-546.
37. Giraud, E. et all. *Science* (2007) **316**: 1307-1312
38. Giraud, E. et all. *Photosyn. Res.* (2004) **82**:115-130
39. Gonzalez-Rizzo S et all. *Plant Cell* (2006) **18**:2680-2693
40. Frugier F et all. *Trends Plant Sciences* (2008) **13**: 115-120
41. Normand P et all. *Genome Research* (2007) **17**:7-15
42. Dazzo FB, Brill WJ, *J. Bacteriol.* (1979) **137**: 1362-1373
43. Kato G, Maruyama Y, Nakamura M. *Agric. Biol. Chem.* (1980) **44**:2843-2855
44. Jeyaretnam B, Glushka J, Kolli VSK, Carlson RW. *The Journal of Biological Chemistry*, (2002) **277**: 41802-4181

Chapter 2

Structural investigation of lipopolysaccharides and lipooligosaccharides

2.1 Extraction and purification of lipopolysaccharide (LPS) and lipopoligosaccharide (LOS).

The approach used for the isolation of S- and R-type of lipopolysaccharides are usually different. Gram-negative bacteria are sequentially extracted with two procedures. Rough-type LPS (LOS) are extracted with a phenol/chloroform/light petroleum (PCP mixture), smooth-type LPS are extracted with the hot phenol-water procedure^[1,2] (see Figure 2.1). Both samples then undergo extensive dialysis and further purification via molecular size exclusion chromatography.

The PCP extraction consists in the treatment of dried bacterial cells with phenol/chloroform/light petroleum in proportions 5/8/2 and then LOS is precipitated from pure phenol adding drops of water. Successively, the obtained pellet is treated with phenol/water 1:1 at 68°. Typically, the presence of the long O-chain moiety increases the hydrophilic nature and generally LPS molecules are extracted in the water phase even though several factors, as the presence of hydrophobic residues, charged groups or the length of the polysaccharide chains, may modulate LPS solubility in water.

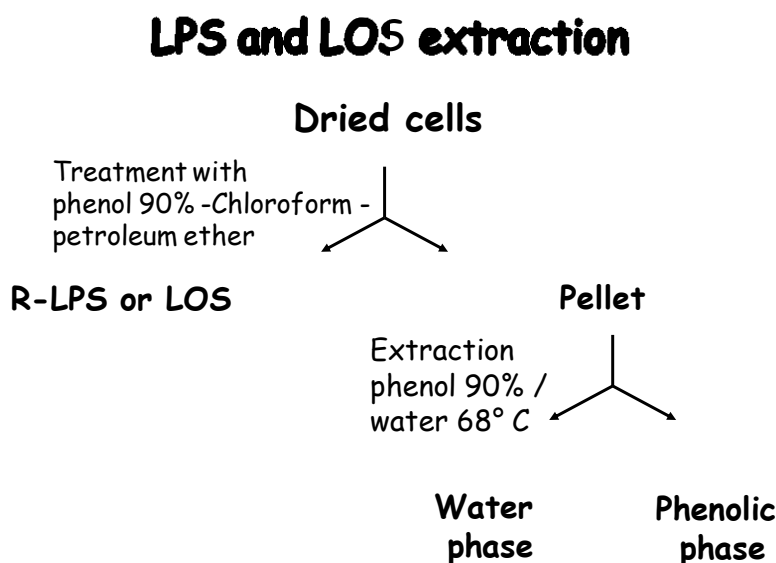


Fig.2.1 Schematic illustration of LPS and LOS extraction

Usually after extraction procedure, enzymatic treatments to remove protein and nucleic acid are performed. The classical protocol consists in LPS/LOS purification with nuclease (DNAse and RNAse) and protease and subsequent dialysis in order to remove the all digested material. In order to visualize the purification degree of the extracted phases, the LPS or LOS molecules are then detected through polyacrylamide SDS electrophoresis gel (PAGE) and stained with silver nitrate.

The electrophoresis analysis, using a denaturing agent, is highly informative and allows to define the typology of the extracted material: a ladder like profile is diagnostic of LPS molecules whereas the presence of material at bottom of the gel profile is related to LOS material. The amphiphilic nature of these molecules is responsible for their low solubility in both aqueous and organic solvents and renders the structural investigation a difficult task. For this reason, the single LPS domains are separately analyzed .

2.2 Structural characterization of LPS and LOS

2.2.1 Acid and alkaline degradations

In order to separate the lipid A fraction from the remaining part of molecule it is possible to execute, directly on LPS or LOS, a mild acid hydrolysis with acetic acid or acetate buffer at 100 °C. In this way the acid-labile ketosidic linkage of Kdo with the glucosamine of the lipid A moiety is selectively hydrolysed. This linkage is very labile for different reasons: 1) the absence of a whichever electron withdrawing group at position adjacent to anomeric (C-3 in this case since anomeric is C-2) favors the formation of the reaction intermediate oxonium carbocation; 2) the passage between chair to half-chair conformation is fastened by the presence of non substituted carbons (less eclipsed interactions in changing conformation; 3). the presence of an axial hydroxyl group at C-5 contributes to a steric energy release in the formation of intermediate carbocation.

After acid treatment the lipid A is precipitated while the polysaccharide or oligosaccharide remains in the supernatant fraction. In this way it is possible to obtain and separately study the glycolipid domain and the poly- oligosaccharides. In case of LPS, the supernatant is constituted by O-antigen still linked to core region, but this does not complicate the structural investigation since, in terms of sugar residues number, the contribute of the core fraction is negligible respect to the O-chain.

The acid treatment, discussed above, is largely used to characterize the O-chain fraction. Usually, to characterize the core region an alkaline degradation is applied because the LOS, after acid treatment, yields an oligosaccharide with a heterogeneous terminal residue (Kdo) that makes difficult the structural investigation of the core domain. The procedure consists in the treatment of LOS with anhydrous hydrazine to remove ester linked fatty acid. Successively, the *O*-de-acylated LOS is hydrolyzed with 4M KOH to remove the remaining amide linked fatty acid. The obtained sugar fraction is constituted by an oligosaccharide that comprises also the lipid A carbohydrate backbone and can be analyzed for its primary structure.

Once oligosaccharide and polysaccharide moieties are isolated, they are subjected to further investigations in order to determine their the primary structure.

Since the combination in which the sugar molecules can be linked are unlimited, the strategy requires combined approaches involving analytical, spectroscopic and spectrometric procedures that allow the determination of:

- the qualitative and quantitative composition of monosaccharide residues
- the absolute configuration of each monosaccharide
- the ring size of each monosaccharide
- the attachment points of the monosaccharides
- the anomeric configuration of each monosaccharide
- the sequence of monosaccharides
- the location of eventually present non-carbohydrates substituents

Additional information on the nature and the sequence of monomers can be obtained from selective cleavages of the polysaccharide (partial acid hydrolysis, acetolysis, periodate oxidation, alkaline degradation , various solvolysis).

2.2.2 Chemical analysis of LPS and LOS

Chemical analyses are very useful to obtain important preliminary information about primary structure of poly/oligosaccharides. The single monosaccharide can be visualized though Gas-Chromatography coupled with Mass-Spectrometry (GC-MS) prior specific derivatization. There are many methods useful to identify the monosaccharides type as well as their glycosylation position.

In order to elucidate the compositional analysis of poly/oligosaccharide, derivatization as peracetylated *O*-methyl glycosides (MGA) can be performed. This method is constituted by a first step of methanolysis with 1 M, 85°C MeOH/HCl and successive acetylation of free hydroxyl groups. The acetylated *O*-methyl glycosides are then injected to GC and identified by comparison with standard or to GC-MS and identified by the fragmentation pattern and the retention time.

An alternative and complementary approache typically used for compositional analysis of LPS and LOS leads to the formation of acetylated alditol derivatives. In this protocol the poly/oligosaccharide is hydrolyzed with 2M TFA followed by reduction of reducing monosaccharides with NaBD4 and acetylation. Derivatization with 2-(+)-octanol^[3] is used to identify the absolute configuration of monosaccharides. They are derivatized as peracetylated 2-(+)-

octyl-glycosides and injected to GC-MS and compared with standards of known absolute configuration.

The determination of the ring size and of the attachment point of the monosaccharides is performed via methylation analysis. This procedure consists in a complete methylation of polysaccharide and successive hydrolysis, reduction with NaBD₄, and acetylation. These partially acetylated methylated alditols are then subjected to GC-MS analysis. The position of the acetyl groups in the fragments accounts for the attachment point or for the position of cyclization of the pyranose or furanose ring. The methyl groups correspond to free positions, not involved in linkages. The reduction of the carbonilic function with sodium borodeuteride discriminates the fragments originated from the reduced position (even masses) from those originated from the last position (odd masses).

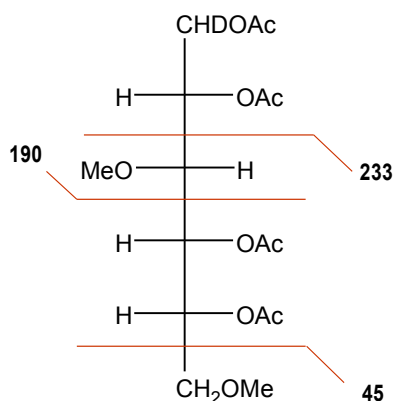


Fig.2.2 A 2,4 di-substituted glucose derivatized with AAPM protocol

Chemical analysis can be useful to determinate also the fatty acid composition in LPS and LOS. Fatty acid derivatized as methyl-ester can be easily analyzed on GC-MS. The procedure consists in the treatment of LPS or LOS with 4M HCl, followed by 4M NaOH, methylation with diazomethane and injection on GC-MS. The retention time and fragmentation pattern is used to determine the fatty acid.

2.2.3 Circular dichroism

The study of chiral molecules is very difficult because the enantiomers have identical chemical and physical properties in a symmetric (non-chiral) environment. For this reason, it can be very complicated to separate a couple of enantiomers as well as to investigate their absolute configuration. There are some spectroscopic techniques able to characterize the chiral components as polarimetry and circular dichroism (CD) methods; in particular, circular dichroic spectroscopy of optically active compounds is a powerful method for studying three-dimensional structures of organic

molecules. Namely, the method provides information on the absolute configuration, conformation, reaction mechanism, etc^[4]. these methods are based on the principle that chiral molecules are able to absorb (in the UV/visible region) in different way the two components (right and left) of circularly polarized light presenting in this way a different absorbance (and also different ϵ coefficients). In fact, a CD spectrum is composed by a graph with $\Delta\epsilon$ in function of wavelength (λ). In a wavelength region where the light is absorbed, the absolute magnitude of the optical rotation at first varies rapidly with wavelength, crosses zero at absorption maximum and then again varies rapidly with wavelength but in opposite direction. This characteristic change is called “Cotton effect” and its sign is defined by the first optical variation. In this frame, circular dichroism can be useful to investigate the absolute configuration of a particular sugar for which it is not possible to obtain a commercial standard. In particular, the “exciton chirality method” is largely applied for the determination of the absolute configuration of monosaccharides, opportunely derivatized with different chromophores. Usually, hydroxyl groups are commonly derivatized as esters with acids having appropriate aromatic chromophores (eg. benzoyl group). Dimethylaminobenzoate or *p*-bromobenzoate are easily accessible chromophores, absorbing in a generally non-interfering UV region (near 310 nm). With this kind of chromophores it is possible to define a simple correlation between the sign of split CD and the disposition of chromophores into the molecule. In fact, according to the Harada and Nakanishi’s Exciton Chirality Rule^[4], when the transition moments of the coupled chromophores are oriented to form a positive torsion angle (positive chirality), the system can be expected to exhibit a positive Cotton effect while when they are oriented to form a negative torsion angle (negative chirality), the Cotton effect is negative (Fig. 2.3). Thus, a couple of enantiomers will present identical CD spectra but with a opposite sign and in this is way it is easy to correlate the split CD sign with disposition of chromofores in chiral molecules and thus to its absolute configuration.

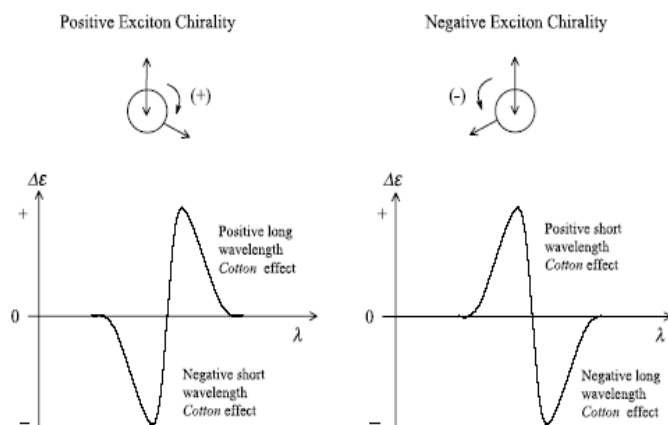


Fig. 2.3 Graphical illustration of the Exciton Chirality Rule that relates the torsion angle or helicity of two interacting electric dipole transition moments to the signed order of the CD Cotton effects

2.2.4 Mass-spectrometry

Mass spectrometry has become a powerful complementary method for structural analysis of lipopolysaccharides and lipooligosaccharides especially with the development of soft ionization techniques like MALDI (Matrix Assisted Laser Desorption Ionisation), ESI (ElectroSpray Ionisation), and the fragment analysis in MS/MS experiments. Usually, for carbohydrates, MALDI- and ESI MS spectra are performed in negative ion mode, due to the presence of the hydroxyl groups that can lose a proton and acquire a negative charge; nevertheless spectra in positive ion mode are also performed. The MALDI and ESI techniques show high sensitivity also at relatively high molecular mass and provides good spectra of intact molecular ions of lipopolysaccharides.

This methodology consists in a soft ionization of a sample that is suspended in a specific matrix that assists the analyte in ionization phenomenon. The matrix has different roles among which the protection of the sample from the laser energy assuring a soft ionization with formation of single charged ions. In case of LOS, the use of high laser power settings in MALDI spectra allows to obtain fragments due to the cleavage of the labile ketosidic linkage of the Kdo (see above). In the deriving spectra three regions of signals can be observed, the one of the lipid A, the core oligosaccharide and the intact LOS. In LPS, due to the dispersion of molecular weight of the O-polysaccharide, information on the size of the repeating unit can be deduced.

2.2.5 NMR spectroscopy

NMR spectroscopy yields the most complete picture of an oligo- and a polysaccharide structure and behaviour in solution. A combination of homo- and hetero-nuclear 2D-NMR experiment (DQF-COSY, TOCSY, NOESY, ^{13}P - ^1H HSQC, ^{13}C - ^1H HSQC, HMBC) are performed in order to assign all the spin systems, to determine the location and the nature of non-glycoside substituents and to characterize the sugar sequence. The evaluation of NMR chemical shifts and coupling constants are sufficient for the identification of the monosaccharide composition. The majority of the protons derived from the sugar bulk of non-anomeric and non-acylated protons are localised in a region comprises between 2.8-4.4 ppm. Anomeric signals appear in a spectral width of 4.4-5.8 ppm. $^1J_{\text{C1,H1}}$ and $^3J_{\text{H1,H2}}$ are diagnostic of the anomeric configuration. In sugar with the H-2 axial (glucose, galactose), a $^3J_{\text{H1,H2}}$ around 8 Hz is indicative of a β -configuration, whereas below 3 Hz of an α -configuration. Sugars with the H-2 equatorial (mannose) show both $^3J_{\text{H1,H2}}$ below 3 Hz. The $^1J_{\text{C1,H1}}$ values are also indicative of the anomeric configuration of pyranose rings, a $^1J_{\text{C1,H2}}$ below 165 indicates a β -anomer whereas above 170 Hz it indicates the presence a α -anomer. The down-field shift of carbon resonances (glycosylation shift) is a useful indication of the positions of glycosylation.

2.2.6 Two-dimensional NMR

Different sequences of bidimensional NMR spectra are largely applied to characterize the structure of oligo and polysaccharides. A combination of homo and heteronuclear 2D NMR experiments (DQF-COSY, TOCSY, HSQC, HMBC, ROESY and NOESY) are performed in order to identify and characterize the spin systems and to localize non-carbohydrate substituents as well as to define the monosaccharide sequence. The proton resonances obtained by COSY and TOCSY spectra are used to assign the spin system and to attribute the carbon resonances in the HSQC spectrum. The *inter*-residual NOE contacts, obtained by NOESY and ROESY experiments, and long range HMBC correlations are very useful to identify the complete sequence of monoses in the poly and oligosaccharides.

Furthermore, the *intra*-residual NOE contacts together with $^3J_{\text{H,H}}$ of the ring protons are fundamental to establish the relative configuration of sugars (e.g. *gluco* or *manno* configuration). NOESY and ROESY spectra are very useful in confirming the *intra*-residue assignment and the anomeric configuration. In fact, in β -configured sugars H-1 gives *intra*-residue NOE effect with H-3 and H-5, in α -configured only with H-2. ^{31}P NMR and ^1H - ^{31}P HSQC allow to localization of the phosphorylation sites.

2.2.7 Lipid A structural investigation

The lipid A may be obtained directly from LPS and LOS with the protocol discussed above (see paragraph 2.2), that consists in a selective hydrolysis of the linkage between Kdo and a GlcNII of lipid A backbone. The glycolipid part is recovered by precipitation or by direct extraction with a specific solvent mixture (e.g. chloroform/methanol/water in different proportions). The complete chemical characterization of lipid A requires the determination of:

1. the sugar backbone
2. the amide and the ester linked fatty acids
3. the distribution of the acyl chains on the sugar backbone
4. the polar heads and their location
5. if present, phosphate substituents and their location

Usually MALDI-TOF and ESI techniques executed on intact and partially degraded lipid A are very useful to define the heterogeneity, e.g. the number of different species of lipid A families and the distribution of fatty acids on the saccharide backbone. The MALDI or ESI spectra on intact lipid A gives information about the number of lipid A species present in the fraction as well as the presence of polar heads (phosphate groups). In order to investigate the distribution of acyl residues on GlcN units, hydrazine treatment and ammonium hydroxide hydrolysis can be executed^[5]. The treatment with hydrazine yields complete *O*-deacylated species. The MALDI spectra carried out on *O*-deacylated lipid A are useful to understand the composition of fatty acid present in amide linkage.

The hydrolysis with ammonium hydroxide is a general and easy methodology to obtain the secondary fatty acid distribution. The procedure exploits the lower stability, under mild alkaline conditions, of acyl and acyloxyacyl esters with respect to that of acyloxyacyl amides. The ammonium hydroxide hydrolysis selectively splits acyl and acyloxyacyl esters, leaving the acyl and acyloxyacyl amides unaffected, thus by this approach not only all the amide-linked groups are revealed but also the acyloxyacyl amides.

MALDI spectra can be executed in positive and negative mode. In positive mode it is possible to visualize also peaks corresponding to oxonium ions, fundamental to differentiate the fatty acid distribution between the two GlcN of lipid A.

The NMR investigation is very important to completely define the lipid A backbone. The amphiphilic nature of lipid A is an obstacle for its solubility in many solvent systems. Sometimes, a different mixture of deuterated solvents with different polarity degree is successful to dissolve the lipid A, as chloroform/methanol or chloroform/methanol/water. Several lipid A have a good

solubility in DMSO-d₆ at relatively high temperature (40 °C). The selection of DMSO as a finer solvent for lipid A seems a good way out of the preparation of complicated mixtures of deuterated solvents and no degradation occurs in these conditions. Furthermore, the solvent and water signals fall neither in the anomeric nor in the sugar ring region of the ¹H-NMR spectrum, allowing easier assignation of all key resonances. In addition, the non exchanged amide protons in the deshielded region of the spectrum are a good alternative starting point to assign all signals of the intact lipid A species. Also in this case, a combination of homo and heteronuclear 2D NMR spectra (DFQ-COSY, TOCSY, HSQC, HMBC, ROESY and NOESY) are performed in order characterize the lipid A backbone, to determinate the localization of non-sugar substitutes as well as to define the monosaccharides sequence. The identification of acylation sites is performed by analysis of proton chemical shift values. In fact, the downfield shift of ring proton signals (acylation shift) is useful to determine O- and N-acylation sites. O-phosphorylated protons undergo a similar down-field shift.

References

1. Galanos C, Luderitz O, Westphal O. A new method for the extraction of R lipopolysaccharides. *Eur. J. Biochem.* (1969) **9**:245-249.
2. Westphal O, Jann K. Bacterial lipopolysaccharides: extraction with phenol-water and further applications of the procedure. *Methods Carbohydr. Chem.* (1965) **5**:83-91
3. Leontein K, Lonngren J. Determination of absolute configuration of sugars by Gas-Liquid Chromatography of their acetylated 2-octyl glycosides. *Methods Carbohydr. Chem.* (1978). **62**: 359-362.
4. Harada N, Nakanishi K. Circular dichroic spectroscopy exciton coupling in organic chemistry. (1983).
5. Silipo A, Lanzetta R, Amoresano A, Parrilli M, Molinaro A. Ammonium hydroxide hydrolysis: a valuable support in the MALDI-TOF mass spectrometry analysis of lipid A fatty acid distribution. *J. Lipid. Res.* (2002) **43**: 2188-2195.

Chapter 3

Structural elucidation of LPS from *Burkholderia rhizoxinica*

Section I

3.1 *Burkholderia rhizoxinica*

The genus *Burkholderia* comprising more than 30 species refers to a group of virtually ubiquitous gram-negative, motile, obligately aerobic rod-shaped bacteria including both animal/human and plant pathogens as well as some environmental bacteria, and inhabits diverse ecological niches and have been isolated from soil, water, plants, insects, industrial settings, hospital environments and from infected humans. Several *Burkholderia* strains have attracted considerable interest from the biotechnological and agricultural industry for bioremediation of recalcitrant xenobiotics, plant growth promotion, and biocontrol purposes. The use of *Burkholderia* species for agricultural purposes (such as biodegradation, biocontrol and as plant-growth-promoting rhizobacteria) is subject to discussions because of pathogenic effects in immuno-compromised people (especially CF-sufferers), e.g., hospital acquired infections.

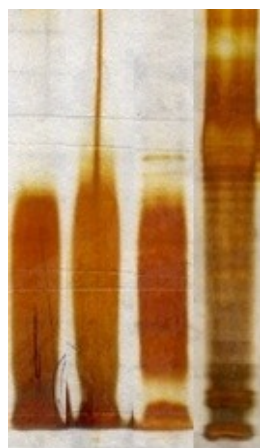
Burkholderia rhizoxinica is an endosymbiotic, that is, intracellular living bacterium isolated from plant pathogenic fungi belonging to the genus *Rhizopus* responsible for causing rice seedling blight. This plant disease is typically initiated by an abnormal swelling of the seedling roots without any sign of infection by the pathogen. This characteristic symptom is caused by the macrocyclic polyketide metabolite rhizoxin that has been isolated from cultures of *Rhizopus* sp. Owing to its remarkably strong antimetabolic activity in most eukaryotic cells, including various human cancer cell lines, rhizoxin has attracted considerable interest as a potential antitumour drug. Recently, the group of Prof. C. Hertwech^[1] has shown that rhizoxin is not biosynthesized by the fungus itself, but by the endosymbiotic *Burkholderia rhizoxinica*. These findings unveil a remarkably complex symbiotic-pathogenic relationship that opens new perspectives for pest control. This symbiotic bacterium/fungus system represents a unique example of a mutualistic life form in which a fungus harbours endobacteria for production of a phytotoxin, the rhizoxin, that exerts its destructive effect by binding to rice β -tubulin, which results in inhibition of mitosis and cell cycle arrest^[2]. Moreover, Hertwech et al.^[1] reported the unexpected observation that in absence of endosymbionts the host is not capable of vegetative reproduction, a form of asexual reproduction that takes place through reproductive structures called spores produced by specific organ (sporangia). In fact, formation of sporangia and spores is restored in the host only after reinfection of endobacteria. Notably, genetic studies demonstrated that the fungal host became resistant to rhizoxin because there is a mutation in the tubulin sequence^[3]. Still, it is a mystery how the endobacteria can survive within fungal host cells and how they interact with their host by ways of chemical recognition and communication^[4].

Given the above premises we wanted to understand if the LPS from *Burkholderia rhizoxinica* is one of the molecular determinants in the interaction of the organism with the fungus and play a role in the symbiotic relationships and in the adaptation to the host. Therefore, we have determined the structure of the LPS from two wild type strains (**B1wt** and **B4wt**) that were isolated from different variants of *Rhizopus* fungi and the LOS from O-antigen ligase mutant of **B1 wt**. The structural elucidation of LPS and LOS has been carried out by a combination of state-of-art spectroscopic analyses on intact and chemically modified LPS.

3.2 Structural characterization of LPS from *Burkholderia rhizoxinica* B1wt

3.2.1 LPS extraction and preliminary analysis

The LPS from B1wt was extracted directly from dried cells using PCP and phenol/water method as previously described (see paragraph 2.1). The Sodium Dodecyl Sulfate gel electoforesis (SDS-PAGE) analysis indicated the presence of LPS in all extracted phases (Fig. 3.1). Chemical analyses showed the presence of a single monosaccharide residue, 2-substituted galactofuranose, suggesting an homopolymeric structure of the O-chain fraction. There were also present, in minor amount, heptose and Kdo, belonging to the core region. The absolute configuration of the galactose residue was deduced from GLC-MS analysis comparing the peracetylated (+)-2-octyl glycosides of galactose with standard^[5] and it resulted to be D.



Line: 1 2 3 4

Figure 3.1 SDS PAGE 13.5 % on PCP (1), phenol (2) and water (3) phases. Line 4 is LPS from *E. coli* as standard

3.2.2 Full characterization of O-chain from LPS of *Burkholderia rhizoxinica* wild type

The LPS was hydrolyzed using mild acid conditions and the O-polysaccharide fraction (PS), purified by gel permeation chromatography, and investigated by a combination of mono- and bidimensional NMR analyses in particular COSY, TOCSY, NOESY, HSQC and F2-coupled HSQC. The ^1H NMR spectrum showed a single anomeric signal indicative of a single-spin system, which was fully assigned by homonuclear 2D NMR spectroscopy, whereas by HSQC spectrum it was possible to assess the furanosidic nature and anomeric configuration of the monosaccharide. These data, in conjunction with chemical analysis, revealed that the PS was consistent with a homopolimeric structure. Chemical shift values are shown in Table 1.

Spin system **A** was identified as a 2-substituted- β -galactofuranose residue. The anomeric configuration was assigned on the basis of C1 chemical shift and $^3J_{\text{H}_1, \text{H}_2}$ coupling constants, whereas the values of vicinal $^3J_{\text{H}, \text{H}}$ ring coupling constants allowed the identification of the relative configuration of hydroxyl groups within the sugar residue^[6]. The evident downfield shift of all carbon signals indicated the presence of a furanose residue and in particular the downfield displacement of the C-2 signal in the HSQC spectrum (figure 3.2 and Table 1) evidently indicated glycosylation at O-2 as confirmed by the H1-H2 NOE contact present in the ROESY spectrum (Figure 3.3). In summary, all chemical and NMR data allowed to establish the structure of PS of the LPS from *B. rhizoxinica* as the following:



Table 1 Chemical shift values of ^1H and ^{13}C of β -(1 \rightarrow 2)-D-Galf polymer

Unit	1	2	3	4	5	6
H	5.18	4.04	4.12	3.89	3.75	3.60/3.58
C	107.5	89.4	76.7	83.5	71.6	64.0

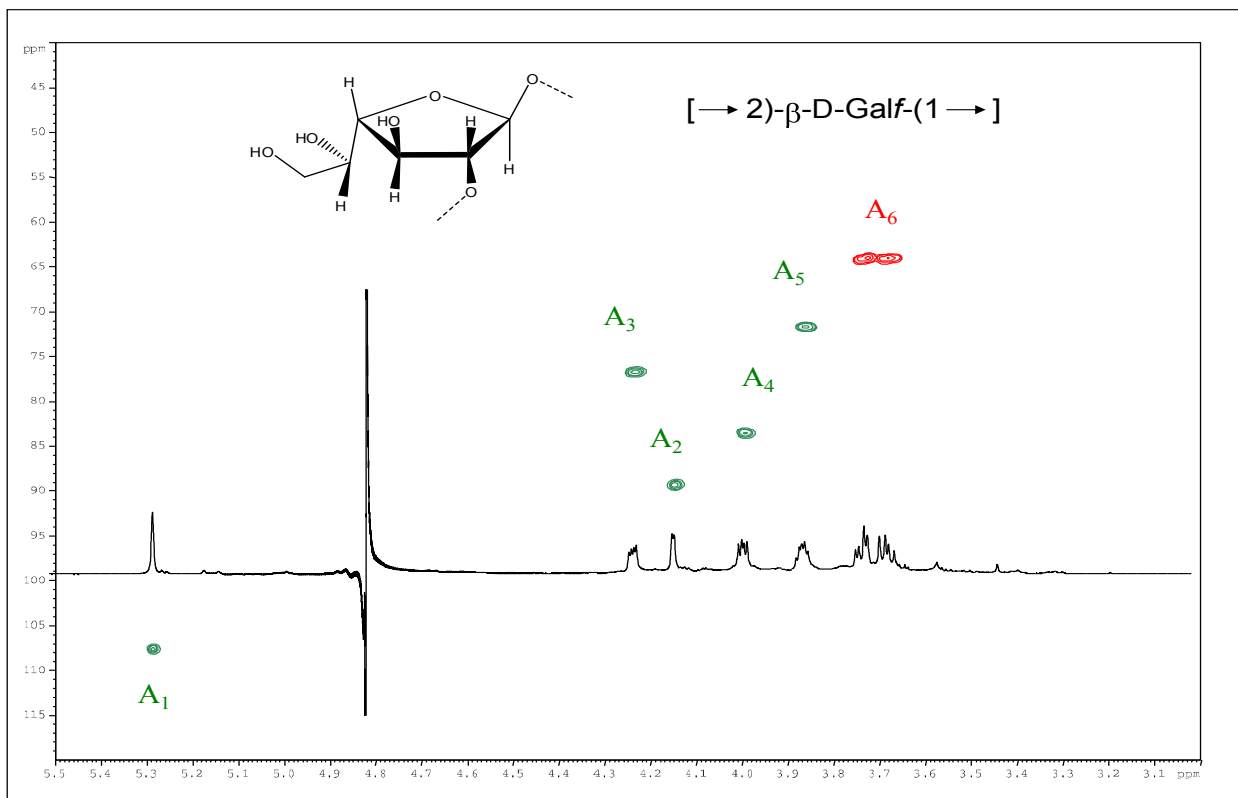


Figure 3.2. ^1H , ^{13}C HSQC spectrum of the O-chain from *B. rhizoxinica* LPS with all cross peaks assignments.

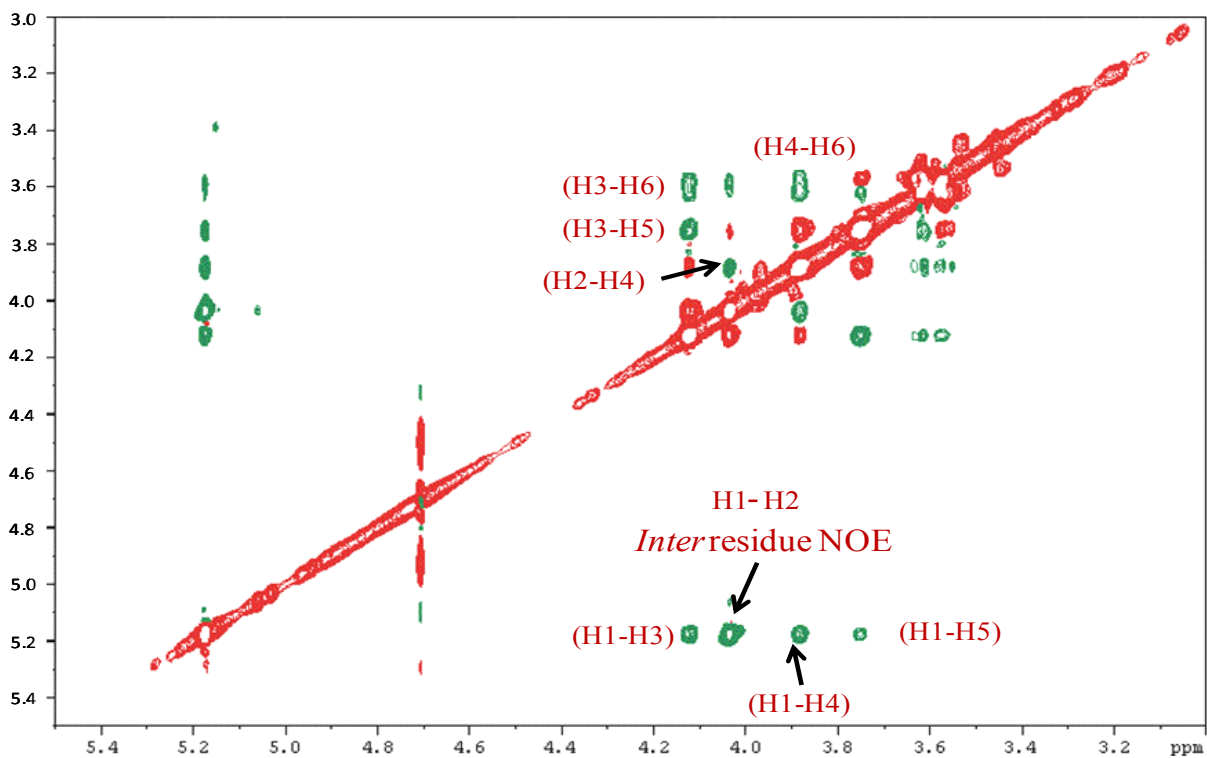


Figure 3.3. ROESY spectrum of the O-chain from *B. rhizoxinica* wt

3.3 Full characterization of LOS from *Burkholderia rhizoxinica* WaaL mutant

In order to investigate the role of this O-chain in both innate immune system and in symbiosis process, the group of prof. Hertwech identified genes responsible for LPS biosynthesis by whole genome shot-gun sequencing of *Burkholderia rhizoxinica* (Fig.3.4 A). Notably, they identified an encoded protein annotated as UDP-galactopyranose mutase (Glf) that together with UDP-glucose 4 epimerase (GalE) are responsible of formation of the LPS building block UDP-D-gactofuranose (Fig.3.4 B). The gene cluster contained several glycosyl-transferase genes and two genes (wzm and wzt) for an ABC transporter system that shuttles membrane-anchored O-antigen chains from the cytosol to the periplasm prior to ligation to the core oligosaccharide. Finally, a *waaL* gene that encodes for a ligase, responsible for the transfer of polymeric O-antigen to the outer core, was identified. An O-antigen ligase mutant ($\Delta waaL::Kan^r$) was created in order to prove the functional assignment of *waaL* and to investigate the lipooligosaccharide (LOS) structure. The obtained mutant presented the expected rough colony phenotype, suggesting the presence of a lipooligosaccharide (LOS) as confirmed by SDS-PAGE experiments (Fig. 3.5). The LOS structure was investigated by means of chemical analysis, mass spectrometry and NMR spectroscopy.

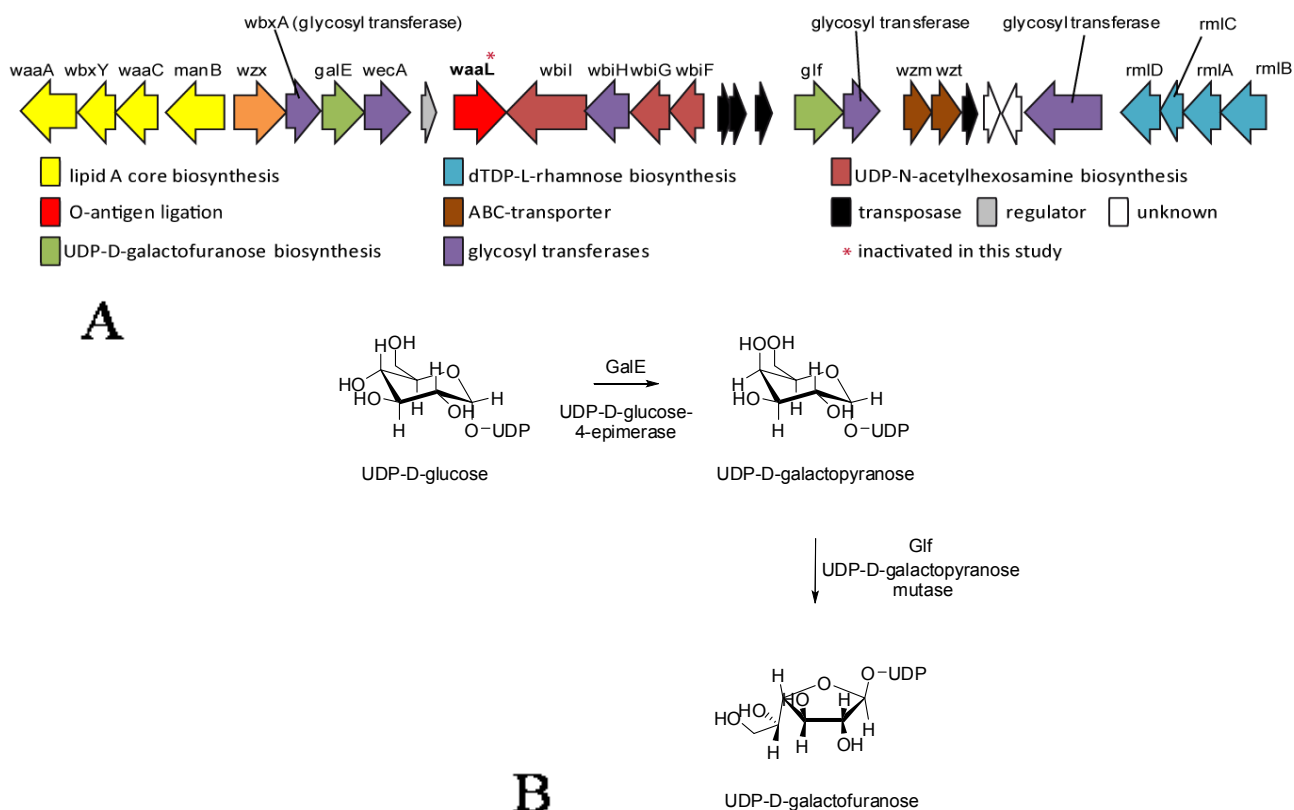
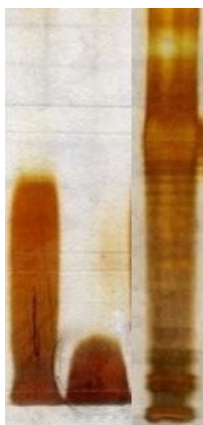


Fig.3.4 (A): Whole genome shot-gun sequencing of *Burkholderia rhizoxinica*; **(B):** biosynthesis of UDP-D-gactofuranose.



Line: 1 2 3

Fig. 3.5 Electrophoresis gel 13,5 % on LPS from B1wt (1), LOS from B1mut (2); Line 3 is LPS from *E.coli* as standard.

3.3.1 NMR characterization of oligosaccharide fraction of LOS from *Burkholderia rhizoxinica waaL mut.*

The oligosaccharide (OS) fraction was obtained from a mild acid hydrolysis with acetate buffer. Monosaccharide analysis on isolated OS molecule revealed the presence of: *L-glycero-D-manno*-heptose (L,D-Hep), 2-amino-2-deoxy-D-galactose (D-GalN), L-rhamnose (L-Rha), D-glucose (D-Glc), 3-deoxy-D-*manno*-oct-2-ulosonic acid (Kdo), D-*glycero-D-talo*-oct-2-ulosonic acid (Ko). Methylation analysis showed the presence of terminal GalN_p, 3-substituted Rha_p, 6-substituted Glc_p, 3,4-substituted Hepp, 3,7-substituted Hepp, terminal Hepp, 4,5-substituted Kdo, terminal Ko. This fraction was analysed through homo- and heteronuclear 2D NMR experiments (DQF-COSY, TOCSY, ROESY, ¹H-¹³C HSQC, ¹H-¹³C HSQC-TOCSY and ¹H-¹³C HMBC) in order to assign all the spin systems and to define the monosaccharide sequence. The fraction analyzed was constituted by a blend of oligosaccharide species characterized by high heterogeneity due to the presence of the Kdo as reducing end, which, in addition, could be present as lactone ring.

It was possible to identify seven major anomeric signals (spin systems **A-G**, Fig.3.6, Table 2), while the signals at 1.94/2.05 ppm were attributed to the H-3 methylene protons of the major α-pyranoside form of the Kdo residue. Spin systems **A**, **B**, **C** and **D** were all identified as α-heptose residues, as indicated by their ³J_{H1,H2} and ³J_{H2,H3} coupling constants (below 3 Hz) and by the *intra*-residual NOE of H-1 with H-2. The ¹³C chemical shift values of C-6 of these heptose residues (all below 71 ppm) confirmed these as *L-glycero-D-manno*-heptose residues. The downfield values of

resonance of C-3 and C-4 of **A** and C-3 and C-7 of **B** indicated glycosyl substitution at these positions. The spin system **C** and **D** resulted to be both terminal units.

Residue **E** (H-1 at 4.81 ppm) was recognized as an α -rhamnose residue, since the TOCSY spectrum showed scalar correlations of the ring protons with methyl signals in the shielded region at 1.18 ppm. Its *manno* configuration was established by the $^3J_{H1,H2}$ and $^3J_{H2,H3}$ values (both below 3 Hz). The α -configuration was assigned by the *intra*-residual NOE contact of H-1 with H-2 and chemical shift of their H-5 and C-5. The chemical shifts of C-3 was evidently displaced downfield because of glycosylation.

Spin system **F** (H-1 4.48 ppm) was identified as 2-deoxy-2-amino-galactose, as indicated by its $^3J_{H3,H4}$ and $^3J_{H4,H5}$ values (3 Hz and 1 Hz, respectively) diagnostic of a *galacto*-configuration. The ^1H - ^{13}C HSQC spectrum showed the correlation of H-2 (4.06 ppm) with a nitrogen bearing carbon signals at 50.9 ppm. The down-field shift of proton resonances of H-2 was diagnostic of *N*-acetylation at these positions. The chemical shifts of H-1 and C-1 (4.60 and 102.4 ppm), the $^3J_{H1,H2}$ value (8.2 Hz) and the *intra*-residual NOE contact of H-1 with H-3 and H-5 evidenced a β -anomeric configuration of the **F** residue.

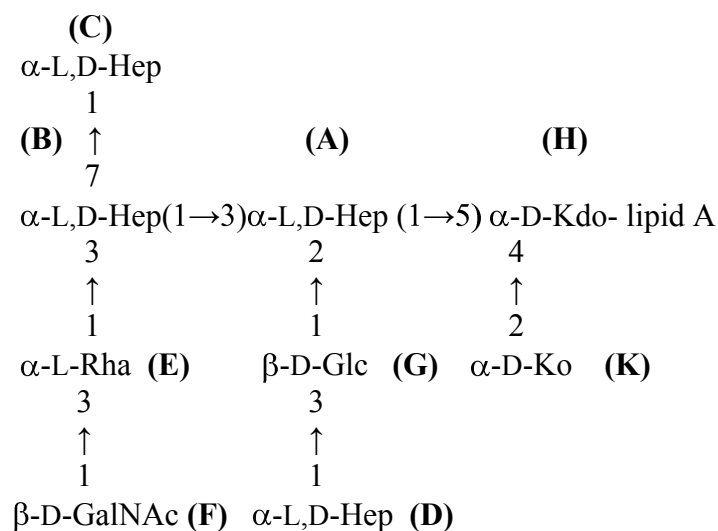
Spin system **G** (H-1 at 4.47 ppm) was identified as glucose residue, as indicated by the large $^3J_{H,H}$ values of the ring protons (above 10 Hz). The chemical shifts of H-1 and C-1 of residue **G** (4.47 and 102.1 ppm respectively), the $^3J_{H1,H2}$ value (8.2 Hz) and the *intra*-residual NOE contact of H-1 with H-3 and H-5 evidenced a β -anomeric configuration for this residue. The downfield chemical shift of C-6 carbon for residue **G** was in agreement with glycosylation at this position.

Because of its free reducing end, the Kdo residue **H** was present in multiple isomeric forms, nevertheless the signals belonging to the α -pyranose reducing unit were clearly assignable starting from the diastereotopic H-3 methylene proton signals, resonating at 1.94 and 2.05 ppm (H-3_{ax} and H-3_{eq}, respectively).

Residue **K** (α -Ko) was assigned starting from its oxymethine H-3 signal at 3.81 ppm. The *talo* and the anomeric configuration of Ko were assigned by the analysis of vicinal $^3J_{H,H}$ coupling constants from the DQF-COSY, and by the comparison with published data^[7].

The oligosaccharide sequence was established evaluating all the inter-residual NOE contacts identified in the NOESY spectrum (Fig. 4.7) and the long range scalar correlations present in the HMBC spectrum. The linkage of the heptose **A** to O-5 of Kdo **H** was proven by the NOE connectivity between H-1 of the heptose **A** (5.15 ppm) and H-5 of Kdo (4.12 ppm). Residue **A** was

in turn substituted at O-3 and O-4. The NOE contacts of H-4 and H-3 **A**, with H-1 of residue **G** (4.30 ppm) showed that the O-4 of α -heptose **A** was glycosylated by residue **G** of β -glucose. This latter residue **G** was glycosylated by the terminal α -heptose residue **D** as attested by the NOE contact between H-1 **D** with H-6_{a/b} **G**. Residue **A** was also substituted at O-3 by α -heptose **B**, according to the NOE effect of H-3 **A** with H-1 **B** (5.14 ppm). Residue **B** was also glycosylated at O-7 by the terminal α -heptose **C**, as attested by the NOE contact between H-1 **C** and H-7 **B**. Additionally, residue **B** was glycosylated at position 3 by the α -Rha **E** as proven by the NOE contact between H-1 of residue **E** and H-3 of residue **B**. Residue **E** was in turn substituted by the terminal α -GalNAc **F** residue at its O-3 as attested by the NOE effect between H-1 **F** and H-3 **E**. From the 2D NOESY and ROESY experiments *inter*-residue NOE contacts between H_{3eq} of Kdo moiety **H** and H-6 of Ko (**K**) were also visible that were diagnostic for the α -D-Ko-(2 \rightarrow 4)- α -D-Kdo linkage. In summary, methylation and NMR analyses allowed to establish the oligosaccharide sequence reported below:



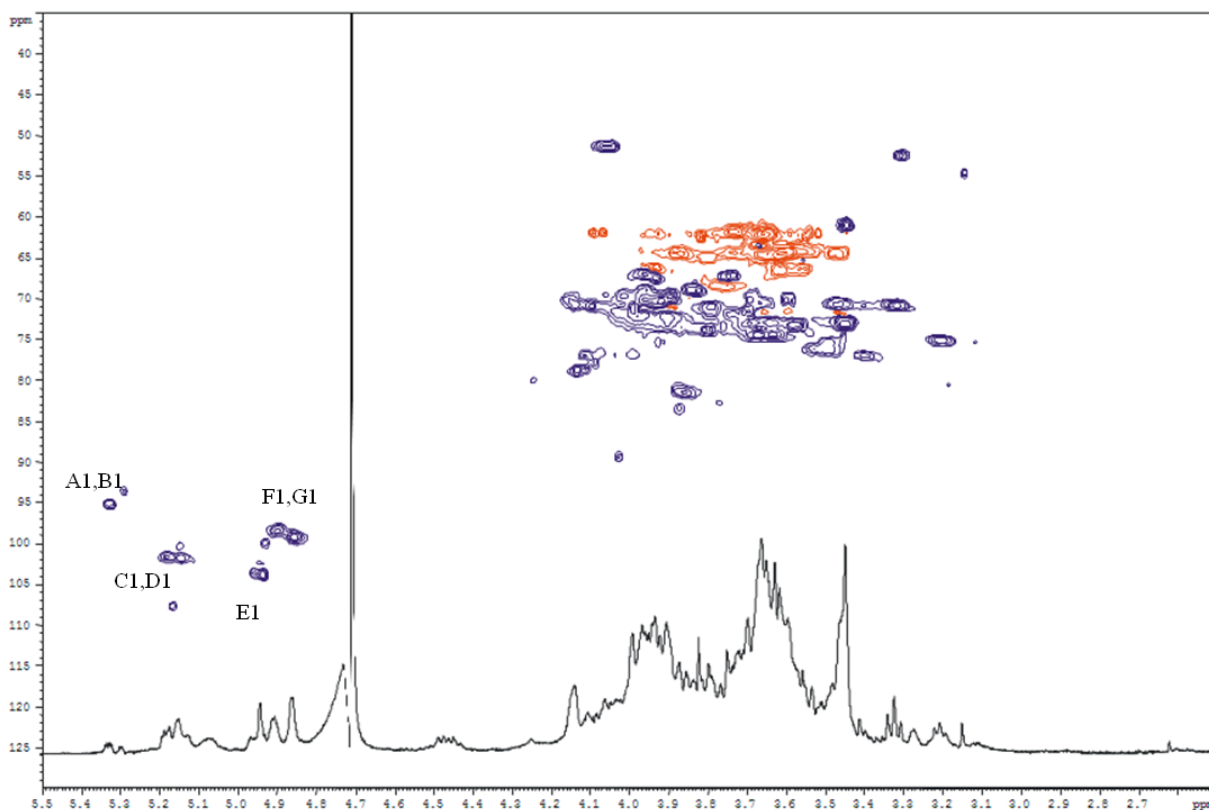


Fig.3.6 ^1H spectrum overlapped to ^1H , ^{13}C HSQC spectrum of the core region from *B. rhizoxinica* mutant

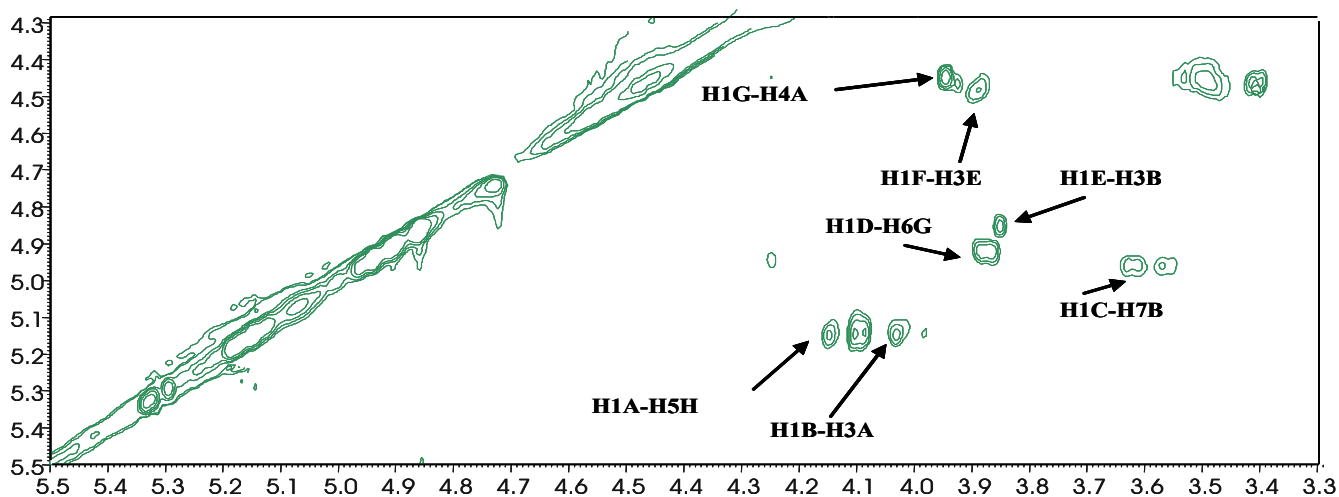


Fig.3.7 Zoom of the NOESY spectrum of the Core region from *B. rhizoxinica* mutant in which the relevant *inter* glycosydic NOE effect are shown

Table 2 Chemical shift values of ^1H and ^{13}C of sugar residues belonging to the core region of the LOS from *Burkholderia rhizoxinica waaL* mutant.

Chemical shift δ ($^1\text{H}/^{13}\text{C}$)								
Unit	1	2	3	4	5	6	7	8
A	5.16	4.13	3.99	3.94	3.62	3.85	3.66/3.57	
3,4- α -Hep	99.0	70.6	74.5	74.2	72.8	68.8	61.7	
B	5.15	4.14	3.88	3.85	3.79	3.79	3.62/3.56	
3,7- α -Hep	99.0	70.2	77.8	69.2	70.4	66.4	70.73	
C	4.94	3.84	3.94	3.89	3.56	4.06	3.52/3.58	
t- α -Hep	101.4	70.0	70.1	71.5	71.8	68.6	62.8	
D	4.91	3.82	3.71	3.71	3.51	4.06	3.52/3.59	
t- α -Hep	101.27	69.9	70.3	70.5	71.6	69.9	62.9	
E	4.86	3.99	3.88	3.32	4.02	1.18		
3- α -Rha	99.2	70.6	77.4	71.9	70.3	16.6		
F	4.48	3.95	3.66	3.99	3.51	3.58/3.67		
t- β -GalNAc	102.4	50.9	71.3	71.9	75.01	60.8		
G	4.44	3.15	3.34	3.28	3.56	3.82/3.87		
6- β -Glc	102.3	73.5	75.6	70.5	72.0	65.3		
H	---	---	3.81	3.87	3.95	3.54	3.92	3.59/3.83
t- α -Ko	---	---	70.8	68.8	70.2	72.3	70.4	63.7
K	---	---	1.94/2.05	3.99	4.12	3.68	3.90	3.61/3.79
4,5- α -Kdo	---	---	33.8	71.6	68.4	71.6	71.8	63.7

3.3.2 Structural characterization by MALDI mass spectrometry of the intact LOS from *Burkholderia rhizoxinica* B1 mut

The intact LOS molecule was analyzed by MALDI-MS in order to gain further information on both lipid A and core regions without any chemical manipulation. The negative ion MALDI mass spectrum of intact LOS is shown in Fig. 3.8. The spectrum presented fragments between m/z 1575

and 1932, originating from the β -cleavage of the glycoside bond between Kdo and the lipid A moiety. Moreover, a single OS oligosaccharide ion peak was found at m/z 1734.4 (Fig.3.8) and exactly consistent with the above core oligosaccharide structure described by NMR spectroscopy. The ion peak at m/z 1575.1 (**L1**) was identified as lipid A with a tetra-acylated bis-phosphorylated disaccharide backbone carrying one Ara4N residue and in ester linkage one 14:0 (3-OH) and in amide linkage two 16:0 (3-OH) acyl chains, one of which, on the GlcN II, was further substituted by a secondary 14:0 fatty acid. Peaks at m/z 1670.3 (**L2**), m/z 1800.8 (**L3**), and m/z 1932.0 (**L4**) were consistent with the penta-acylated lipid A carrying two ester-linked 14:0 (3-OH) with one and or two Ara4N residues respectively. The ion peaks that range from m/z 3310.7 to 3665.3 represented a LOS moieties with the combination of lipid A species (**L1**, **L2**, **L3**, **L4**) and the core oligosaccharide.

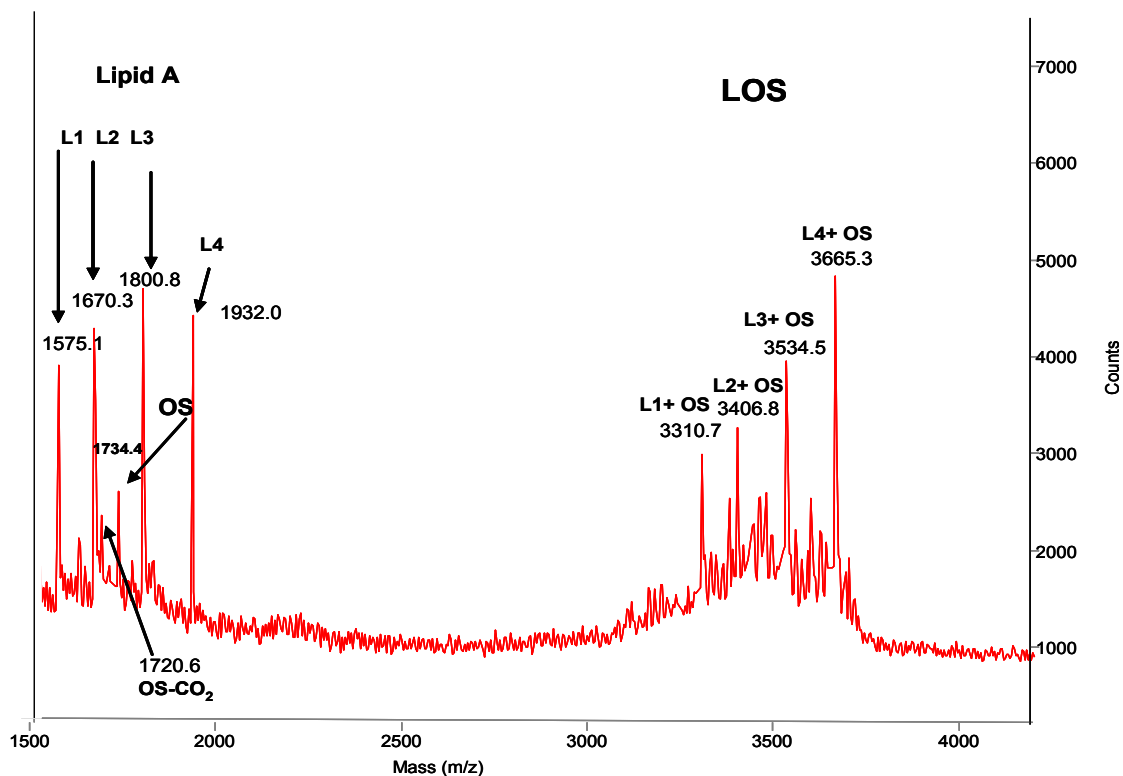


Fig. 3.8 Negative-ion MALDI mass spectrum of intact LOS

3.4 Biological activity of *Burkholderia rhizoxinica* strain B1wt and WaaL mutant

In order to establish a relation between structural data and biological activity, the two strains of *Burkholderia rhizoxinica* strain B1wt and waaL mutant were checked for their bioactivity. The biological testes consist in a sporulation assay in order to check if both endosymbiont were capable of initiate a stable symbiosis. Thus, the pure cultures of *B. rhizoxinica* (wild-type and mutant) were

mixed with endosymbiont-free (cured) *R. microsporus* cultures and the sporulation behavior was monitored over time both on agar plates and in liquid culture by using 48-well plates (Fig.3.9). Six cultures were observed in parallel and each experiment was repeated four times to calculate mean values and standard deviations.

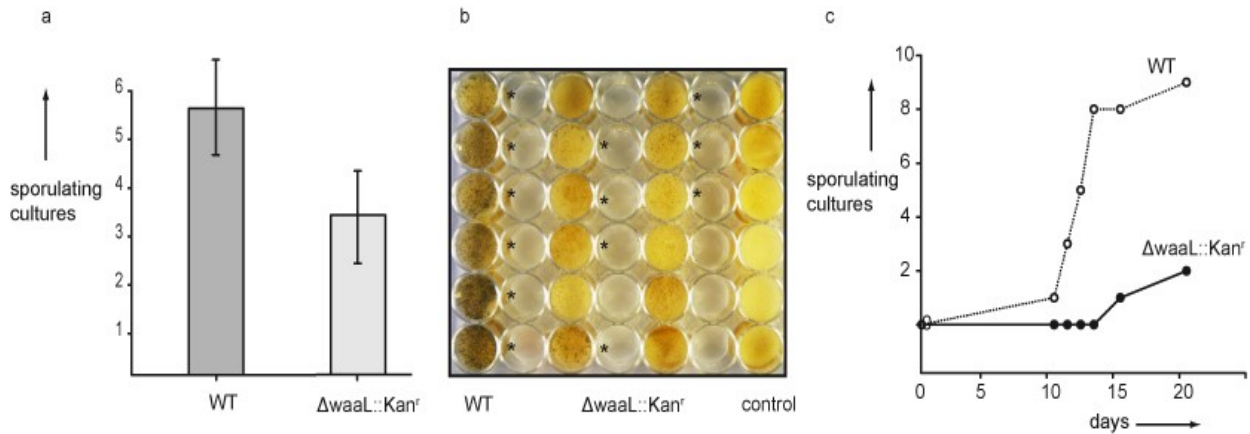


Fig.3.9 Sporulation and reinfection assay **a**: Bar charts illustrate reinfection/sporulation rates in liquid cultures. (error bars). **b**: Photograph of a completed reinfection/sporulation experiment (liquid culture): Sporulating cultures are marked with asterisk. Negative controls (endosymbiont-free *R. microsporus*) do not sporulate. **c**: Reinfection experiment on agar plate observed over time.

In the experiments co-cultivation with wild type bacteria resulted in high successful reinfection while the *waaL* mutant showed a significantly reduced reinfection and sporulation rates^[4]. It means that the endosymbionts need the presence of LPS O-polysaccharide chain domain in order to establish a correct symbiosis with host fungus.

Discussion

In summary, we have completely characterized the LPS and the LOS produced by the endosymbiont *Burkholderia rhizoxinica* strain B1. The lipid A moiety possessed a carbohydrate backbone characterized by a [P→4-β-D-GlcpN-(1→6)-α-D-GlcpN-1→P→] sequence and revealed to be constituted by a mixture of penta and tetra acylated species carrying a non-stoichiometric presence of two Ara4N units. The lipid A is further glycosylated by a Kdo unit that is in turn substituted at O-5 with a Ko residue. The presence of Ko monosaccharide is limited to few bacterial LPS, like *Acinetobacter*^[8], *Yersinia*^[9] and *Serratia*^[10]. The core oligosaccharide consists of a nonasaccharide backbone comprising four heptose (Hep) residues, a GalNAc, a Glc, a Rha, a Kdo, and a Ko unit. The core oligosaccharide structure of *B. rhizoxinica* LOS strictly resembles the one from *B. multivorans*^[11] especially for what concerns the inner core and the presence of a further

heptose residue attached to the β -Glc. The outer core is different but still coherent with LOS structures from *Burkholderia* spp^[12]

The analysis of O-chain fraction from *Burkholderia rhizoxinica* strain B1 revealed the presence of a homopolymer of [2- β -Gal f]_n. This polysaccharide is completely new respect to the O-chain from other known *Burkholderia* species and related bacteria. The discovery of poly-D-galactofuranose chains in an endofungal bacterium is particularly intriguing since Gal f conjugates are especially abundant in cell wall of filamentous fungi and, furthermore, structurally related galactofuranan bioactive polysaccharides have been identified in fungi^[13,14]. These observations suggest that the biosynthesis of this particular O-antigen is a strategy used by bacteria to mimic the fungi-self structure in order to avoid the immune system response. This process is referred to as “molecular mimicry” and there are many other example in which pathogenic bacteria mimic structural components of the host cell. For example, beneficial bacteria inhabiting mammalian intestines decorate their surface with fucose, which is an abundant surface molecule of intestinal epithelial cells^[4].

In order to investigate the biological role of the O-chain, the complete genomes sequence of LPS biosynthesis was performed. The sequence shown a couple of genes responsible to encode a UDP-galctopyranose mutase (Glf) and a UDP-glucose 4 epimerase (Gale), that form the LPS building block UDP-D-gactofuranose. In addition of this, the cluster encoded an O-antigen ligase (*waaL*), required for transfer of polymeric fraction to the outer core. Thus, it was created an O-antigen ligase mutant ($\Delta waaL::Kan^r$) and the LOS produced was structurally investigated.

The strains wt and its *waaL* mutant were subjected to biological assays in order to confirm the molecular mimicry process that we have proposed. In normal conditions, when preparations of *Burkholderia rhizoxinica* wild type are injected in cured fungi, they are capable to reestablish the symbiosis and the fungus start to sporulate again. It means that we can use the sporulation assay like a test in order to understand if bacteria establish a correct symbiosis with the fungus. Therefore the sporulation assay was executed on both strains and the results showed that the B1wt strain reinfected the cured fungi and sporulated with higher level with respect to B1 *waaL* mutant. These observations demonstrated that the O-chain fraction is indispensable for bacteria to establish the symbiosis process since it mimics the fungus self structure in order to escape the response by the fungus immune system. In summary, we clarified the role of the LPS in this peculiar bacteria/fungus system that constitutes a unique example of symbiosis in which the fungus use endosymbiont bacterium to exert its pathogenic activity.

Section II

3.5 Structural elucidation of LPS from *Burkholderia rhizoxinica* strain wt B4

Burkholderia rhizoxinica strain wt B4 is an endosymbiont of an other isolated plant pathogenic fungus, *Rhizopus microsporus* var. *microsporus*. Also in this case the endosymbiont is capable to biosynthesise, during the mutualistic life form instauration, a phytotoxin, constituted by the rhizoxin and their derivatives that present a great antimetabolic activity. Particularly, the bacterial cells of *Burkholderia rhizoxinica* strain B4 were recovered directly from pathogenic fungus and grown in Tryptic Soy Broth in specific conditions of temperature (see Paragraph 6.1). In this section the results from chemical elucidation of LPS from *Burkholderia rhizoxinica* strain B4 were presented.

3.5.1 LPS Extraction and preliminary analysis

The LPS extraction was carried out directly on dried cells with hot phenol/water method (see chapter 2.1). The SDS-PAGE analysis (not shown) revealed that the LPS was present mainly in the watery phase. Compositional analysis of the polysaccharide revealed the presence of 2-substituted and 3-substituted Rhamnose (Rha) and 3-substituted N-acetyl Glucosamine (GlcNAc). There were also present, in minor amount, Glucose, Heptose and Kdo that belonged to the core fraction. In order to recover the polysaccharide fraction we carried out a mild acid hydrolysis with acetate buffer at pH 4.4 to selectively cleave the glycosidic bond between Kdo and GlcNII of lipid A. The isolated O-chain was purified by gel-filtration chromatography (Sephadex S-100) and two fractions were recovered and investigated.

3.5.2 Full characterization of the O-chain from LPS of *Burkholderia rhizoxinica* strain B4

The two fractions obtained from gel-filtration chromatography were analysed with mono and bidimensional NMR experiments.

The ^1H spectrum of the second fraction (Fig. 3.10) contained three different signals in the anomeric region suggesting a trisaccharide repeating unit. All ^1H and ^{13}C chemical shifts of each spin system were assigned by homo- and heteronuclear NMR spectra.

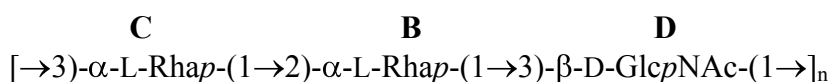
Spin systems **B** (H1-C1 5.17/100.13 ppm) and **C** (H1-C1 4.97/102.71 ppm) were respectively identified as 2-substituted and 3-substituted α -rhamnose residues as testified by the downfield chemical shift of carbon 2 and 3 and in accordance with chemical analysis. Their *manno* configuration was established by the $^3J_{\text{H1,H2}}$ and $^3J_{\text{H2,H3}}$ values (both below 3 Hz). The α -

configuration was assigned by the *intra*-residual NOE contact of H-1 with H-2 and chemical shift of their H-5 and C-5. (Table 3)

The chemical shift value of C-2 at 56.41 ppm of residue **D** (4.90/101.17 ppm) suggested the presence of a nitrogen bearing carbon signal. The down-field shift of proton resonance of H-2 **D** was diagnostic of *N*-acetylation at this position. The $^3J_{H,H}$ values of the ring protons (above 10 Hz) and the *intra*-residual NOE contact of H-1 with H-3 and H-5 evidenced a β -anomeric configuration for this residue that was identified as a β -GlcNAc substituted at position 3 as confirmed by the glycosylation shift at carbon 3.

The monosaccharide sequence in the O-chain repeating unit was defined through *inter*-residual NOE contacts (Fig. 3.11) and long range correlations present in HMBC spectrum. In particular, the strong *inter*-residual NOE contacts of H1 **B** with H3 of residue **D** demonstrated that the O-3 of **D** unit was glycosylated by residue **B** of α -rhamnose. Residue **B** was in turn substituted at O-2 by residue **C** of α -rhamnose as demonstrated by the NOE connectivity between H-2 of rhamnose **B** and H-1 of rhamnose **C**. Finally, H-3 of rhamnose **C** showed a strong NOE contact with the anomeric position of residue **D** of β -GlcNAc indicating that the O-3 of rhamnose **C** was glycosylated at this position by residue **D**.

Thus, the NMR data were in accordance with the following repeating unit:



Comparing ^1H spectra of the two fractions isolated by size exclusion chromatography (figure 3.10) it was possible to note that in the first one there was an additional anomeric signal, spin system **A**, identified as a 2-substituted rhamnose that also constituted a homopolimeric repeating unit of $[\alpha\text{-}(1\rightarrow 2)\text{-L-Rhap}]_n$ as confirmed by the strong NOE contact of the anomeric proton with H-2 (Fig.3.12).

In summary, all NMR data suggested that the LPS from *Burkholderia rhizoxinica* strain B4 is built up of two different O-polysaccharide chain:



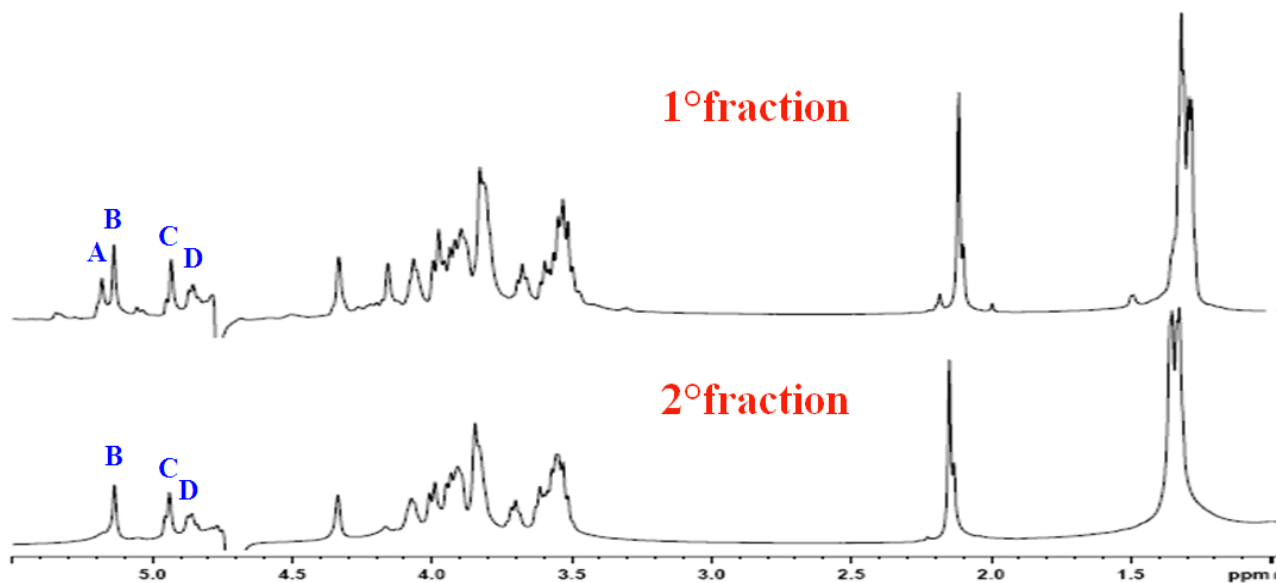


Fig. 3.10 ^1H NMR spectra of two fractions from gel-filtration chromatography.

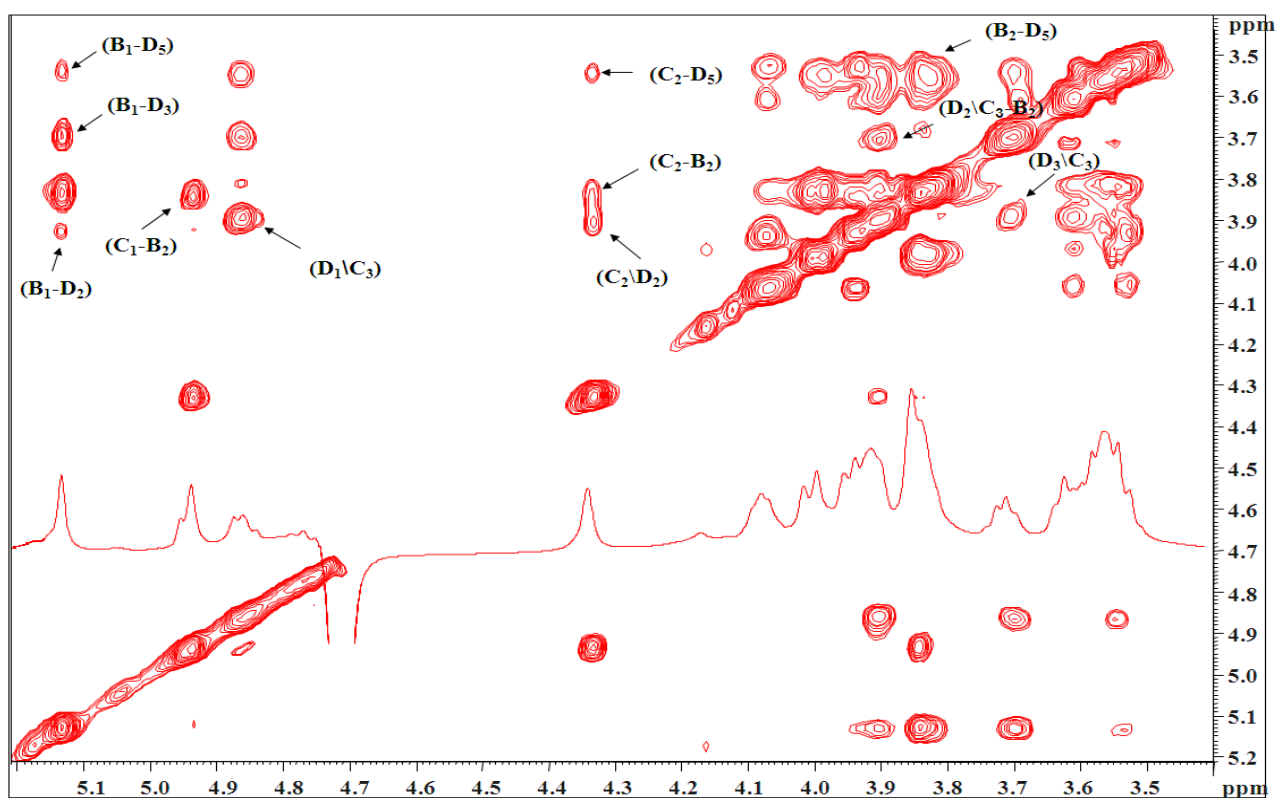


Fig. 3.11 Section of NOESY of second fraction. Monosaccharide labels are as indicated in Table 3. The relevant *inter*-residue NOE cross-peaks are indicated.

Table 3 Chemical shift values of ^1H and ^{13}C of sugar residues belonging to the O-chain fraction from *Burkholderia rhizoxinica* strain B4

Unit	1	2	3	4	5	6
A	5.21	4.20	3.99	3.60	3.85	1.39
2- α -Rha	101.2	78.6	70.4	71.4	69.7	17.3
B	5.17	3.88	3.97	3.56	4.11	1.36
2- α -Rha	100.1	80.6	70.4	72.7	69.6	17.3
C	4.97	4.36	3.94	3.60	3.85	1.39
3- α -Rha	102.7	70.2	80.4	71.4	69.7	17.3
D	4.9	3.95	3.66	3.64	3.58	4.04/3.87
3- β -GalNAc	102.2	56.4	82.0	69.1	76.2	61.2

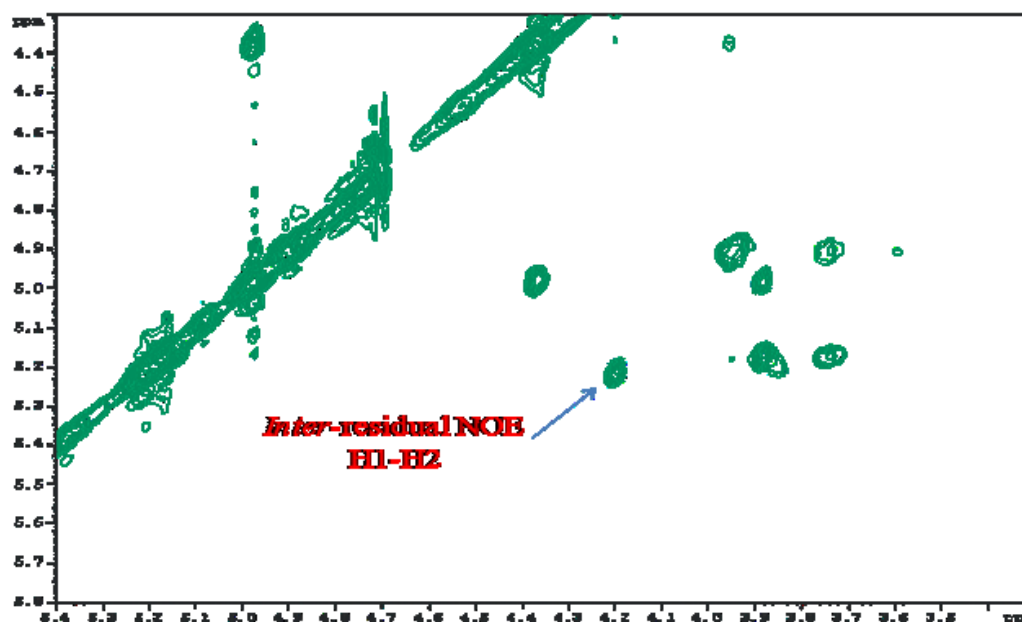


Fig. 3.12 Section of NOESY of first fraction

3.6 Structural elucidation of lipid A from *B. rhizoxinica* strain B4

As discussed in paragraph 3.3 of section I, lipid A was characterized by a combination of chemical analysis and MALDI mass spectrometry. The lipid A fraction was recovered by a mild acid

hydrolysis. Chemical analyses showed the presence of 6-substituted-GlcN and terminal-GlcN, both in D-configuration and terminal-4-amino-4-deoxy-arabinose with L-configuration. The negative ion MALDI spectrum is shown in Fig.3.13. In analogy with lipid A structures from *Burkholderia*^[15] even in this case the classical β -(1 \rightarrow 6)-GlcN_p carbohydrate backbone was phosphorylated at the α -anomeric position of the reducing GlcN and at O-4 of the non-reducing β -GlcN. At these phosphate groups β -Ara4N residues were attached through a phosphodiester linkage.

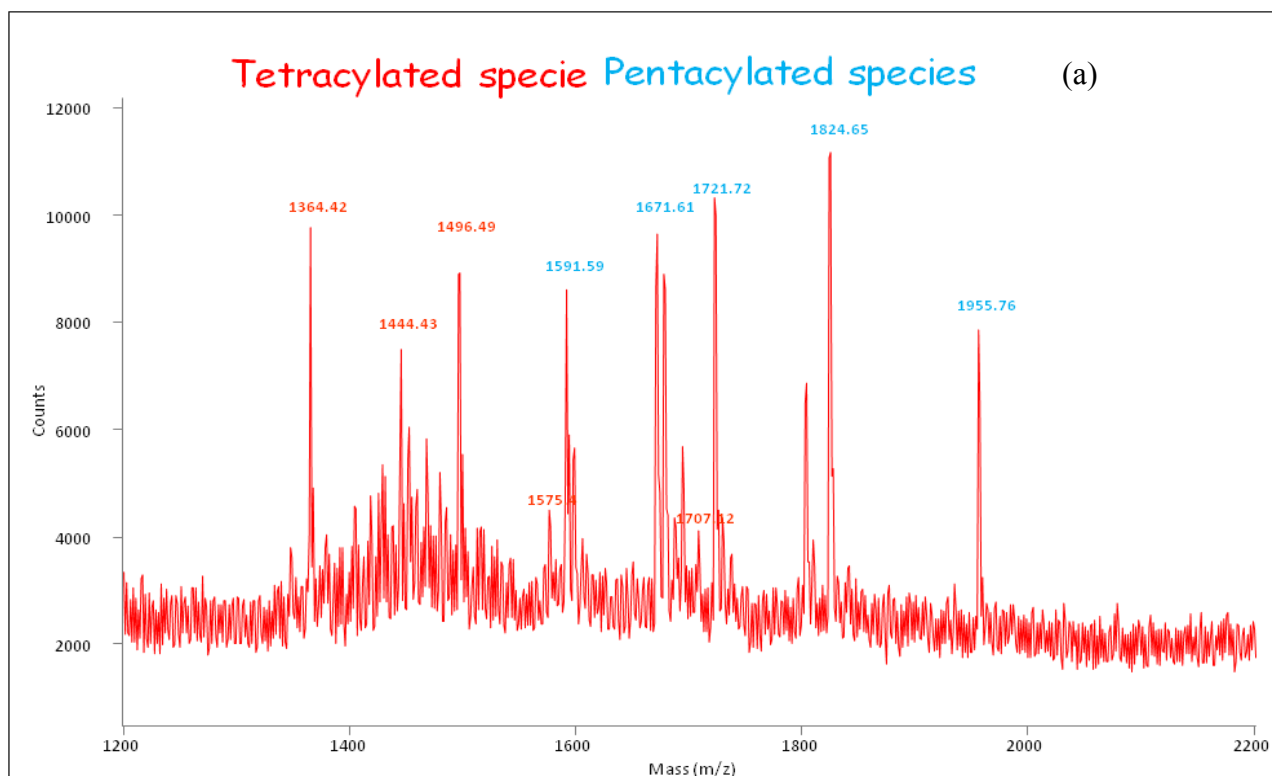
The peaks at m/z 1364.4 and 1444.43 (specie 1 and 2) were identified both as tetra-acylated lipid A, mono and *bis*-phosphorylated respectively, possessing in ester linkage one 14:0 (3-OH) and one 14:0 residues, and in amide linkage two 16:0 (3-OH) residues. The specie at 1496.49 m/z (specie 3) corresponded to tetra-acylated lipid A, that carried an additional L-Ara4N residue respect to the specie 1. The peaks at 1591.75 and 1671.89 m/z (specie 4 and 5) corresponded to a penta-acylated lipid A, mono and *bis*-phosphorylated respectively, that carrying two 14:0 (3-OH) and one 14:0 residues in ester linkage, and two 16:0 (3-OH) residues in amide linkage. The ion at 1721.9 and 1824.65 $[M+Na^+]$ m/z (specie 6 and 7) were identified as penta-acylated species with an additional L-Ara4N respect to the specie 4 and 5 respectively. In the spectrum, a non negligible amount of specie 8 at 1955.7 m/z was also present and identified as $[M+Na^+]$ adduct, *bis*-phosphorylated, pentacylated carrying two Ara-4N units. The positive-ion mode MALDI mass spectrum showed two oxonium ions. In particular, the ion m/z 933.8 could be ascribed to a triacylated GlcN II oxonium ion carrying one 14:0 (3-OH), one 14:0, and a 16:0 (3-OH) residues, whereas the ion at m/z 1064.8 carried an additional Ara4N.

An aliquot of lipid A fraction was then selectively de-*O*-acylated by treatment with NH₄OH and then analyzed via MALDI MS. This approach allowed the location of the amide-bound acyloxyacyl moieties, left unaltered by this mild hydrolysis. The ion-negative MALDI spectrum of de-*O*-acylated lipid A (Fig.3.14) showed two pattern of peaks corresponding to a mixture of tri- and tetra-acylated lipid A. The ion at 1138.19 m/z (specie 9) was consistent with a tri-acylated lipid A, monophosphorylated that possessed two primary fatty acid (16:3OH) in amid linkage and one secondary fatty acid (14:0) in ester linkage. The peak at 1269.13 m/z possessed an additional Ara-4N respect to the specie 9. Both species were present in low amount as *bis*-phosphorylated form (+80). The ion at 1442.50 m/z was attributed at tetracylated lipid A, *bis*-phosphorylated with an additional 14:0 (3-OH) residue with respect to species 10. A small ion peak at 1574.92 m/z was present in the spectrum and it corresponded to tetra-acylated structure *bis*-phosphorylated with a Ara-4N residue linked to the phosphate group.

All the data allowed to identified the classical *Burkholderia* lipid A existing as mixture of differently acylated and phosphorylated species as illustrated in table 4.

Table 4 Proposed fatty acid and carbohydrate composition of the main ion peaks of the MALDI -MS spectrum

Observed ion (<i>m/z</i>)	Acyl substitution	Proposed fatty acid, phosphate and carbohydrate composition
1364.42.0	Tetra-acyl	1 x 14:0 (3-OH), 2 x 16:0 (3-OH), 1 x 14:0, , 1P
1444.43	Tetra-acyl	1 x 14:0 (3-OH), 2 x 16:0 (3-OH), 1 x 14:0, 2P
1469.51	Tetra-acyl	1 x 14:0 (3-OH), 2 x 16:0 (3-OH), 1 x 14:0, 1P, 1 x Ara4N
1591.59	Penta-acyl	2 x 14:0 (3-OH), 2 x 16:0 (3-OH), 1 x 14:0, 1P
1671.61	Penta-acyl	2 x 14:0 (3-OH), 2 x 16:0 (3-OH), 1 x 14:0, 2P
1721.72	Penta-acyl	2 x 14:0 (3-OH), 2 x 16:0 (3-OH), 1 x 14:0, 1P, 1 x Ara4N
1824.65	Penta-acyl	2 x 14:0 (3-OH), 2 x 16:0 (3-OH), 1 x 14:0, 1 x Ara4N, 2P, Na ⁺
1955.76	Penta-acyl	2 x 14:0 (3-OH), 2 x 16:0 (3-OH), 1 x 14:0, 2 x Ara4N, 2P, Na ⁺



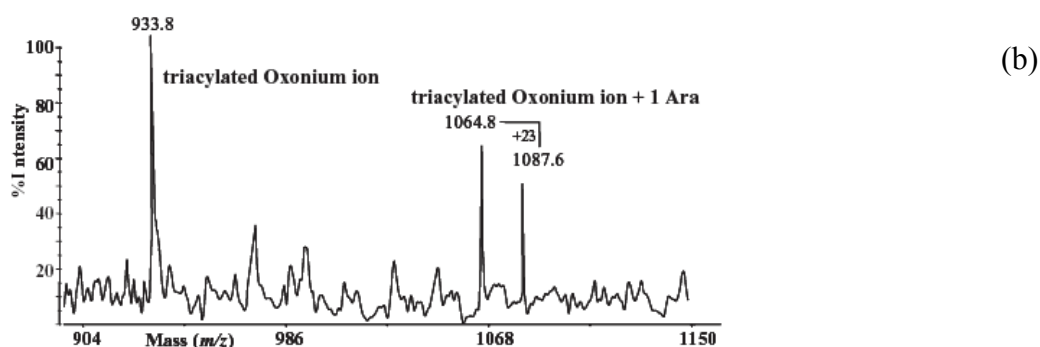


Fig.3.13 (a) Ion-negative MALDI spectrum of lipid A from *Burkholderia rhizoxinica* strain B4. The m/z values marked in red are referred to a tetracylated species with different degree of phosphorylation and substitution of Ara-4N. Pentacylated species are instead marked in blue. (b) Section of the positive-ion MALDI mass spectrum of the same product in which two oxonium ions are visible.

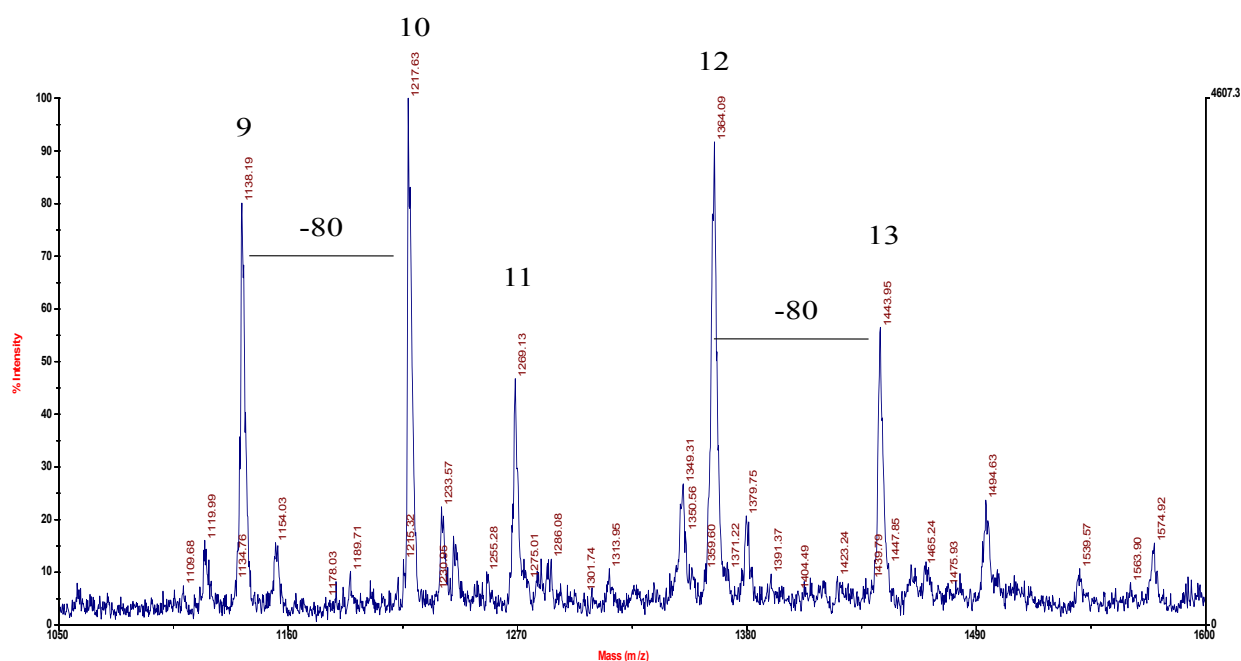


Fig.3.14 Negative MALDI spectrum of NH_4OH treated lipid A from *Burkholderia rhizoxinica* strain B4.

Discussion

We have here reported the chemical characterization of the LPS from *Burkholderia rhizoxinica* strain B4. The O-chain domain was constituted by a mixture of two different polysaccharides. The first one was a homopolymer of 2-substituted α -L-Rhap; the other was formed by a heteropolysaccharide with a repeating unit of $[\rightarrow 3)\text{-}\alpha\text{-L-Rhap-(1}\rightarrow 2)\text{-}\alpha\text{-L-Rhap-(1}\rightarrow 3)\text{-}\beta\text{-D-GlcpNAc-(1}\rightarrow]_n$. Usually O-chains isolated from *Burkholderia* genus are rather simple structures with few sugars constituting the repeating unit very often containing 6-deoxysugar (typically L-rhamnose), It was demonstrated that the presence of these deoxy-sugars increases the hydrophobicity of polysaccharide and this has been deemed to play a key role in bacterial interaction with host recognition system e.g., in plant innate immunity^[15]. The biosynthesis of two different O-chain polysaccharides in Gram-negative bacteria is not so common, even though is usual for *Burkholderia* spp.^[16]. *B. cariphilly*^[17,18], *B. cepacia*^[18], *B. vietnamensis*^[18] *B. multivorans* C1576^[19] are all remarkable examples of *Burkholderia* bacteria that biosynthesize a mixture of different LPS O-chain.

The lipid A fraction from *Burkholderia rhizoxinica* strain B4 was constituted by a mixture of tetra and pentacylated species, mono or bisphosphorylated and with one or two residues of Ara4N. The presence of one or two residues of Ara4N is very usual for the lipid A from *Burkholderia* species. This constitute an expedient used by bacteria to avoid the attack from host-released cationic antimicrobial peptides and from different classes of antibiotic molecules

In order to understand the molecular basis of the microbe-bacteria interaction and to clarify the LPS roles in both plant immune system and in symbiosis process, further studies will be performed on mixture of characterized polysaccharides including conformational analysis as well as biological assays.

References

1. Partina Martinez LP, Monajembashi S, Greulich KO, Hertweck C, *Current Biology* (2007) **17**:773-777.
2. L. P. Partida-Martinez, C. Hertweck, *Nature* (2005) **437**: 884-888.
3. Schmitt I, Partida-Martinez LP, Winkler R, Voigt K, Einax A, Wöstemeyer J, Hertweck C. *ISME J.* (2008) **2**: 632-641.
4. Leone, M. R.; Lackner, G.; Silipo, A.; Lanzetta, R.; Molinaro, A.; Hertweck C.; *Angewandte Chemie* (2010). **49**: 7476 –7480
5. König H, Herald C, Varma A, *Prokaryotic cell wall*, chapter 4 : 133-15 Leontein K, Lonngren J. Determination of absolute configuration of sugars by Gas-Liquid Chromatography of their acetylated 2-octyl glycosides . *Methods Carbohydr. Chem* (1978). **62**: 359-362.
6. Costantino V, Fattorusso E, Imperatore C, Mangoni A. *Eur. J. Org. Chem.* (2001) **23**: 4457-4462.
7. Silipo, A. Molinaro, T. Ieranò, A. De Soyza, L. Sturiale, D. Garozzo, C. Aldridge, P. A. Corris, C. M. A. Khan, R. Lanzetta, M. Parrilli, *Chemistry* (2007), **13**, 3501-3511
8. Vinogradov EV, Müller-Loennies S, Petersen BO, Meshkov S, Thomas-Oates JE, Holst O, Brade H, *Eur. J. Biochem.* 1997, **247**: 82– 90.
9. Vinogradov EV, Lindner B, Kocharova N A, Senchenkova S N, Shashkov A S, Knirel Y A, Holst O, Gremyakova TA, Shaikhutdinova R Z, Anisimov A P, *Carbohydr. Res.* 2002, **337**:775 – 777.
10. Vinogradov EV, Lindner B, Selmann G, Radziejewska-Lebrecht J, Holst O, *Chem. Eur. J.* 2006, **12**: 6692 – 6700.
11. Ieranò T, Silipo A, Sturiale L, Garozzo D, Brookes H, Khan CMA, Bryant C, Gould FF, Corris PA, Lanzetta R, Parrilli M, De Soyza A, Molinaro A, *Glycobiology* 2008, **18**: 871.
12. De Soyza A, Silipo A, Lanzetta R, Govan JR, Molinaro A, *Innate Immun.* 2008, **14**: 127.
13. Latge JP, *Med. Mycol.* 2009, **47**,: S104.
14. Corsaro MM, De Castro C, Evidente A, Lanzetta R, Molinaro A, Mugnai L, Parrilli M, Surico G, *Carbohydr. Res.* 1998, **308**: 349.
15. De Soyza A, Silipo A, Lanzetta R, Govan JR, Molinaro A. Chemical and biological features of *Burkholderia cepacia* complex lipopolysaccharides. *Innate Immunity* (2008) **14**: 127-144.
16. Vinion-Dubiel AD, Goldberg JB, *Journal of Endotoxin Research* 2003, **9(4)**, 201-213
17. Adinolfi M, Corsaro MM, De Castro C, Evidente A, Lanzetta R, Molinaro A, Lavermicocca P, Parrilli M. *Carbohydrate Research* (1996) **284**: 119-133.
18. Vinion-Dubiel AD, Goldberg JB, *Journal of Endotoxin Research* (2003) **9**: 201-213.

19. Ieranò T, Silipo A, Cescutti P, Leone MR, Rizzo R, Lanzetta R, Parrilli M, Molinaro A. *Chemistry-A European Journal* (2009) **15**: 7156-7166.

Chapter 4

Structural elucidation of lipid A from *Burkholderia cepacia* strain ASP B 2D

4.1 introduction

Burkholderia cepacia ASP B 2D is an endophytic bacterium belonging to the *Burkholderia* genus, that comprises more than 30 species, including both mammalian and plant pathogens as well as some environmental bacteria (see chapter 3). Strain of *Burkholderia* are naturally found in river sediments and in the most areas of soil around the roots of plants. Some strain of *Burkholderia* have been implicated as biological control of plants diseases and bioremediation, while other strains are recognized as phytopathogens or human opportunistic pathogens^[1].

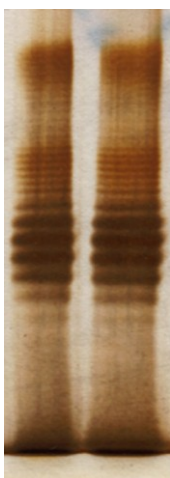
It was amply shown that LPS from *Burkholderia cepacia* can be recognized as MAMPs (Microbe Associated Molecular Pattern, see chapter 1) inducing a plant defense-related response also if the MAMP-active eliciting part(s) of LPSs have not yet been fully investigated. Furthermore, there are many observations in accordance with the idea that lipid A is the inducing part of LPSs due to the overall chemical architecture of lipid A that is conserved in Gram-negative bacterial LPSs^[2,3,4]. Concerning the lipid A domain, several structure/biological activity relationships have been indentified in animals that include the number and location of acyl chains, the overall charge of the lipid A molecule, i.e. phosphorylation of the disaccharide backbone and presence of further polar heads^[5,6,7,8]. The chemical composition, structure and conformation of lipid A are important because influence the pathogenesis of bacteria as well as the their adaptation to host environment.

Conversely, the role of lipid A in plant immune system is less studied. Some studies showed that lipid A is an agonist of plant defense responses while others show a contrary, antagonist effects. For example, lipid A from *Xanthomonas campestris* has been shown to induce both PR1 and 2 (Pathogenesis Related proteins 1 and 2, see paragraph 1.5.1) in *Arabidopsis thaliana*^[9]. On the other hand, lipid A from *Sinorhizobium meliloti* suppresses the oxidative burst in host plants (*Medicago sativa* and *M. truncatula*) and *Nicotiana tabacum*^[10,3]. Due to the limited number of lipid A structures determined from plant-associated bacteria, it is no possible to clearly correlate the structure of lipid A to its biological activity. Here we have investigated the chemical structure of lipid A from *Burkholderia cepacia* ASP B 2D in order to extend the knowledge about its biological activity in plant immunity system as well as about the molecular basis of LPS perception in plants.

4.2 Chemical characterization of lipid A structure

The LPS was isolated from dried cells with phenol/water extraction (see Par. 2.1) and it was identified in the water phase as confirmed by sodium dodecyl sulfate (SDS)–polyacrylamide gel electrophoresis (PAGE) (Fig.4.1). After enzymatic treatment with DNase, RNase, Protease-K, the LPS was dialyzed and subjected to the gel permeation chromatography (Sephacryl S100). The lipid

A moiety was isolated from LPS with a mild acidic hydrolysis and the glycolipidic fraction was recovered as precipitate by centrifugation. The results from chemical analysis revealed the presence of 6-linked-GlcN and terminal-GlcN, both in D-configuration, 4-amino-4-deoxy-arabinopyranose with L-configuration, and phosphate. Fatty acid analysis showed the presence of (*R*)-3-hydroxyhexadecanoic (16:0(3-OH)) in amide linkage and (*R*)-3-hydroxytetradecanoic (14:0(3-OH)) and tetradecanoic acid (14:0) in ester linkage. We have determined the lipid A structure with the combination of chemical degradations, NMR analyses and the use of negative/positive-ion matrix assisted laser desorption ionization (MALDI) mass spectra on native and opportunely degraded lipid A.



Line: 1 2

Fig.4.1 Electrophoresis gel 13,5 % on purified LPS (in both lanes 1 and 2) from *Burkholderia cepacia* strain ASP B 2D showing the banding pattern of the repeating units of the O-antigen.

4.2.1 NMR spectroscopy of lipid A

A combination of homo- and heteronuclear NMR experiments was performed in DMSO, at 343K, on the *O*-deacylated lipid A aiming at the definition of the carbohydrate backbone, phosphorylation and acylation sites. All assignment of ^{13}C , ^1H and ^{31}P resonances were performed with DQF-COSY, TOCSY, ROESY, ^{13}C - ^1H and ^{31}P - ^1H HSQC spectra. The NMR data were in accordance with the presence of the typical $[\beta\text{-D-GlcpN-(1}\rightarrow\text{6)-}\alpha\text{-D-GlcpN}]$ disaccharide backbone with a variety of acyl chains that resulted in a heterogeneous mixture of species. The presence in non-stoichiometric amount of a $\beta\text{-L-Arap4N}$ residue attached via phosphodiester bond at O-4 of GlcN II was demonstrated by ^{31}P - ^1H HSQC where a correlation between H-4 of GlcN II and the anomeric proton of Ara4N was evident (Fig. 4.2). Conversely, the anomeric position of GlcN I was either

present as a free reducing end or, when bound to phosphate, as an α -configured residue. The NMR characterization was performed as described in Par. 5.4 and is not further discussed.

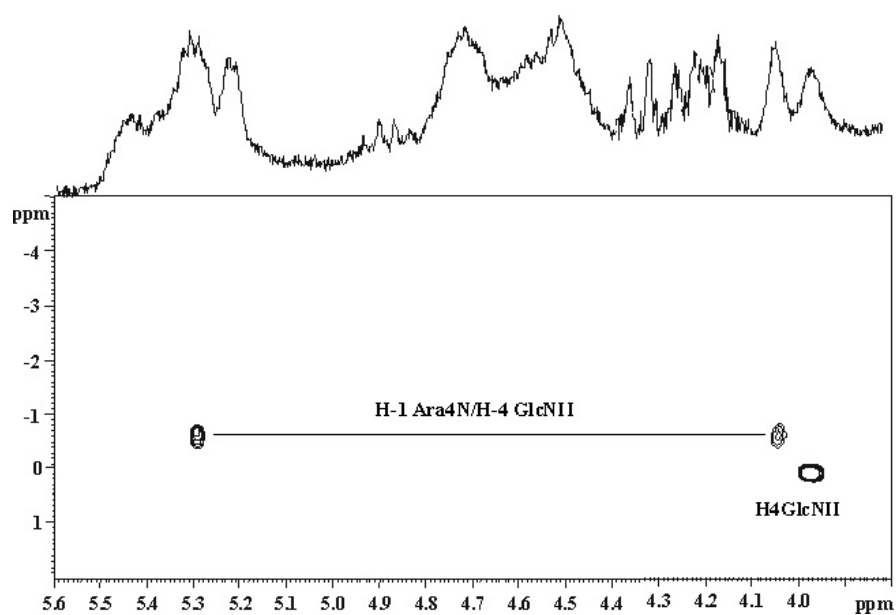


Fig.4.2 ^{31}P - ^1H HSQC NMR of de-*O*-acylated lipid A in DMSO in which are evident the phosphodiester correlation of anomeric proton of Ara4N and H-4 of GlcN II and also the phosphate correlation with H-4 of GlcNII

Unit	1	2/NH	3	4	5ax/eq	6ax/eq
A	5.46	3.65/7.28	3.56	3.00	3.81	3.60/3.71
α -GlcN-I	94.8	53.4	71.3	69.6	69.3	69.7
	-0.66					
B	5.44	3.60/7.38	5.12	3.16	3.80	3.50/3.66
α -GlcN-I	94.8	53.5	69.1	68.7	69.3	68.7
	-0.66					
C	5.13	3.58/7.33	3.49	3.06	4.04	3.50/3.64
α -GlcN-I	91.9	53.4	71.3	69.6	69.5	68.7
D	5.19	3.56/7.31	3.49	3.06	4.04	3.50/3.64
α -GlcN-I	90.0	52.9	70.3	68.6	69.5	68.7
E	5.29	3.55	3.82	3.38	3.57/3.97	/
β -Ara-4N	93.8	70.2	69.3	50.1	58.8	/
	-0.66					
F	4.74	3.68/7.68	4.99	4.00	3.36	3.66/3.48
β -GlcN-II	99.5	52.6	73.7	72.5	74.2	61.8
				-0.16		

Table 1 Chemical shift values of ^1H and ^{13}C of sugar residues belonging to the core region of the LOS from *Burkholderia cepacia* strain ASP B 2D .

4.2.2 MS analysis on intact and selectively degraded lipid A

Analysis of native lipid A

The ion-negative MALDI spectrum on intact lipid A (Fig. 4.3) showed the heterogeneous mixture of penta- and tetra-acylated species substituted in a different way. The peak at m/z 1363.3 (species 1) was identified as monophosphorylated tetra-acylated lipid A, possessing in ester linkage one 14:0 (3-OH) and one 14:0 residues, and in amide linkage two 16:0 (3-OH) residues. The specie at m/z 1493.76 corresponded to a tetra-acylated lipid A, that carried an additional L-Ara4N residue with respect to the species 1. The peaks at 1442.75 m/z and 1573.89 m/z (species 2 and 4) were identified as the corresponding *bis*-phosphorylated species. The ion at 1668.6 m/z (species 5) corresponded to a penta-acylated lipid A, bis-phosphorylated that carried two 14:0 (3-OH) and one 14:0 residues in ester linkage, and two 16:0 (3-OH) residues in amide linkage. The ion at 1798.9 m/z (species 7) was identified as penta-acylated specie with an additional L-Ara4N respect to species 5. In the spectrum traces of species 6 at 1719.7 m/z was also present and identified as monophosphorylated penta-acyl lipid A, carrying two C14:0 (3-OH) and one C14:0 residues in ester linkage, and two C16:0 (3-OH) residues in amide linkage. Thus, the complete distribution of all fatty acid has been carried out by negative and positive mass spectrometry on the de-*O*-acylated and dephosphorylated Lipid A.

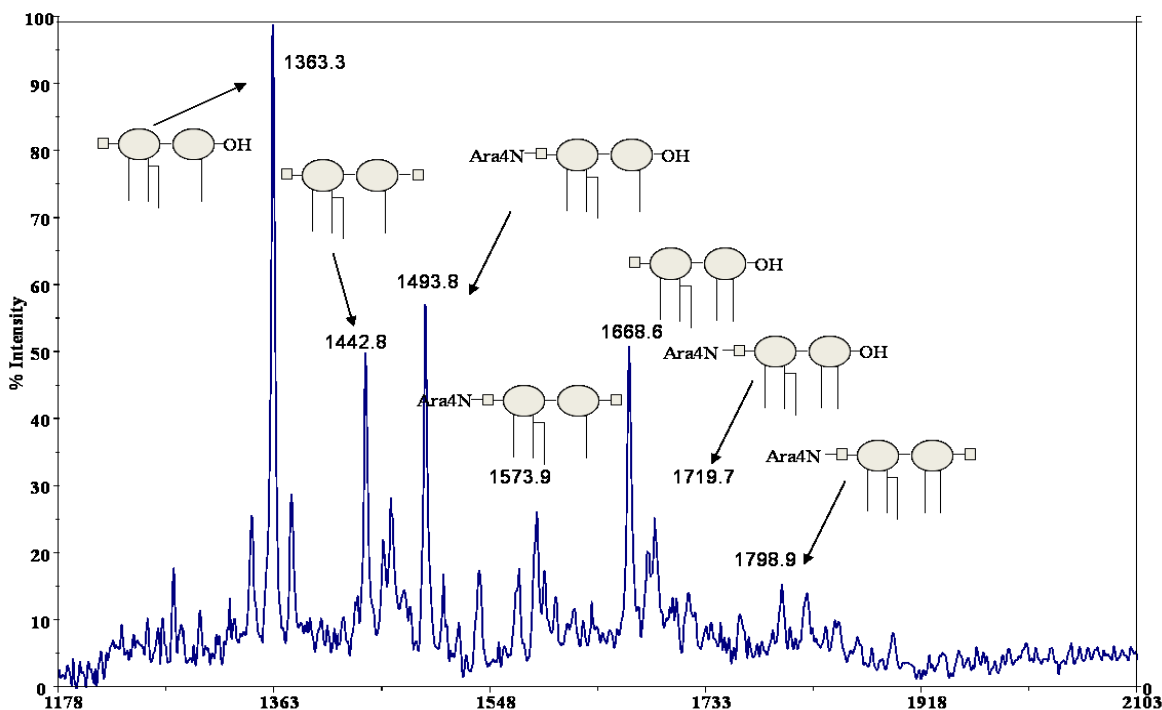


Fig4.3 Negative ion MALDI mass spectrum of the lipid A fraction of LPS from *B. cepacia* ASP 2D.

Analysis of *O*-de-acylated lipid A

An aliquot of lipid A was treated with 32% NH₄OH in order to obtain selectively *O*-deacylated lipid A and then analyzed with ion-negative MALDI-TOF (Fig. 4.4). This mild alkaline-hydrolysis is useful to comprehend the position of the amide-bound acyloxyacyl residues since this procedure selectively removes ester-linked acyloxyacyl and acyl moieties and leaves the amide-linked acyloxyacyl groups unaffected^[11]. The negative ion MALDI spectrum of the obtained product showed two pattern of peaks corresponding to a mixture of tri-acylated lipid A. The ion at 1138.0 *m/z* (specie **1**) was consistent with a tri-acylated lipid A, monophosphorylated that possesses two primary fatty acid (16:3OH) in amide linkage and one secondary fatty acid (14:0) in ester linkage. The peak at 1268.8 *m/z* possessed an additional Ara-4N respect to the specie **1**. Both species were present in also in *bis*-phosphorylated form (specie +80). The positive ion mode MALDI mass spectrum showed the presence of two oxonium ions, a major one at *m/z* 706.1 and a minor one at *m/z* 837.6. The first ion was identified as a GlcNII oxonium ion carrying one 14:0 and one 16:0(3-OH) residues. The latter ion at *m/z* 837.6 carried an additional Ara4N. Thus, by the analysis of the ammonium treated lipid A fraction, it was evident that the secondary 14:0 fatty acid residue substituted the amide bound 16:0(3-OH) residue on GlcN II and that Ara4N, when present, is very likely attached to GlcN II.

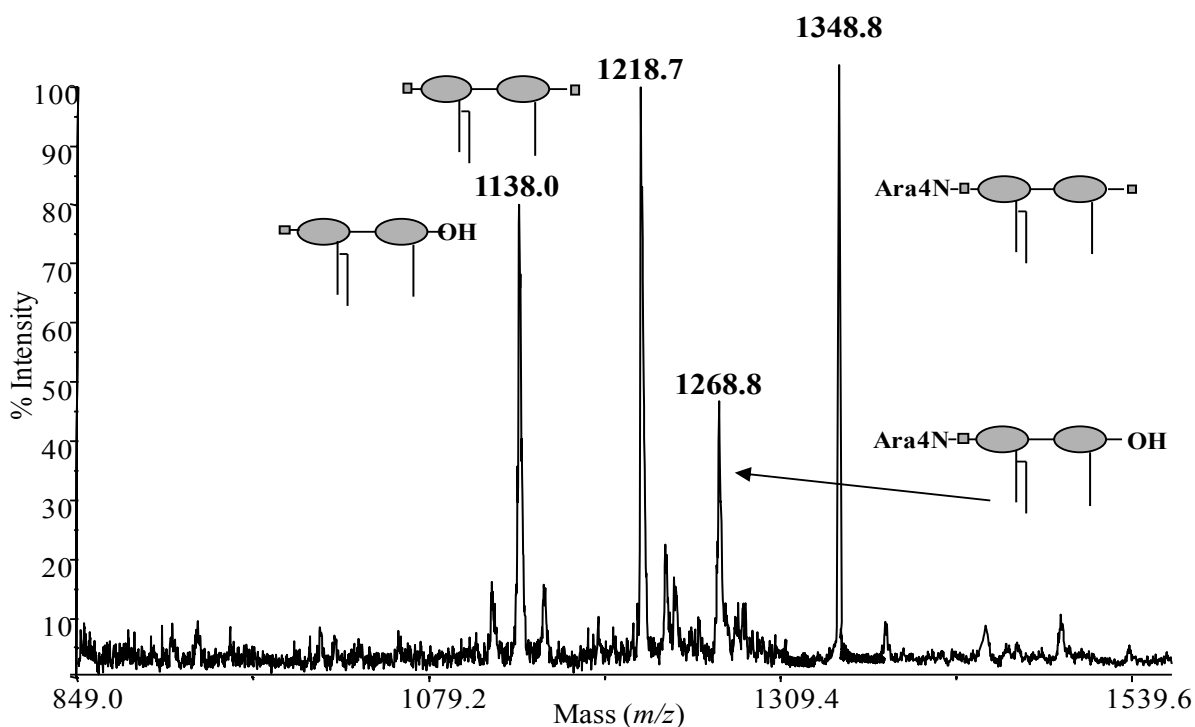


Fig4.4 Negative ion MALDI mass spectrum of NH₄OH treated lipid A fraction of *B. cepacia* ASP 2D.

Analysis of de-phosphorylated lipid A

A small fraction of lipid A was dephosphorylated with 48% HF treatment and then analyzed with ion-positive MALDI-TOF. The spectrum showed the presence of several pseudomolecular ions $[M+Na]^+$ lipid A, with the same acylation pattern of native lipid A. Species carrying Ara-4N residues are completely absent confirming that this sugar is linked to the lipid A backbone via phosphodiester linkage. In particular, one ion m/z 933.8 could be ascribed to a tri-acylated GlcN II oxonium ion carrying one 14:0(3-OH), one 14:0 and a 16:0(3-OH) residue, whereas the ion at m/z 1064.8 carried an additional Ara4N^[12]. In low amounts, two other ions peaks were found assignable to the two oxonium ions above that lacked the 14:0(3-OH) residue ($\Delta m/z = 228$) indicating that, in the native tetra-acylated lipid A species, the 14:0(3-OH) residue may also lack the GlcN II, even though this does not exclude that it may lack the GlcN I as well.

Table 2 Main MALDI-MS negative ion peaks of Fig.5.3 and proposed interpretation of the acyl, phosphate and carbohydrate substituents on the lipid A backbone of the LPS from *B. cepacia* ASP B 2D.

Observed ion (m/z)	Predicted mass (m/z)	Species	Acyl substitution	Proposed fatty acid, phosphate and carbohydrate composition
1363.3	1363.95	1	Tetra-acyl	2 x 16:0(3-OH), 1 x 14:0(3-OH), 1 x 14:0, 1P
1442.8	1440.89	2	Tetra-acyl	2 x 16:0(3-OH), 1 x 14:0(3-OH), 1 x 14:0, 2P
1493.8	1495.01	3	Tetra-acyl	2 x 16:0(3-OH), 1 x 14:0(3-OH), 1 x 14:0, 1 x Ara4N, 1P
1573.9	1572.96	4	Tetra-acyl	2 x 16:0(3-OH), 1 x 14:0(3-OH), 1 x 14:0, 1 x Ara4N, 2P
1668.6	1667.09	5	Penta-acyl	2 x 16:0(3-OH), 2 x 14:0(3-OH), 1 x 14:0, 2P
1719.7	1721.2	6	Penta-acyl	2 x 16:0(3-OH), 2 x 14:0(3-OH), 1 x 14:0, 1 x Ara4N, 1P
1798.9	1799.15	7	Penta-acyl	2 x 16:0(3-OH), 2 x 14:0(3-OH), 1 x 14:0, 1 x Ara4N, 2P

On the basis of the MS and NMR data on the native and selectively degraded lipid A, all lipid A species can be assigned. The lipid A fraction was constituted by a heterogeneous mixture of tetra- and penta-acylated lipid A species differing by phosphorylation pattern and substitution by Ara4N as illustrated in Fig. 5.5. The chemical composition of all lipid A species is illustrated in Table 2.

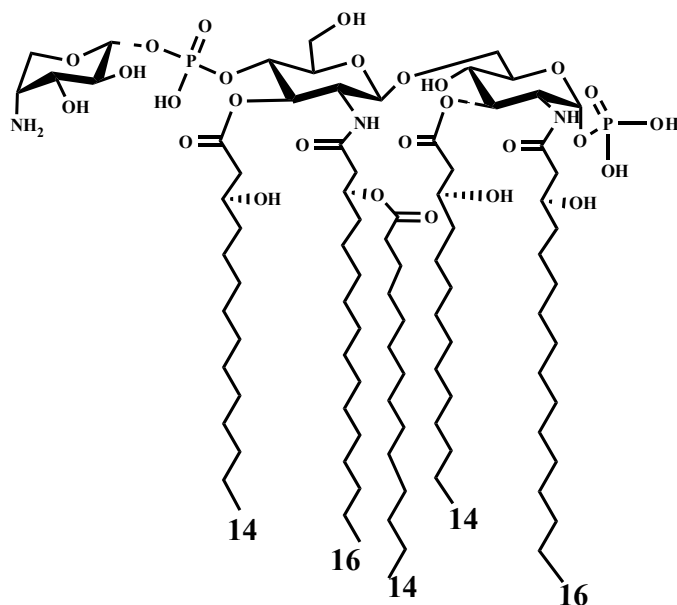


Fig.4.5. The structure of the molecules present in the lipid A blend from the LPS of *B. cepacia* ASP B2D sketched in a single formula.

4.3 Biological activity of lipid A from *B. cepacia* ASP B2D

This work was accomplished in collaboration with the group of Prof. Ian Dubery from Department of Biochemistry, University of Johannesburg. They investigated the biological activity of lipid A fraction monitoring the up-regulation of genes in *Arabidopsis thaliana* seedling following treatment with lipid A purified from LPS. Table 3 shows a partial list of genes that are up-regulated in *A. thaliana* after 8h of treatment with a preparation of 20 μg/ml of lipid A, using water-treatment as negative control. The genes were classified into different categories that include transcriptional regulation, signal transduction, cell transporters, protein degradations, etc. These findings constituted a molecular evidence that lipid A induces an immune response in *A. thaliana* that was very similar to that reported for other MAMPs such as flagellin, Ef-Tu, PGN and LPS^[13,14,15,16]. For further information concerning the biological section of this work, it is possible to refer to our paper published on *Glycobiology*^[17] and enclosed to this thesis.

Functional category	Gene number	Gene description
DNA binding proteins, transcription factors and transcriptional regulation.	At1g20340	DNA damage repair/toleration protein 112
	At1g21570	Zinc (CCH-type) family protein
	At1g24300	GYF domain-containing protein
	At1g80070	Abnormal suspensor 2
	At2g19430	Transducin family protein/WD-40 repeat family protein
	At2g32070	CCR4-NOT transcription complex protein
RNA binding proteins.	At1g18630	Glycine-rich RNA-binding protein 6
	At4g17390	60S ribosomal protein L15
	At4g27000	RNA binding
Signal transduction, protein kinases and - phosphatases.	At1g10210	Mitogen activated protein kinase 1
	At1g09870	Histidine acid phosphatase family protein
	At3g46280	Protein kinase-related protein
	At4g03460	Ankyrin repeat family protein
	At4g08180	Oxysterol-binding family protein
	At4g24740	FUS3-compl gene 1 (CLK/STY lammer-type protein kinase)
	At4g27280 #	Calcium binding EF hand family protein
	At5g58150	LRR transmembrane RLK
At5g60548	Geminivirus REP interacting kinase 2	
Stress-responsive and defense proteins.	At1g02920	Glutathione S-transferase
	At1g20440	Cold regulated 47
	At1g72610	Germin-like protein
	At2g05790	Glycosyl hydrolase family 17 protein, beta glucanase
	At2g32150 *	Haloacid dehalogenase-like hydrolase protein
	At2g44060	Late embryogenesis abundant family protein
	At3g49120	Peroxidase 34
	At3g53280	Cytochrome P450 71B5 monooxygenase
	At4g34180	Cyclase family protein
	At4g37930	Serine hydroxymethyltransferase 1
	At4g02380 #	Senescence-associated responsive protein 21
	At4g12470	Lipid transfer protein
	At4g21960 #	Peroxidase 42
At5g64120	Peroxidase	
Molecular chaperones.	At1g08570	Thioredoxin family protein (disulfide reductase)
	At1g13690	ATPase E1 / peptidyl-prolyl cis-trans isomerase
	At4g22670	Hsp 70 interacting protein
Cell transporters and ion homeostasis.	At1g11260 #	Sugar transporter 1
	At2g26900	Bile acid: sodium symporter family protein
	At2g34250	Protein transport protein Sec 61, putative protein
	At5g25050	Integral membrane transporter family protein
Protein degradation, ubiquitin and proteasome function.	At1g21780	BTB/POZ domain-containing protein
	At1g75990	26S proteasome regulatory subunit S3
	At3g12700	Aspartyl protease family protein
	At3g19390	Cysteine proteinase
	At3g59940	Kelch repeat-containing F-box family protein
	At5g48430	Aspartic-type endopeptidase/ pepsinA

Table 3. Genes up-regulated in *A. thaliana* seedlings following an 8 h treatment with lipid A purified from LPS of *B. cepacia* cell walls.

Discussion

We have reported the chemical characterization of lipid A fraction from *B. cepacia* ASP B2D, an endophytic species belonging to *Burkholderia* genus. The importance of this work resides in fact that there is a limited number of characterized lipid A structures from plant-associated bacteria and so its role in immune plant system is not clear.

All structural data (chemical degradation, mass and NMR analysis) demonstrated that the lipid A is composed by a mixture of glycoforms of tetra- and penta-acylated lipid A species differing by phosphorylation pattern and substitution by Ara4N. The saccharidic backbone is constituted in all cases by [GlcN-*p*- β -(1 \rightarrow 6)-GlcN-*p*] disaccharide. Furthermore, the lipid A has been found to possess a large amount of under-acylated and a low amount of phosphate. The acylation and phosphorylation pattern constitutes important factors in elicitation of mammalian immune system. Studies on lipid A moiety demonstrated that this structural variability is responsible of different three-dimensional lipid A arrangements, leading to changes in the toxicity degree of the lipid A itself. Particularly, the higher acylation degree in the lipid A family with asymmetrical fatty acid distribution on the glucosamine backbone increases the toxicity of lipid A. It was also observed that the absence of one phosphate group on the disaccharide reduces the pathogenicity associated with the microorganism^[18]. Therefore, an interesting parallel with basal resistance in plant can be drawn. Probably, a presence of under-acylated/phosphorylated species and substitution of lipid A with Ara4N residues might allow *B. cepacia* to survive as an endophyte in plant host by reducing the net charge in order to avoid the attach from cationic antimicrobial peptides. In addition to these data, new insights into the biochemical action mechanism of *B. cepacia*-derived lipid A as a MAMP, a resistance elicitor and triggering agent of transcriptional changes during defense responses have been obtained^[18]. The results showed that the lipid A was perceived by *A. thaliana* leading to up-regulation of a large broad of genes, some of which are associated with defense responses and biotic and abiotic stresses, while others are associated with metabolic reprogramming of cellular activities in support of immunity and defense. The nature of the physical interaction between lipid A as a ligand and plant receptors that can act in its perception, are topics that warrants further investigation^[17].

References

1. Govan JRW, Deretic V. *Microbiol Rev.* (1996), **60**: 539–574.
2. Molinaro A, Newman M-A, Lanzetta R, Parrilli M. The structure of lipopolysaccharides from plant-associated Gram-negative bacteria. *Eur J Org Chem* 2009; **34**: 5887-5896.
3. Silipo A, De Castro C, Lanzetta R, Parrilli M, Molinaro A. Lipopolysaccharides. In: *Prokaryotic Cell Wall Compounds - Structure and Biochemistry*. König H, Claus H, Varma A. Eds.; Springer, Heidelberg, 2010; pp 133-154.
4. Silipo A, Erbs G, Shinya T, Dow, JM, Parrilli, M, Lanzetta R, Shibuya N, Newman, M-A, Molinaro A. Glyco-conjugates as elicitors or suppressors of plant innate immunity. *Glycobiol* 2010; **20**: 406-419.
5. Schromm ABE, Lien E, Henneke P, Chow JC, Yoshimura A, Heiner H, Latz E, Monks BG, Schwartz DA, Miyake L, Golenbock DT. Molecular genetic analysis of an endotoxin non-responder mutant cell line: a point mutation in a conserved region of MD-2 abolishes endotoxin-induced signaling. *J Exp Med* 2000; **194**: 79-88.
6. Alexander C, Rietschel ET. Bacterial lipopolysaccharides and innate immunity. *J Endotoxin Res* 2001; **7**: 167-202.
7. Raetz CR, Whitfield C. Lipopolysaccharide endotoxins. *Annu Rev Biochem* 2002; **71**: 635-700.
8. Raetz CR, Reynolds CM, Trent MS, Bishop RE. Lipid A modification systems in Gram-negative bacteria. *Annu Rev Biochem* 2007; **76**: 295-329.
9. Silipo A, Sturiale L, Garozzo D, Erbs G, Jansen TT, Lanzetta R, Dow MJ, Parrilli M, Newman MA, Molinaro A. The acylation and phosphorylation patterns of lipid A from *Xanthomonas campestris* strongly influence its ability to trigger the innate immune response in *Arabidopsis*. *ChemBioChem* 2008; **9**: 896-904
10. Scheidle H, Grob A, Niehaus K. The lipid A substructure of the *Sinorhizobium meliloti* lipopolysaccharides is sufficient to suppress the oxidative burst in host plants. *New Phytol* 2004; **165**: 559-566.
11. Leontein K, Lönnigred J. Determination of the absolute configuration of sugars by gas-liquid chromatography of their acetylated 2-octyl glycosides. *J Meth Carbohydr Chem* 1978; **62**: 359-362.
12. Silipo A, Molinaro A, Cescutti P, Bedini E, Rizzo R, Parrilli M, Lanzetta R. Complete structural characterization of the lipid A fraction of the clinical strain of *Burkholderia cepacia* genomovar I lipopolysaccharide. *Glycobiology* 2005; **15**: 561-570.

13. Navarro L, Zipfel C, Rowland O, Keller I, Robatzek S, Boller T, Jones JDG. The transcriptional innate immune response to flg22: interplay and overlap with Avr gene-dependent defense responses and bacterial pathogenesis. *Plant Physiol* 2004; **135**: 113-128.
14. Zeidler D, Zahringer U, Gerber IB, Dubery IA, Hartung T, Bors W, Hutzler P, Durner J. Innate immunity in *Arabidopsis thaliana*: Lipopolysaccharides activate nitric oxide synthase (NOS) and induce defense genes. *Proc Natl Acad Sci U.S.A* 2004; **101**: 15611-15816.
15. Gust AA, Biswa R, Lenz HD, Rauhut T, Ranf S, Kemmerling B, Götz F, Glawischnig E, Lee J, Felix G, Nürnberger T. Bacteria-derived peptidoglycans constitute pathogen-associated molecular patterns triggering innate immunity in *Arabidopsis*. *J Biol Chem* 2007; **282**: 32338-32348.
16. Livaja M, Zeidler D, Von Rad U, Durner J. Transcriptional responses of *Arabidopsis thaliana* to the bacteria-derived PAMPs harpin and lipopolysaccharide. *Immunobiology* 2008; **213**: 161-171.
17. Ntakadzeni EM, Leone MR, Molinaro A, Dubery I A. Deciphering the structural and biological properties of the lipid A moiety of lipopolysaccharides from *Burkholderia cepacia* strain ASP B 2D, in *Arabidopsis thaliana*. *Glycobiology*, (2010).
18. Seydel, U.; Oikava, M.; Fukase, K.; Kusumoto, S. and Brandeburg, K. 2000. Intrinsic conformation of Lipid A is responsible for agonistic and antagonistic activity. *Eur. J. Biochem.* **267**: 3032-3039

Chapter 5

Structural elucidation of LPS from *Bradyrhizobium* bacteria

5.1 Introduction

Bradyrhizobium species are Gram-negative nitrogen-fixing bacteria that form nodules on host plants and are capable to establish a mutualistic symbiotic relationship with plants of *Leguminosae* genus. As a consequence of the endosymbiotic process, bacteria cause the development of root nodules on plant host in which the rhizobia bacteriods fix atmospheric nitrogen into forms easily available to other organisms and use carbon and energy from the plant in the form of dicarboxylic acids. Legume plants cannot live without these bacteria's essential nitrogen-fixing processes. *Bradyrhizobium* bacteria, as other *Rhizobia* (*Rhizobium*, *Mesorhizobium*, *Sinorhizobium*, and *Azorhizobium*), have been largely used in agriculture system to enhance the natural nitrogen sources avoiding the use of chemical fertilizer^[1]. The early stages of this process are mediated by exchange of different chemical compounds between the eukaryotic host and prokaryotic symbiont. Lipochitoligosaccharides nodulation factors (nod factors), secreted by bacteria during symbiosis, belong to these key molecules and they are considered the principle responsible of nodule organogenesis. In fact, the process has a beginning with a release, from host plants, of broad range of molecular patterns, mainly flavonoids and isoflavonoids, that are able to activate the *nod-ABC* genes, responsible of biosynthesis of nod factors leading to formation of root nodules (Fig.5.1). In this frame, the nod factors seem to be pivotal to develop nodules and thus to establish a correct symbiosis with host organisms.

Giraud et al^[2] have recently shown, by complete genome sequencing, that in two strain of *Bradyrhizobium* (BTAi1 and ORS278) the canonical *nod-ABC* genes, and thus the nod factor, are absent although bacteria are still able to induce the nodule formation in plants as *Aeschynomene sensitiva* and *Aeschynomene indica*. This finding suggests an alternative strategy, used by bacteria, to establish the symbiosis and actually there are many studies in progress in order to understand which molecular patterns are involved in this nod factors independent mechanism (see Par. 1.5.3). The lipopolysaccharides (LPSs), very important cell wall glyco-conjugates with a central role in the mechanisms of bacterial invasion and adaptation to the host environment, could play a role as signaling compounds and act as suppressors of plant defense reactions in initial colonization. In fact, the genome sequences of *Bradyrhizobium sp.* BTAi1 and ORS278 have revealed a number of LPS and exopolysaccharide (EPS) biosynthetic genes involved during the symbiotic bacterial interaction with the host plants.

In order to shed light on the role that lipopolysaccharides have during the symbiotic process of *Bradyrhizobia* strains, with particular interest to those devoid of nod factors, we have performed the structural characterization of the LPSs isolated from *Bradyrhizobium sp.* BTAi1 and ORS278. The pure compounds will be used for testing their biological activity with the aim of clarifying their

structure to function relationship and to supply information about the role of LPS in both plant immune system and in the symbiotic process.

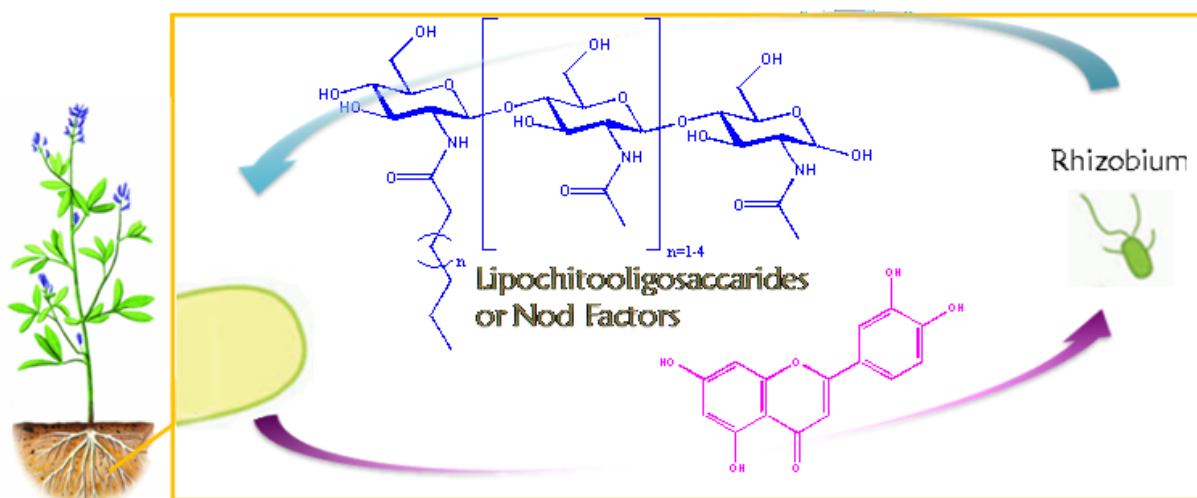
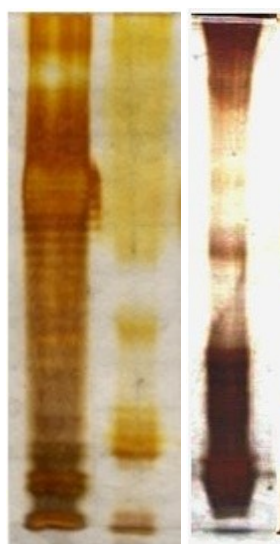


Fig.5.1 Nodules formation through the Nod factors (lipochitooligosaccharides) dependent mechanism

5.2 Isolation and structural characterization of LPS from *Bradyrhizobium* BTAi1 and ORS278

Bradyrhizobia belong to the “slow growing bacteria” group. It means that during the growth there are many risks of contaminations by other bacteria that grow quickly. There are many literature data that report specific growth conditions for *Rhizobia* to avoid contaminations; starting from the medium used, namely AGM (Arabinose-Gluconate medium; for composition see Par.6.1) dried cells from both strains BTAi1 (Br1) and ORS278 (Br2) were accumulated and the LPS extraction was performed with the usual PCP and hot phenol/water protocol (see Paragraph 2.1). The SDS-PAGE analysis of the LPS from Br1 and Br2 (Fig. 5.2) showed that they differed for the molecular weight. In particular, the LPS from Br1 was a smooth type, as suggested by the SDS-PAGE showing the presence of high molecular-weight species in the upper part of the gel (Fig. 5.2); on the other side, the electrophoretic profile of the LPS from Br2 showed a run mainly at the central/terminal part of the gel, revealing the presence of lower molecular weight LPS species (see Fig. 5.2).



line: **1** **2** **3**

Fig.5.2 Electrophoresis gel (13,5 %) on LPSs from *Bradyrhizobium sp.* BTai1(Br1) (line 2) and ORS278 (Br2) (line 3) using LPS from *E.coli* as standard (line1).

In order to elucidate the structure of both O-chain and lipid A fractions, different chemical degradation were used. The usual mild acid hydrolysis on LPS fraction was performed to isolate and characterize the lipid A moiety, while for the O-chain elucidation, a complete de-acylation of both LPS was performed using a strong alkaline treatment (see Par. 2.2).

5.2.1. NMR structural elucidation of O-chain fraction from *Bradyrhizobium sp.* BTai1 (Br1).

After the complete de-acylation of LPS, the obtained polysaccharide (PO) from Br1 was characterized by an extensive 2D NMR analysis. In Table 1 $J_{H,H}$ and $J_{C,H}$ (Hz) coupling constants, long-range correlations and *intra*- and *inter*-residue NOE contacts measured on PO are reported. The 1H -NMR spectrum (Fig. 5.3) contained nine signals, with a single peak in the anomeric region (H1 4.97 ppm, Table 1), suggesting a homopolymeric structure of the O-chain fraction. There were also present four peaks corresponding to ring protons, a methylene group and two singlets, among which one corresponded to a methyl group and the other one was identified as an isolated CH-OH. The combined analysis of both ^{13}C and DEPT NMR spectra showed, despite the already identified groups (see Fig. 5.4 and Table 1) two quaternary carbons at 75.0 (C4) and 74.5 (C8) ppm.

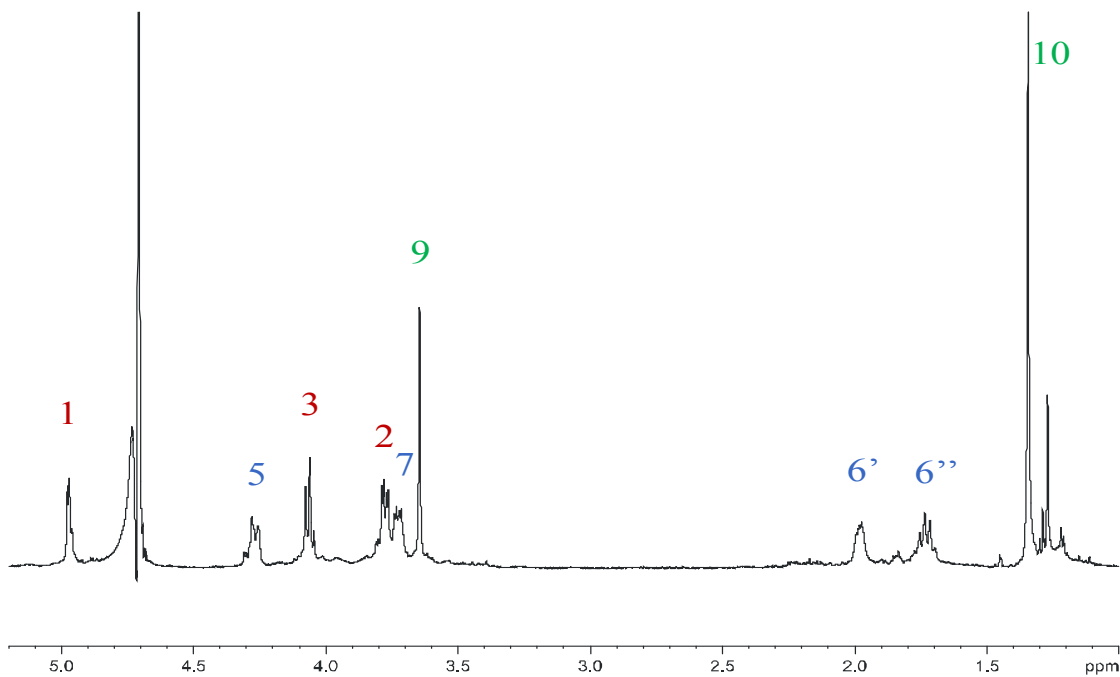


Fig. 5.3 ^1H spectrum of the O-chain domain from *Bradyrhizobium sp.* BTAi1

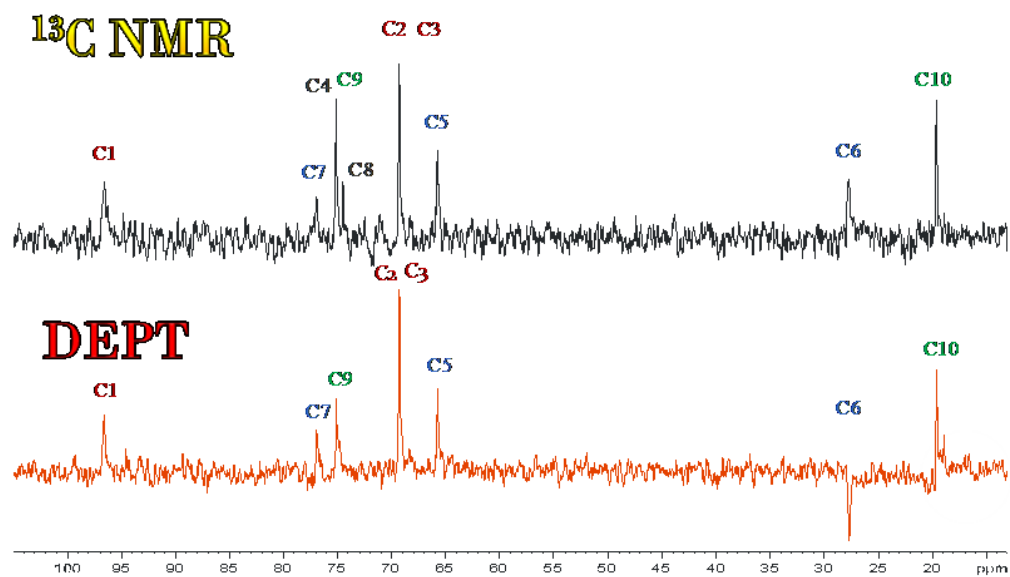


Fig. 5.4 ^{13}C and DEPT NMR spectra of the O-chain fraction from *Bradyrhizobium sp.* BTAi1. A comparison of the two spectra allowed the identification of two quaternary carbon signals: C4 at 74.5 ppm, as confirmed by the disappearing in DEPT spectrum of this signal and C8 at 75.0 ppm, coincident as chemical shift with C9, as testified by the sensible decrease of the signal in DEPT spectrum.

By COSY and TOCSY experiments (Table 1, Figure 5.6) different spin systems were identified. The first started from the anomeric position at 4.97/96.6 ppm and correlated with H-2 at 3.77/69.2 ppm and H-3 at 4.06/69.2 ppm. The multiplicities and the ring coupling constant values ${}^3J_{H2,H3}$ around 10 Hz (see Table 1) suggested an axial disposition of H2 and H3 substituents; the α -anomeric configuration was supported by the value of ${}^3J_{H1-H2}$ coupling constant of 3.9 Hz and by the ${}^1J_{C,H}$ coupling constant of 174 Hz. The second spin system involved the diastereotopic methylene protons at 1.73-1.97/27.5 ppm (H-6ax/H-6eq) correlated with signals at 3.72/77.2 ppm (H-7) and 4.26/65.8 ppm (H-5). The multiplicities and the ${}^3J_{H,H}$ coupling constants values, used to define the relative configuration of protons (table 1), evidenced a ring fragment where both protons at 3.72 and 4.26 ppm were *axial*-oriented and spaced out by methylene group. NMR data (Figure 5.3, 5.4, 5.6) gave evidence of a methyl singlet at 1.34 ppm, suggesting its location on tetra-substituted carbons, and a carbinolic residue at 3.65 ppm, that appeared like a singlet likely due to its location between two quaternary carbons. By a combination of data from NOESY (Fig.5.6) and HMBC (Fig.5.7) experiments, it was possible to establish the disposition of spin systems in the monosaccharide unit as well as the glycosilation linkage in the polysaccharide. Thus, data allowed to identify a carbocyclic monose with a trans-decaline junction as shown in the following figure 5.5.

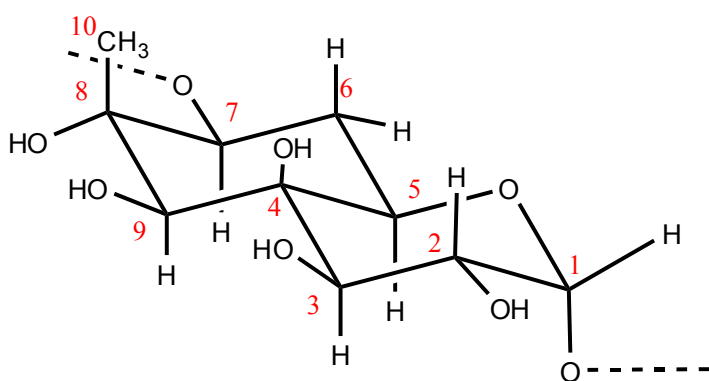


Fig.5.5 O-chain structure from *Bradyrhizobium* sp. BTAi1.

The long range correlations in the HMBC spectrum (Figure 5.7 and Table 1) were useful to locate the quaternary carbons and to identify the above suggested structure. In particular, the cyclohexane ring fragment with *gluco*-configuration containing the anomeric position was identified by the long range correlations of the quaternary carbon C4 with H2 and H3 (Table 1 and figure 5.5 and 5.7) and of C1 with H5; moreover, the chemical shift value of C5 confirmed the α -anomeric configuration. The other ring was identified through the long range correlation of H9 with C4, H6ax/eq with C5;

the methyl group at position 10 and the quaternary carbon at position 8 were located by the long range correlations of H10 with C8, H9 with C8, H7 with C8. The NOE correlations were useful in order to confirm the relative configuration of monose component. In particular, the *intra*-residue NOE contacts between H-3 with H-5 and H-9 (Figure 5.6) indicated their syn axial disposition, as also for H-5 and H-7. The *axial* orientation of CH₃ was endorsed by its *intra*-residual NOE with the axial methylene proton H6 at 1.73 ppm (Figure 5.6).

The downfield shift of the carbon resonance at position 7 (77.2 ppm) identified this as the glycosylated position. The analysis of the scalar and dipolar *inter*-residual correlations in the 2D NMR spectra (Figure 5.6 and 5.7) yielded the polysaccharide sequence. The *inter*-residue NOE contact of H-1 with H-7 (Figure 5.6) was diagnostic of the presence of a α -(1 \rightarrow 7) homopolymeric structure, as confirmed by the long range scalar correlation (Figure 5.7) of C1/H1 with H7/C7 present in the HMBC spectrum (Figure 5.7)

The alternative pyranose ring closure with the hydroxyl at position 9 was excluded on the basis of the H, C long range correlation between H-1 and the C-5 at 65.8 ppm.

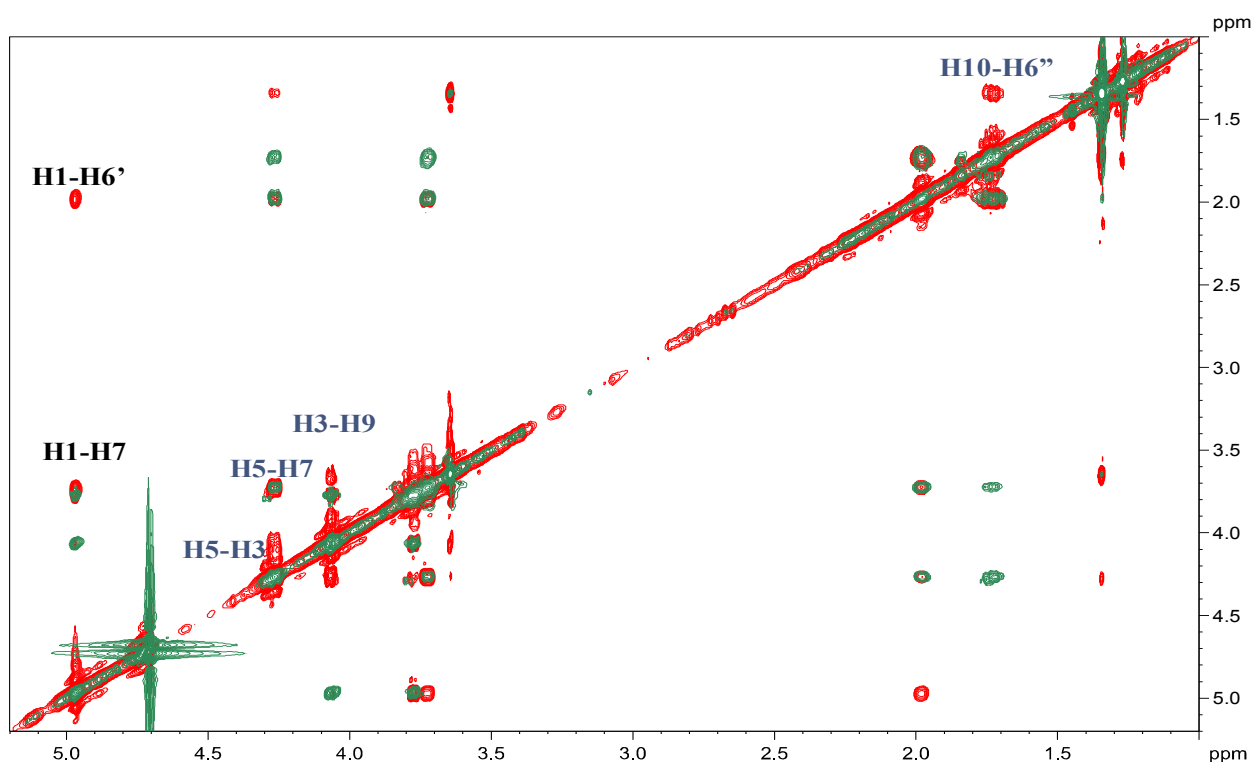


Fig 5.6 NOESY (red) and TOCSY (green) spectra of the O-chain fraction from *Bradyrhizobium sp.* BTAi1. The black marked correlations correspond to *inter*-residual NOE contacts. Conversely, the blue ones are *intra*-residual NOE correlations.

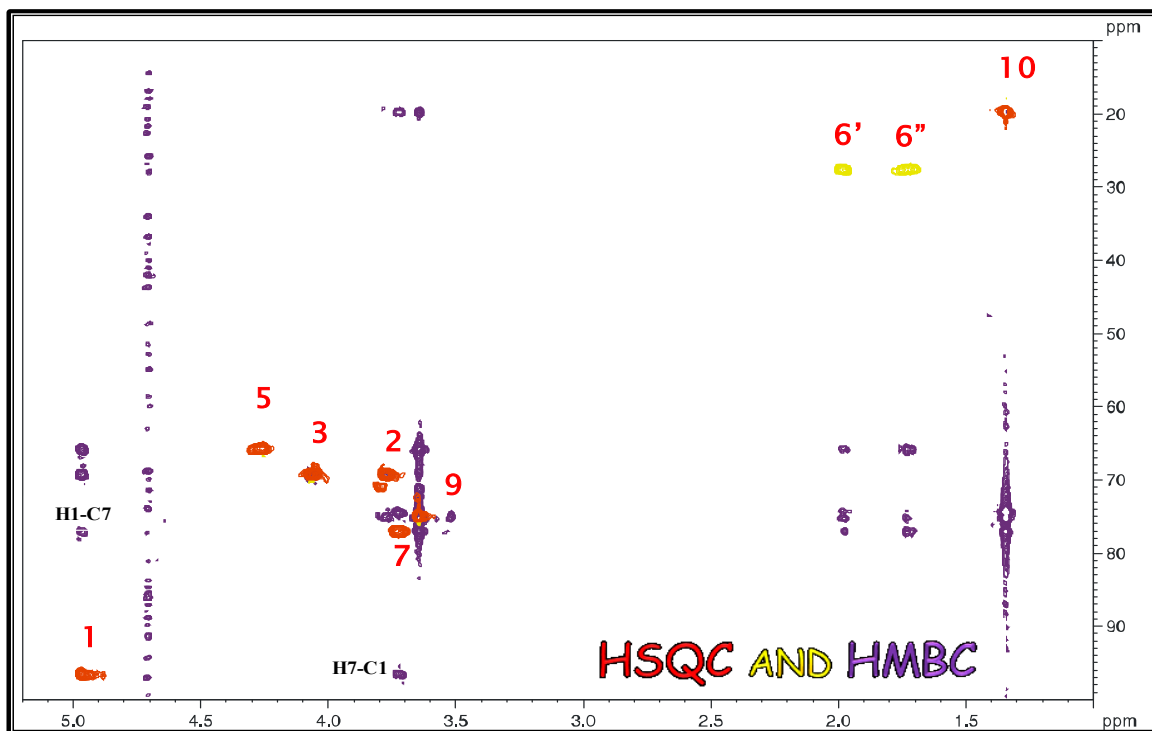


Fig 5.7. HMBC (violet) and DEPT-HSQC (red and yellow) spectra of the O-chain fraction from *Bradyrhizobium sp.* BTAi1

These structural data were further confirmed by the chemical analysis performed derivatizing the sugars as alditol acetate partially methylated (AAPM). From GC-MS analysis, the carbocyclic monose 1-7 linked was detected. In Fig.5.8 the fragmentation pattern of the monosaccharide unit has been reported.

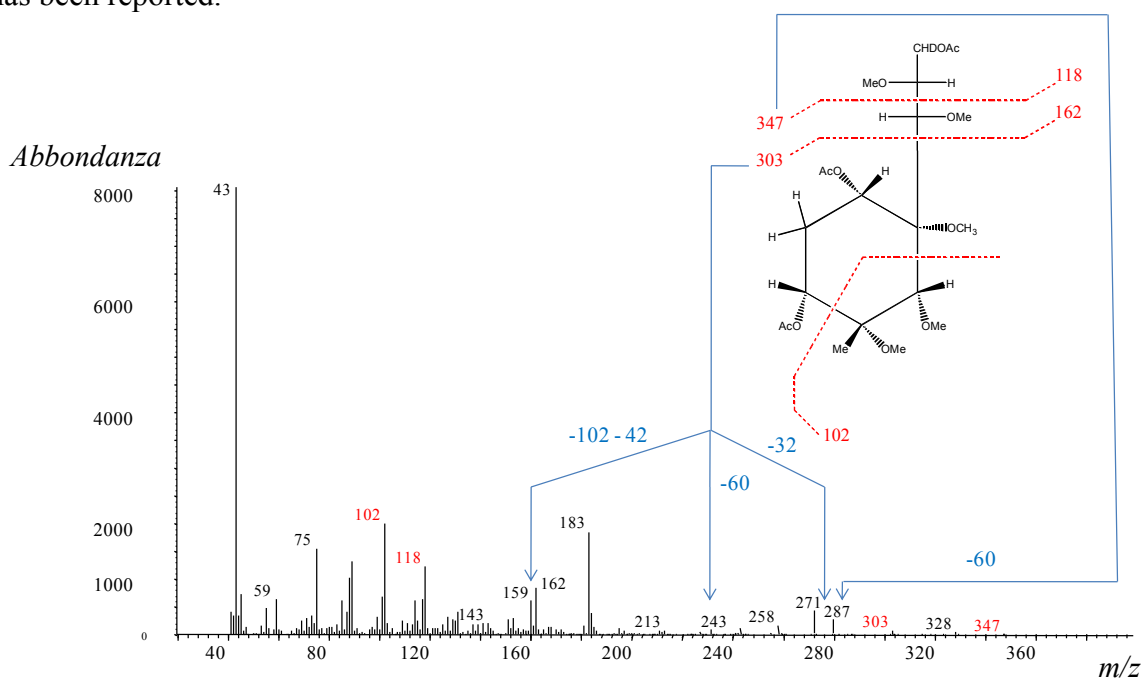


Fig. 5.8 Fragmentation pattern of alditol acetate partially methylated of 7-substituted Bradyrhizose from O-chain fraction of *Bradyrhizobium sp.* BTAi1.

Table 1 ^1H and ^{13}C chemical shifts (ppm), coupling constants $^3J_{\text{H,H}}$ and $^1J_{\text{C,H}}$ (Hz), H-long-range correlations and ^1H NOE contacts both *intra*- and *inter*-residue measured on PO.

	^1H	^{13}C	H-C long - range	<i>intra</i> -NOE	<i>inter</i> - NOE
1	4.97 (<i>d</i>) $^3J_{\text{H,H}}=3.9$ Hz	96.6 $^1J_{\text{C,H}}=174$ Hz	65.8 (C-5) 69.3 (C-3/2) 77.2 (C-7)	3.77(H-2)	1.97 (H-6 _{eq}) 4.06 (H-3) 3.72 (H-7)
2	3.77 (<i>dd</i>) $^3J_{\text{H,H}}=3.9; 10.0$ Hz	69.2	75.0 (C-4)	4.97 (H-1)	
3	4.06 (<i>d</i>) $^3J_{\text{H,H}}=10.0$ Hz	69.2	69.2 (C-2)	3.65 (H-9) 4.26 (H-5)	1.34 (H-10) 4.97(H-1)
4	-	75.0	-		
5	4.26 (<i>dd</i>) $^3J_{\text{H,H}}=3.5; 11.6$ Hz	65.8	-	1.97 (H-6 _{eq}) 3.72 (H-7) 4.06 (H-3)	1.34 (H-10) 1.97 (H-6 _{eq})
6 _{ax}	1.73 (<i>m</i>)	27.5	65.8 (C-5) 77.2 (C-7)	1.34 (H-10) 1.97 (H-6 _{eq})	
6 _{eq}	1.97 (<i>q</i>) $^3J_{\text{H,H}}=11.6$ Hz	27.5	65.8 (C-5) 77.2 (C-7)	4.26 (H-5) 3.72 (H-7) 1.73 (H-6 _{ax})	4.97(H-1)
7	3.72 (<i>dd</i>) $^3J_{\text{H,H}}=4.5; 11.6$ Hz	77.2	19.5 (C-10) 74.5 (C-8) 96.6 (C-1)	4.97(H-1) 4.26 (H-5)	1.97 (H-6 _{eq}) s 1.73 (H-6 _{ax}) w
8	-	74.5	-		
9	3.65 (<i>s</i>)	75.0	19.5 (C-10) 65.8 (C-5) 74.5 (C-8) 75.0 (C-4) 77.2 (C-7)	1.34 (H-10) 4.06 (H-3)	
10	1.34 (<i>s</i>)	19.9	74.5 (C-8) 75.0 (C-9) 77.2 (C-7)	1.73 (H-6 _{ax}) 4.26 (H-5) 3.65 (H-9)	

5.2.2 Absolute configuration of the novel monosaccharide from the O-chain fraction of *Bradyrhizobium sp.* BTAi1.

In order to establish the absolute configuration of the novel monosaccharide isolated from *Bradyrhizobium sp.* BTAi1, circular dichroic spectra (CD) were performed after appropriate derivatization of monose. To this purpose the methyl glycoside (mixture of α and β glycoside) was treated with *p*-brombenzoyl chloride in pyridine using a stoichiometric ratio for the four hydroxyls groups and following the reaction progress by MALDI spectra. In this way, adding a stoichiometric amounts of chloride, it was possible to detect by MALDI spectrum only a tri-*O*-benzoyl derivative. The product was purified with preparative TLC and NMR analyses were performed in order to

define the positions involved in derivatization. The NMR data (Fig. 5.9) were in accordance with the presence of a methyl 2,3,7-tri-*O*-benzoyl α/β glycoside, as shown in Fig. 5.10. In fact, H2, H3 and H7 protons of the derivatised monosaccharide were shifted in the region between 5.2 and 5.9 ppm, indicating an acylation at these positions. Clearly, steric hindrance prevented the acylation of the secondary hydroxyl group at position 9. Thus, CD spectra were performed on the obtained product using methanol as solvent and acquiring in the near UV (220-380 nm) (Fig. 5.11).

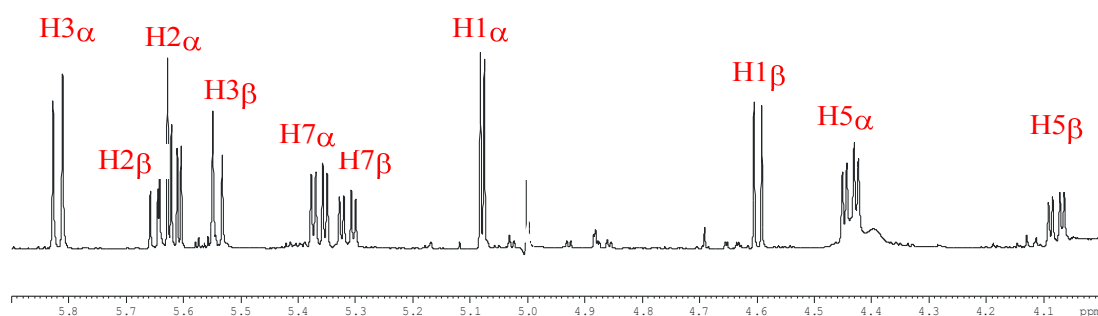


Fig. 5.9 ^1H NMR spectrum of methyl 2,3,7-tri-*O*-benzoyl glycoside.

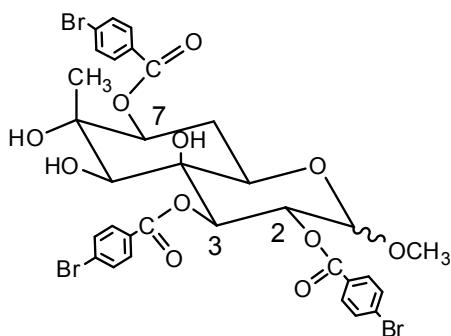


Fig.5.10 Methyl 2,3,7-tri-*O*-benzoyl glycoside of carbocyclic monose

It was amply demonstrated^[3] that with benzoyl derivatives the positive split CD effect is directly connected with a clockwise disposition of chromophores (and thus of the hydroxyl groups). Conversely, a negative split CD effect indicates a counterclockwise disposition of chromophores (see Par. 2.2.3). With the presence of three chromophores, it is necessary to consider the additive CD split effect, due to the single coupling of each couple of chromophores, in relation to their spatial relationships. Considering the minimized structure of **2**, it was possible to evaluate the module and sign of the dihedral angles between each couple of chromophores: The dihedral angle between position 2 and 3 and between 3 and 7 of derivatised Bradirhizose (figure 5.10 and 5.11)

were both about 60° , while that between position 2 and 7 was of the opposite sign and with a value close to 170° . The absolute value of CD split amplitude results to be dependent on the dihedral angle and in particular it results to be maximum for dihedral angles near 60° and zero for 0° and 180° . Thus the contribution to the split CD by couple of chromophores 2-7 was negligible. On the basis of these observations and also considering the distance between the chromophores, it was possible deduce that the total effect of the three split CD effects gave a clear indication about the absolute configuration of Bradirhizose and was mainly contributed by couples 2-3 and 3-7. Actually, compound **2** displayed an overall positive split CD amplitude ($\Delta\epsilon = +60$) (Fig.5.11) indicating a clockwise arrangement for chromophores in position 3-2 and 3-7 and a counterclockwise arrangement for the couple 2-7 (Figure 5.11).

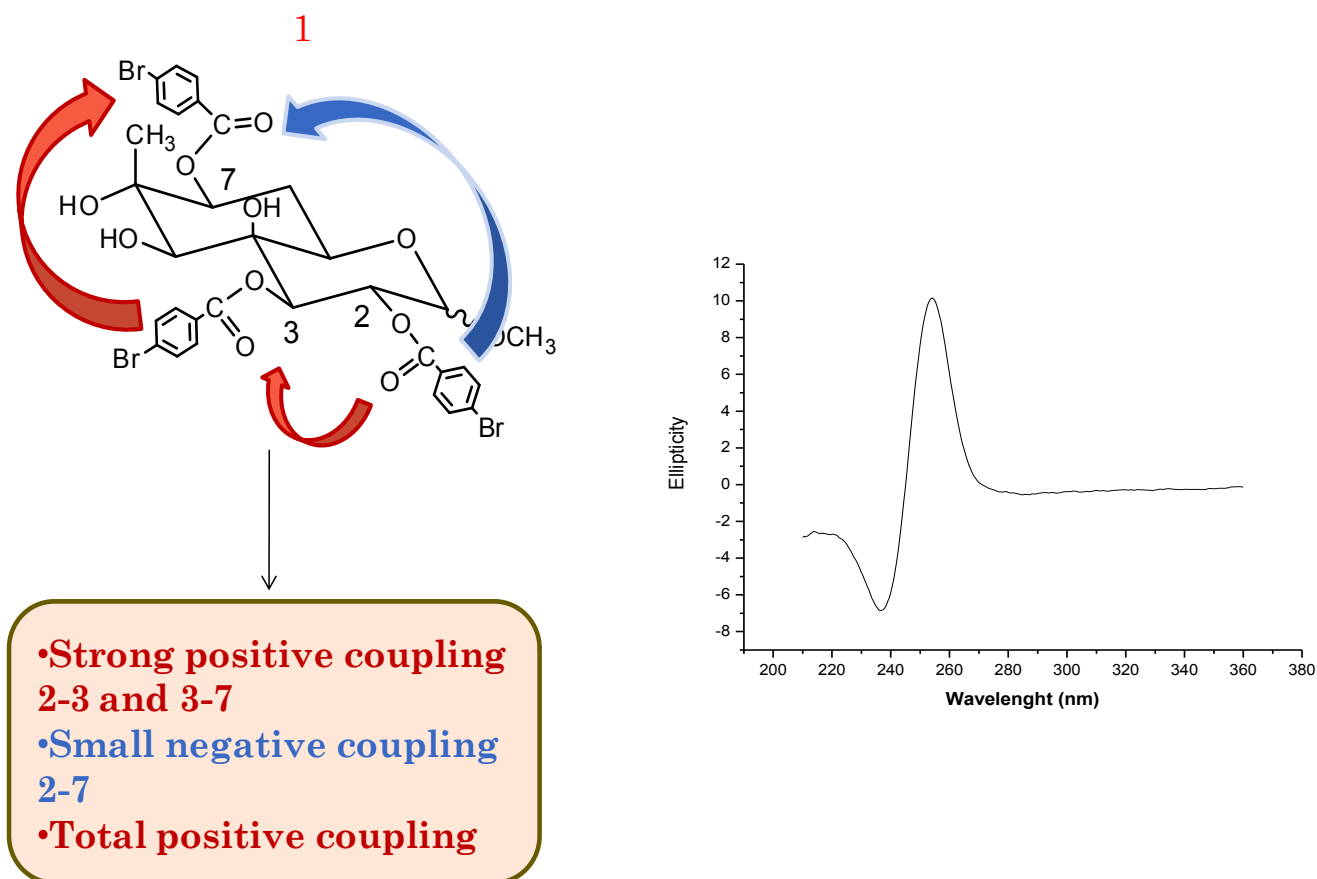


Fig.5.11 CD spectrum of derivatized carbocyclic monose. The solvent was MeOH and the spectrum was acquired between 220-380 nm. positive split CD amplitude is diagnostic of clockwise arrangement for the chromophore in position 3-2 and 3-7 and of counterclockwise arrangement for the couple 2-7.

All structural data allowed to define the structure of carbocyclic monose shown in Fig.5.12. This novel monosaccharide represents the second example of a carbocyclic monosaccharide that contains ten carbons with a trans-decaline junction type. The first example was constituted by caryose, a carbocyclic sugar found as a component of the O-chain fraction from a phytopathogenic bacterium *Burkholderia caryophylli*^[4,5].

As far as the systematic name we suggested, on the basis of the nomenclature used for caryose, the name 4,9-cyclo-6-deoxy-8-C-Methyl-D-xilo-D-galacto-nonose and as trivial name bradyrhizose.

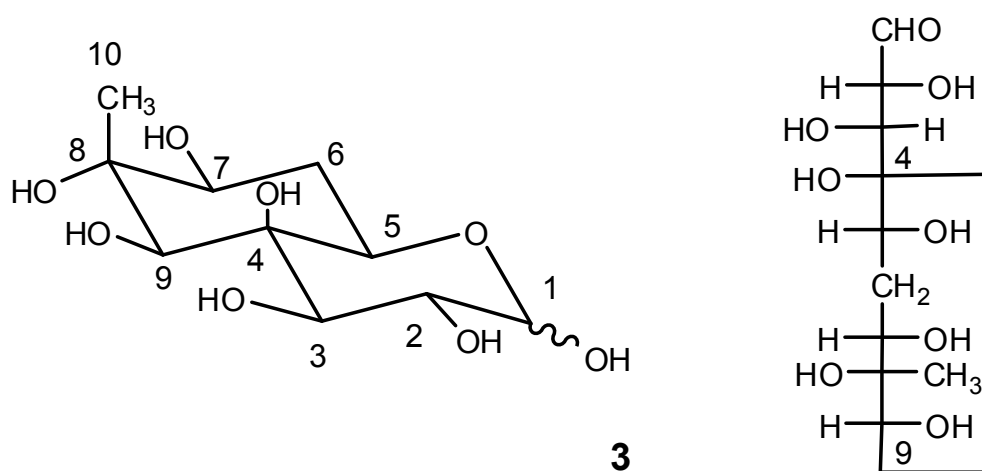


Fig.5.12 Definitive structure of bradyrhizose

5.2.3 Full characterization of the O-chain fraction from *Bradyrhizobium sp.*ORS278

The O-chain fraction from *Bradyrhizobium sp.*ORS278 (Br2) was obtained, similarly to Br1, with a complete de-acylation of LPS. The polysaccharide was investigated with a combination of mono and bidimensional NMR spectra.

The ¹H spectrum showed two main signals in the anomeric region among which one (spin system **B**) appeared as a singlet at 4.97 ppm, and the other was splitted in three signals (**A'**, **A''**, **A'''**) resonating at 5.05, 5.03 and 5.02 ppm that differed for a minimal difference in chemical shift and that were attributable to the same spin system **A**. The proton chemical shifts were assigned on the basis of COSY and TOCSY spectra (Fig. 5.13 and Table 2) while the carbon resonances were assigned by ¹H-¹³C HSQC (Fig. 5.14 and Table 2). The *intra*-residual NOE contacts, obtained from NOESY and ROESY, were used to establish the relative configuration of all protons present in the monosaccharide units. NMR data suggested the presence of a mixture of two homopolymers

referred to as **A** and **B** that were both composed of bradyrhizose (see par.5.2.1, Fig.5.2.2 and Table 2) linked in the two A and B polysaccharides at different positions. The $^1J_{C-H}$ coupling constant (above 170 Hz) and a small value of coupling constant $^3J_{H1-H2}$ (below 3 Hz) were diagnostic for α -configuration of both homopolymers. In particular, homopolymers **A** resulted to linked at position 9 as confirmed by the strong *inter*-residual NOE contact between the anomeric position and position (Figure 5.13 and Table 2) and by a HMBC correlation between these two positions involved in the glycosidic linkage (Figure 5.14); thus homopolymer **A** was constituted by an α -(1→9) bradyrhizose polysaccharide. The splitting of **A** into three slightly different spin systems, A', A'', A''', was likely attributable to the presence of species with significantly different molecular weight belonging to the same homopolymer **A** (see SDS-PAGE). These conditions may create small difference in chemical environment, thus causing the splitting of **A** in three signals. As for homopolymer **B**, the NOE contact of H1 with H-7 and the corresponding long range correlations suggested the presence of a α -(1→7) bradyrhizose polysaccharide, as that we found in the O-chain from *Bradyrhizobium sp.* BTAi1.

GC-MS analysis performed on the O-chain fraction isolated from the LPS of *Bradyrhizobium sp.*ORS278 confirmed the presence of two differently linked Bradyrhizose residues. The fragmentation of the 1→7 linked Bradyrhizose matched with the one showed in Fig. 5.8 while the fragmentation pattern of 1→9 linked Bradyrhizose is shown in Fig. 5.15.

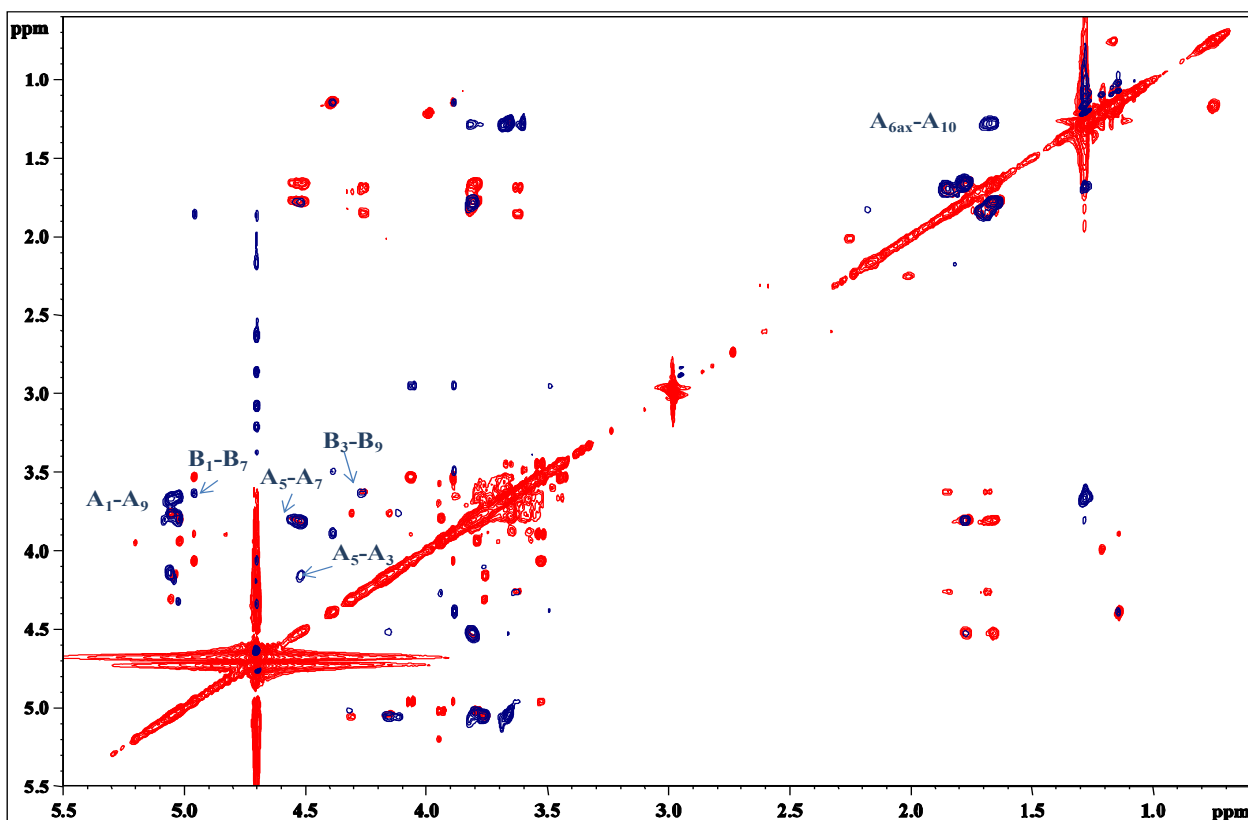


Fig 5.13. TOCSY (red) and ROESY (blue) spectra of the O-chain fraction from *Bradyrhizobium sp.* ORS278.

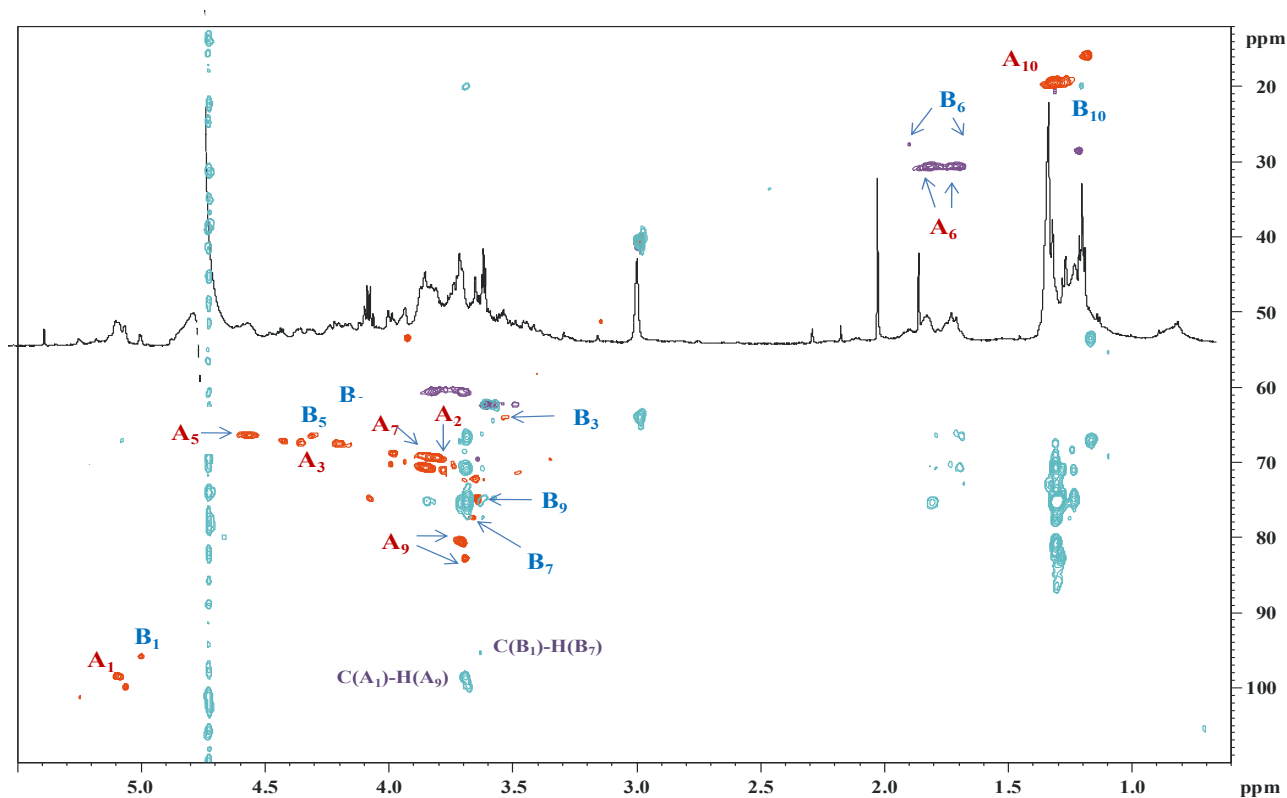


Fig 5.14. ¹H, ¹³C HSQC (red and blue) and HMBC (azure) spectra of the O-chain from *Bradyrhizobium sp.* BTAi1 LPS with all cross peaks assignments.

Table 2 Chemical shift values of ^1H and ^{13}C of both bradyrhizose α -(1 \rightarrow 9) (A) and Bradyrhizose α -(1 \rightarrow 7) (B) residues.

	Chemical shift δ ($^1\text{H}/^{13}\text{C}$)									
Bradirozoze α-(1\rightarrow9) (A)	1	2	3	4	5	6ax/6eq	7	8	9	10
^1H	5.05/ 5.03/ 5.02	3.76/ 3.76/ 3.79	4.31/ 4.15/ 3.94	-----	4.55/ 4.51/ 4.32	1.77/1.66 1.77/1.66 1.72/1.82	3.79/ 3.81/ 3.83	----- -	3.68/ 3.65/ 3.64	1.2
^{13}C	98.5/ 98.5/ 99.9	69.3/ 69.3/ 69.2	67.2/ 67.5/ 68.7	75.7	66.3/ 66.3/ 67.2	30.0/ 30.0/ 30.7	69.2/ 70.6/ 69.2	75.0	80.4/ 80.5/ 82.7	19.8

	Chemical shift δ ($^1\text{H}/^{13}\text{C}$)									
Bradirozoze α-(1\rightarrow7) (B)	1	2	3	4	5	6ax/6eq	7	8	9	10
H	4.96	4.06	3.53	---	4.25	1.85/1.67	3.63	----	3.59	1.13
^{13}C	95.7	63.5	64.1	75.0	66.3	27.6	77.4	74.2	74.9	19.2

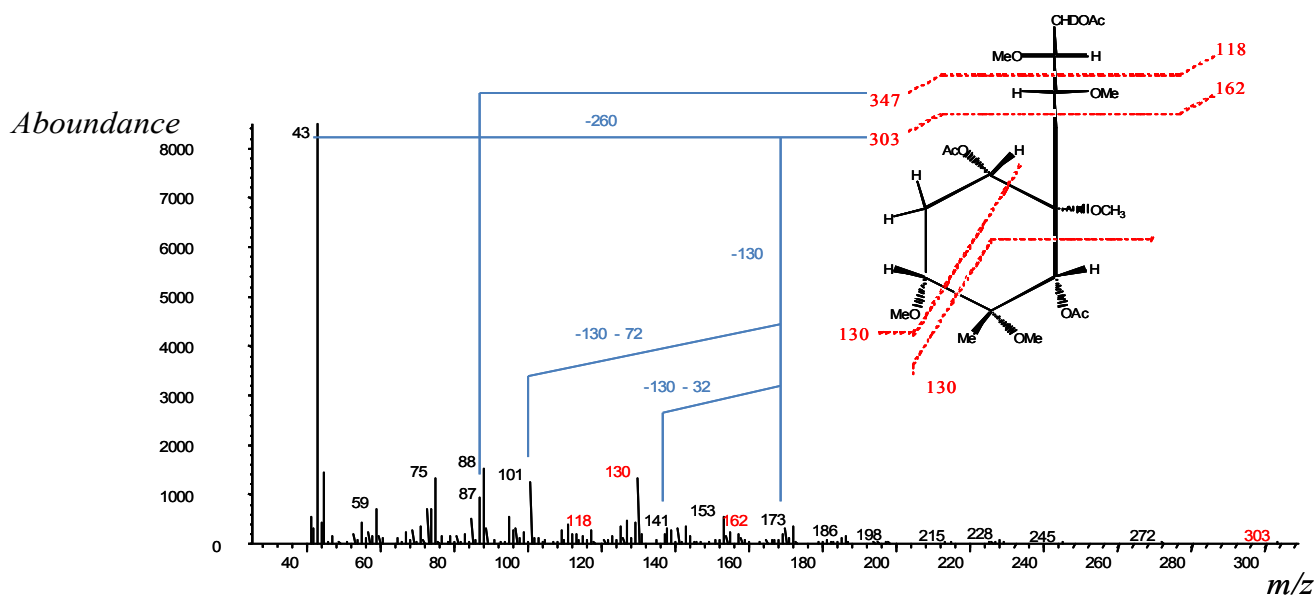


Fig.5.14 Fragmentation pattern of alditol acetate partially methylated of 9-substituted Bradyrhizose.

5.3 Structural characterization of lipid A from *Bradyrhizobium sp.* BTAi1 and ORS278

The lipid A fraction was directly obtained from LPS after acid treatment (see par. 2.2). The glycolipid portion was recovered with a selective extraction with chloroform/methanol/water 2:2:1.8. The organic phase was analysed with chemical degradations, MALDI experiments and NMR spectroscopy.

Chemical analysis performed directly on lipid A showed the presence of Mannose (Man), 2,3-diamino-2,3-dideoxy-glucose (diaminoglucose, DAG) and Galcturonic acid (GalA) and as fatty acid residues of C14:0(3-OH), C12:0(3-OH), C12:1 α,β -unsaturated and long chain C24:0, C26:0, C26:0(25-OH), C28:0(27-OH), C30:0(29-OH-),. Furthermore, the presence of C30:0 (x,yOH), C32:0 (x,y-OH), residues was detected and specific analysis are in progress to understand the position of both hydroxyl groups. Methylation analysis (see par. 2.2.3) allowed to identify the presence of 3-linked Man, 4-6 linked DAG and terminal GalA.

5.3.1 MALDI/TOF analysis of Lipid A

Mass spectrometric experiments on the native and partially degraded lipid A from both strain of *Bradyrhizobium* were performed in positive ion mode.

The first information on the lipid A structure were obtained from positive-ion MS/MS spectra performed on the *O*-deacylated lipid A (Fig. 5.15). The spectrum showed a pseudomolecular ion peak $[M+Na^+]$ at 1691.00 m/z corresponding to a tetra-acylated species composed of two GlcN3N, two Man, one GalA, two N-linked C₁₄:0 (3-OH), a N-linked C₁₂:0 (3-OH) and a N-linked unsaturated C₁₂:1. The ion peaks at 1529.92 and 1369.83 m/z fitted with a tetra-acylated structure lacking one and two units of Man, respectively. Furthermore, there was also a species at 1517.91 m/z that lacked the GalA unit. The ion peak at 931.44 m/z corresponded to an oxonium Na^+ adduct composed of two Man residues, one GlcN3N, one unit of C₁₄:0 (3-OH) and one of C₁₂:0 (3-OH), allowing the full primary fatty acid distribution on each GlcN3N, i.e., the unsaturated fatty acid is present on the proximal GlcN3N and that the distal GlcN3N was substituted by a Man-Man disaccharide.

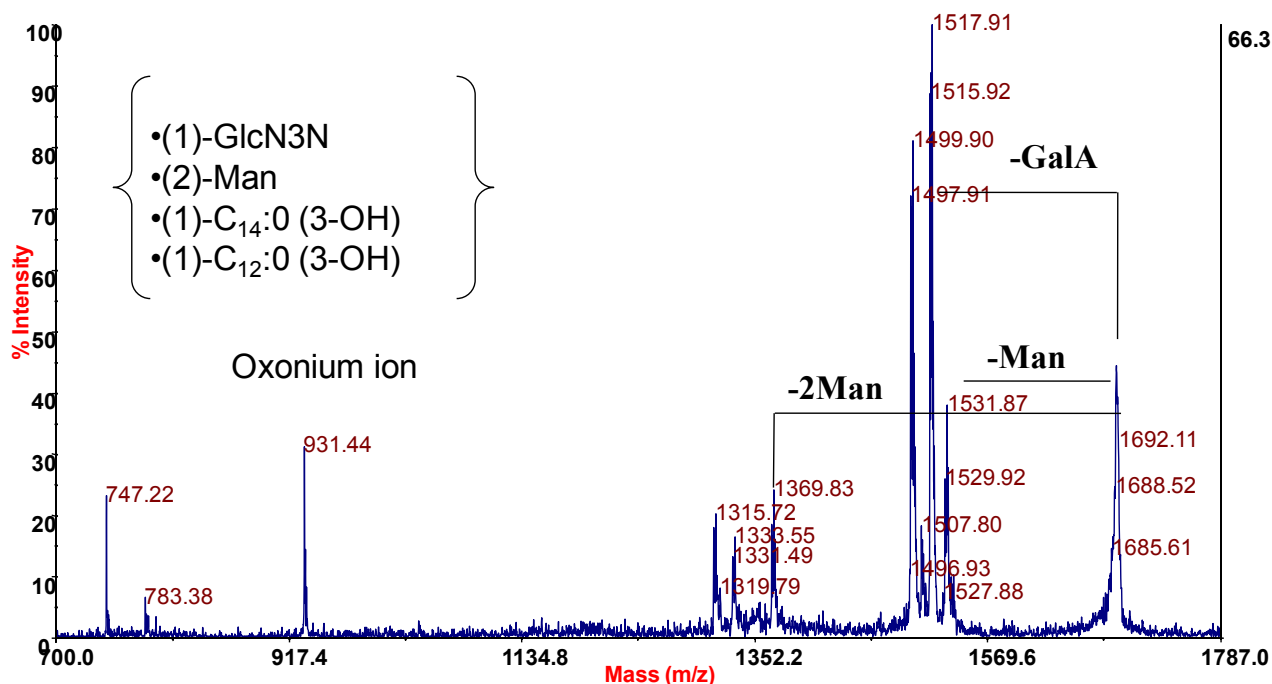


Fig.5.15 TOF/TOF MALDI spectrum performed on peak at 1692.11 m/z of the *O*-deacylated species. In the figure the chemical composition of oxonium ion has been reported.

In Fig.5.16 is shown the positive ion MALDI MS spectrum performed on the intact lipid A in which we have identified an heterogeneous mixture of peaks, all present as adduct with Na^+ and corresponding to three main families of lipid A species centered in the region of m/z 2606, 2128 and 3091.0 that differed for a long chain fatty acid. Based on the compositional analyses we have assigned the peak at 2606.1 m/z (Figure 5.16) to a hexa-acylated species with the following composition:

- two residues of GlcN3N
- two residues of Man
- one unit of GalA
- two $\text{C}_{14:0}$ (3-OH)
- one $\text{C}_{12:0}$ (3-OH)
- one unsaturated $\text{C}_{12:1}$
- one $\text{C}_{30:0}$ (x,y-OH)
- one $\text{C}_{30:0}$ (29-OH)

The pattern of the neighboring peaks of m/z 2606 suggested heterogeneity in length (peaks at ± 28 m/z) and hydroxylation (peaks at ± 16 m/z) of the fatty acids. A third minor ion family centered at

m/z 3118 corresponding to an equivalent structure of 2606.1 m/z but with a difference in mass of 512. Further investigations are in progress in order to identify the chemical structure of this residue.

MALDI spectrum obtained from lipid A after de-phosphorylation treatment (not shown) was identical to that performed on the intact lipid A indicating the absence of phosphate group on the lipid A backbone.

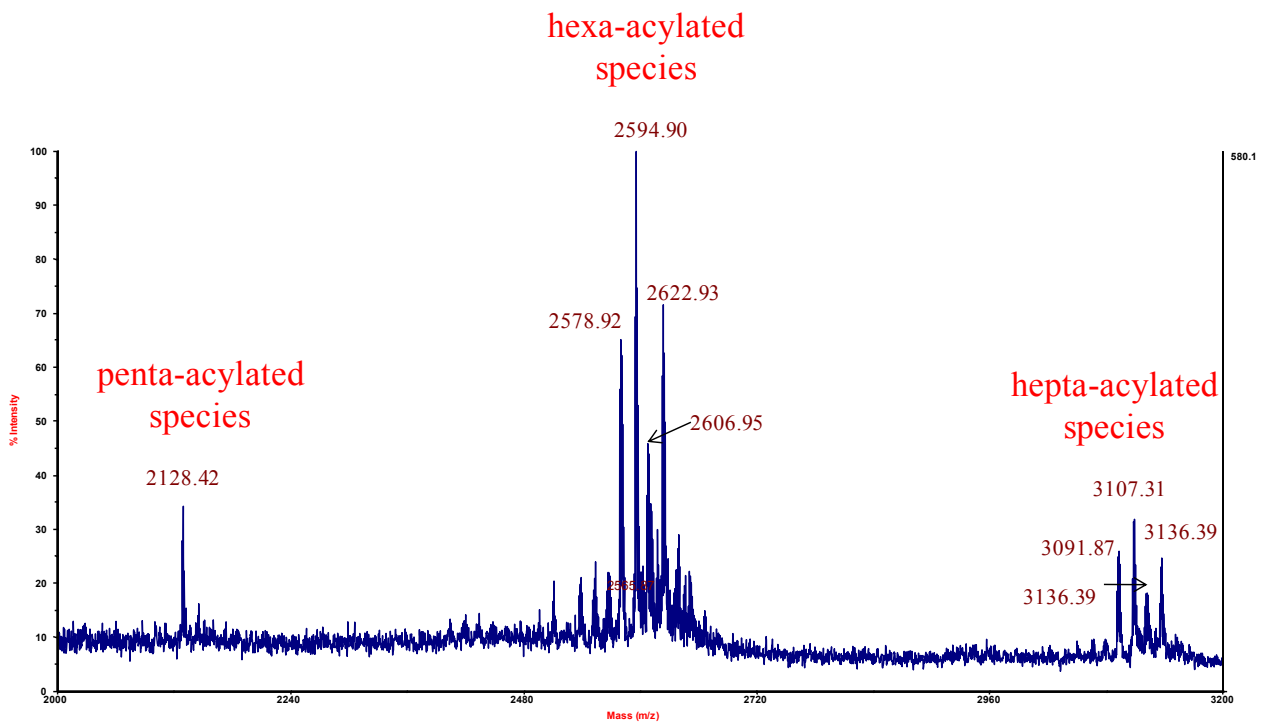


Fig.5.16 Ion-positive MALDI spectrum on native Lipid A. The chemical composition of the specie at 2606.2 m/z has been reported.

To delve deeper into these structural data, MS/MS (TOF-TOF) experiments on the ion peaks at m/z 2606.11 and 2622.93 were performed; the obtained spectra are shown in Fig.5.17 a and b. The positive ion MS/MS spectrum on 2606.11 m/z showed two different ion fragments at 2412.58 and 2281.58 m/z that corresponded to the species without GalA and two residues of Man respectively. There was also present the oxonium ion at m/z 1845 deriving from cleavage of the glycosidic linkage of the DAG disaccharide with the following composition:

- one residue of GlcN3N
- two residues of Man
- one C₁₄:0 (3-OH)
- one C₁₂:0 (3-OH)
- one C₃₀:0 (x,y-OH)

- one C₃₀:0 (29-OH)

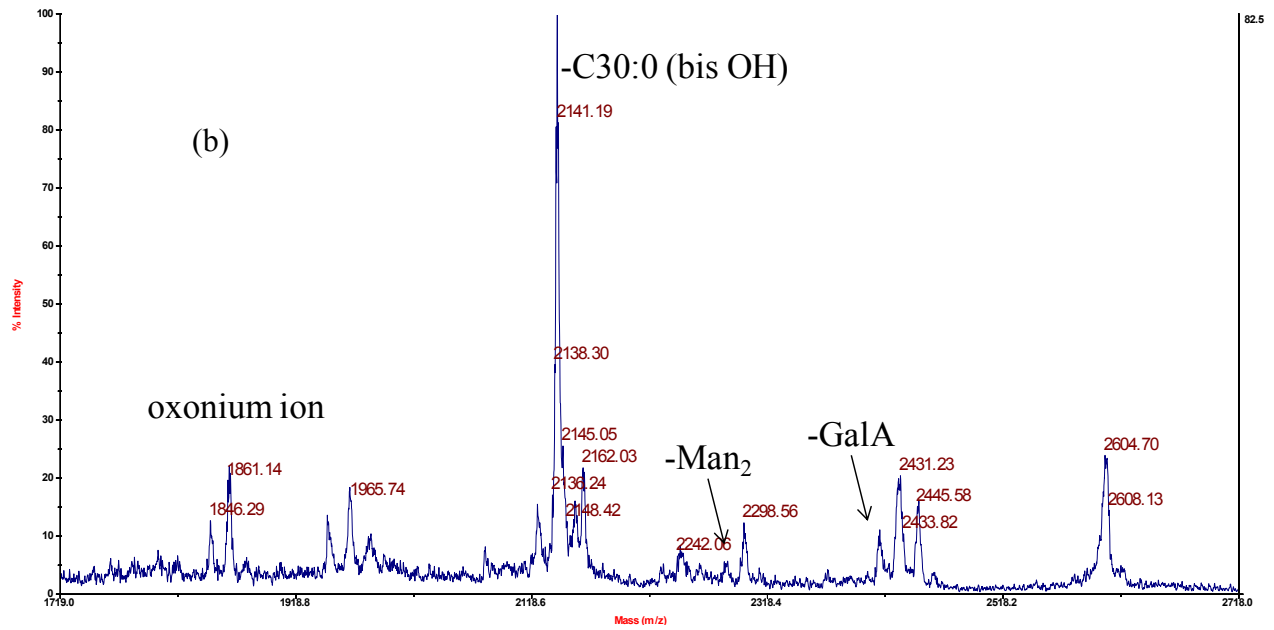
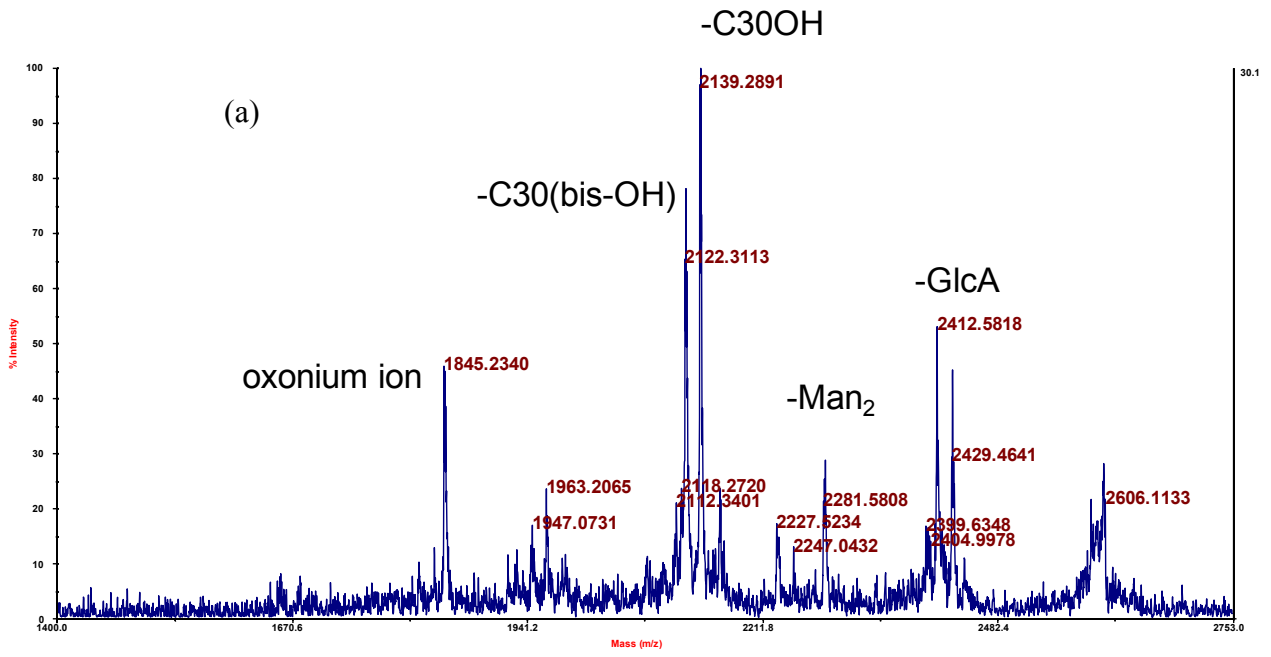
the presence of two residues of Man in the oxonium ion confirmed that they were both linked to the non reducing DAG of the lipid A saccharide backbone while the GalA unit was located on reducing DAG. Furthermore, the oxonium ion was also useful to identify the fatty acid distribution on each DAG residue and thus the asymmetric distribution of the acyl chains with respect to the DAG disaccharide backbone of the hexa-acylated lipid A species (4+2 arrangement). The peaks at m/z 2139.00 and 2122.0 both corresponded to penta-acylated lipid A fragments, lacking a residue of C₃₀:0 (29-OH) and of C₃₀:0 (x,y-OH) respectively. This suggested that both fragments were present in ester linkage (more labile respect to amide linked fatty acids) and thus their secondary fatty acid nature.

The positive ion MS/MS spectrum at m/z 2622.93 (+ 16 with respect to 2606) showed the same pattern of fragmentation of. In fact, the peak 2622.93 m/z was in accordance with a hexacylated with this following composition:

- two residues of GlcN3N
- two residues of Man
- one unit of GalA
- two C₁₄:0 (3-OH)
- one C₁₂:0 (3-OH)
- one unsaturated C₁₂:1
- two C₃₀:0 (x,y-OH)

the presence of a second C₃₀:0 (x,y-OH) that replaced a C₃₀:0 (29-OH) residue was suggested by a single peak at 2141.19 m/z in MS/MS spectrum (Fig.5.17 b) that corresponded to the simultaneous lack of two C₃₀:0 (x,y-OH).

In order to obtain further information about the fragment at 512 m/z , the MS/MS (TOF-TOF) experiment was performed on specie at 3091 m/z (Fig.5.17 c). This peak corresponded to a heptacylated specie carrying the additional 512 m/z respect to hexacylated ion at 2578.92 m/z found in MALDI on intact lipid A (Fig.5.16). The MS/MS spectrum of 3091 m/z presented one peak at m/z 2561.23 corresponded to hexa-acylated lipid A fragments lacking a residue of 512 m/z . The peak at 2110.66 m/z corresponded to the ion lacking of fragment of C₃₀:0 (29-OH) and 512 m/z simultaneously. This finding suggested a tertiary substitution of 512 m/z residue.



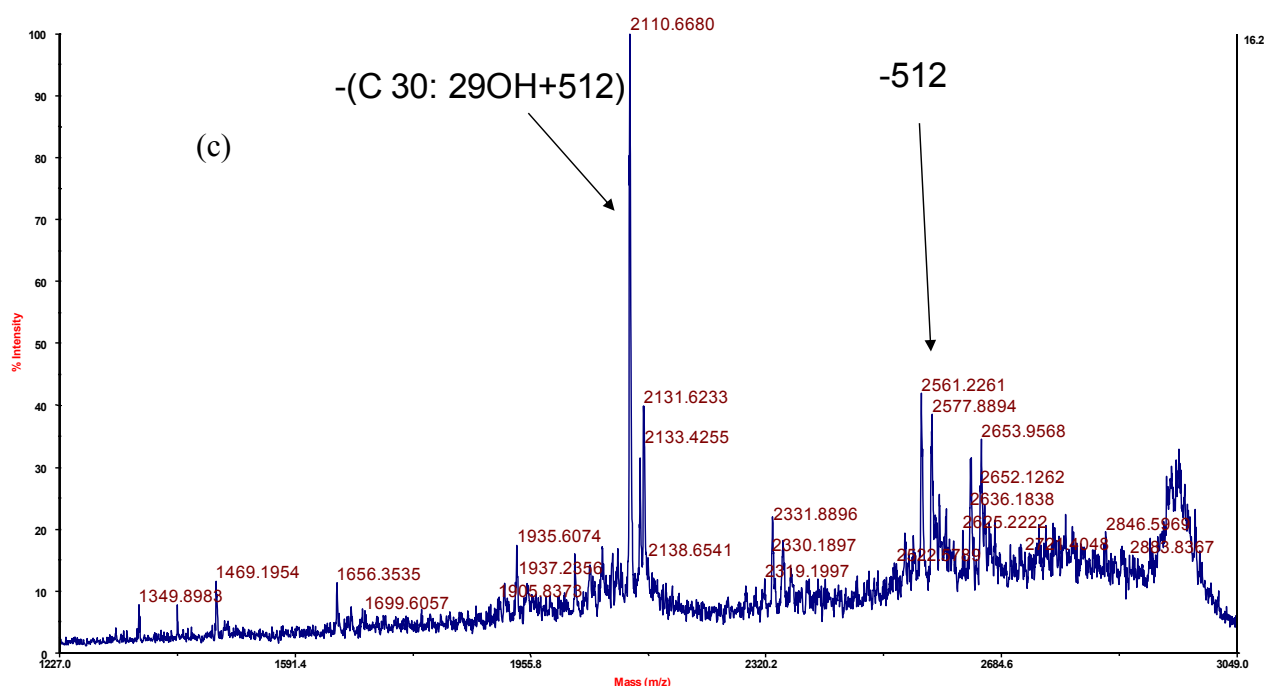


Fig.5.17 TOF/TOF MALDI spectra performed on peaks at 2606.11 m/z (a), 2622.93 m/z (b) and 3091 m/z (c)

5.3.2 NMR spectroscopy of lipid A

The structural characterization of lipid A backbone from *Bradyrhizobium sp.* ORS278 and BTAi1 was performed with 1D and 2D NMR spectroscopy. The NMR spectra were executed on the extracted lipid A (see Par.5.4) that was dissolved in $CDCl_3/CD_3OD$ (1/1 v/v). All 1H and ^{13}C assignments of each sugar were based on 2D homonuclear experiments: DQF-COSY, TOCSY and $^1H/^{13}C$ heteronuclear experiments (HSQC and HMBC). The anomeric region of the HSQC spectrum (Fig. 5.18) presented five signals, suggesting a pentasaccharide structure for lipid A backbone. Four cross peaks were found between 50 and 55 ppm and they corresponded to nitrogen-bearing carbons. The remaining signals, observed in the region from 60 to 78 ppm, were generated from ring carbons among which we found two groups of unsubstituted as well as two of substituted C-6 carbon atoms. The coupling constants and the chemical shift values were in agreement with the presence of two 2,3-diamino-2,3-dideoxy-Glucose (DAG), two residues of Mannose (Man) and one of Galacturonic acid (GalA), all present in 4C_1 chair conformation. The chemical shift values of 1H and ^{13}C are shown in Table 3.

The anomeric protons at 5.06 ppm (**B**) and 4.41 ppm (**C**) were respectively identified as α and β DAG residues. The α and β configuration of **B** and **C** was determined by the $^1J_{C1,H1}$ constants

(Figure 5.20 and Table 3) derived from F2-coupled HSQC measurements, and were confirmed by ^{13}C , ^1H chemical shift values and by the *intra*-residual NOE contacts observed in the ROESY spectrum. In fact, spin system **B** presented a $^1J_{\text{C1,H1}}$ value of 176 Hz and *intra*-residual NOE contact of **B**-1 only with **B**-2, confirming α -configuration; spin system **C**, instead, presented a $^1J_{\text{C1,H1}}$ value of 162 Hz and NOE correlations of **C**-1 with **C**-2, **C**-3 and **C**-5, typical of β -configuration. The carbon chemical shifts of **B**-2/**B**-3 (51.3/51.78 ppm) and **C**-2/**C**-3 (53.48/54.17 ppm) corresponded to *N*-linked carbon in accordance with the nature of diaminoglucose of both residues; the downfield shift of proton resonance of H-2 and H-3 of residues **B** and **C** was diagnostic of *N*-acylation at these positions. The carbon resonances of **B**-6'/**B**-6'' (69.19 ppm) were evidently displaced downfield suggesting a glycosylation in this position. The anomeric proton of residue **C** presented a strong NOE correlation with **B**6' indicated that the two GlcN3N were bound with β -(1 \rightarrow 6) linkage, as also confirmed by the corresponding long range correlation (Figure 5.18).

Spin system **A** (5.22, 94.3 ppm) was assigned to α -galacturonic residue. The $^3J_{\text{H3,H4}}$ and $^3J_{\text{H4,H5}}$ values (below 1 Hz) were in accordance with a *galacto*-configuration. The α -configuration was inferred by the heteronuclear $^1J_{\text{C1,H1}}$ value of 180 Hz, and confirmed by the chemical shifts of H-1 and C-1 and by the *intra*-residual NOE contact of H-1 with H-2. The ring carbons resonances of **A** were not evidently displaced downfield suggesting that this residue was linked only with anomeric position, in accordance with the chemical analysis. The strong NOE contact between the anomeric protons of residues **A** and **B** and the long-range correlations between these two positions were diagnostic of their α -(1 \rightarrow 1) linkage (Figure 5.18 and 5.19).

Residues **D** and **E** were identified both as α -mannose units. The *manno*-configuration was assigned by $^3J_{\text{H1-H2}}$ and $^3J_{\text{H2-H3}}$ values (below 3 Hz) whereas the anomeric configuration was established by $^1J_{\text{C1,H1}}$ value and the *intra*-residual NOE contact of H-1 with H-2. The downfield shift of C-6 from residue **D** together with the strong NOE contact between **E**1 and **D**6'/**D**6'' and the corresponding long range correlation (Figure 5.18, 5.19 and table 3) indicated that they were bound through an α -(1 \rightarrow 6) glycosidic linkage. Furthermore, the anomeric carbon of residue **D** presented a strong HMBC correlation with H-4 from residue **C** (Fig. 5.18) suggesting that the Mannose **D** is α -(1 \rightarrow 4) linked with the distal β -DAG unit.

In summary, all the NMR data were in accordance with the following pentasaccharide lipid **A** backbone:



The NMR spectra showed other spin systems attributable to acyl moieties. In the HSQC spectrum the cross peak at 3.83/68.1 ppm corresponded to H3/C3 of primary 14:0 (3-OH) and 12:0 (3-OH) moieties while the downfield signals at 5.29/71.32 ppm and 5.14/71.2 ppm were assigned to *O*-acylated H3/C3 of the same residues. The chemical shifts for α , β and γ atoms of 3-hydroxy fatty acids, *O*-acylated and with a free OH group, are listed in Table 3. The proton signal at 3.72 ppm, correlated in HSQC spectrum to a carbon at 67.3 ppm, was attributed to ω -1 methine of the long chain fatty acids. This ω -1 proton in COSY and TOCSY spectra, correlated with a methyl group at 1.15 ppm and to the ω -2 methylene protons at 1.4/1.38 ppm. Other two different signals at 4.97/4.87 ppm, correlated in HSQC spectrum with 72.3 and 71.3 ppm respectively, were assigned to ω -1 methine of the long fatty acids with geminal *O*-acylation. The nature of substitution is not yet known but, based on mass spectrometry experiments, it must be ascribable to the 512 *m/z* fragment (see above) that both lipid A from *Bradyrhizobium sp.* BTAi1 and ORS278 carries as additional residue. In addition, two low field proton and corresponding carbon signals were present in the spectra, at 6.80/ 145.6 and 5.96/123.2 ppm; they were straightforwardly attributed to the double bond of the unsaturated fatty acid C₁₂:1.

Table 3. $^1\text{H}/^{13}\text{C}$ chemical shift values of relevant signals of lipid A from *Bradyrhizobium sp.* BTAi1 and ORS278

Chemical shift δ ($^1\text{H}/^{13}\text{C}$)						
Unit	1	2	3	4	5	6
A	5.22	3.95	4.05	4.29	4.54	/
1- α -GalA	94.3	67.8	71.9	70.3	70.9	171.0
B	5.06	4.08	4.29	3.46	4.07	3.79/3.90
6- α -GlcN-3N	92.4	51.3	51.78	68.3	71.9	69.1
C	4.41	3.8	4.07	3.65	3.44	3.91/3.80
4- β -GlcN-3N	102.53	53.4	54.1	75.19	76.5	61.1
D	4.89	3.70	3.60	3.55	3.72	3.84/3.78
6- α -Man	101.75	70.7	70.7	67.0	72.5	66.5
E	4.82	3.90	3.83	3.71	3.79	3.84/3.76
<i>t</i> - α -Man	99.7	70.2	71.1	67.1	73.3	61.5

Fatty acid	α_1/α_2	β	γ	$(\text{CH}_2)_n$	CH_3
I-(3-OR) fatty acid	2.48/2.55	5.29	1.6	1.31	0.88
	40.63	71.32	34.08	28.6	13.0
II-(3-OR) fatty acid	2.40/2.53	5.14	1.59	1.31	0.88
	40.57	71.2	35.08	28.6	13.9
3-OH fatty acid	α_1/α_2	β	γ	$(\text{CH}_2)_n$	CH_3
	2.23/2.29	3.83	1.4	1.27	0.94
C₁₂:1	42.9	68.1	36.6	28.6	
	α	β			
Fatty acid	6.80	5.96			
	145.6	123.2			
long chain (ω-1) -OH	ω -2	ω -1	ω		
	1.4/1.38	3.72	1.15		
Ist long chain (ω-1) -OR	38.6	67.3	22.4		
	1.51/1.62	4.97	1.24		
IInd long chain (ω-1) -OR	35.6	72.3	19.1		
	1.59/1.50	4.87	1.20		
	35.5	71.3	19.0		

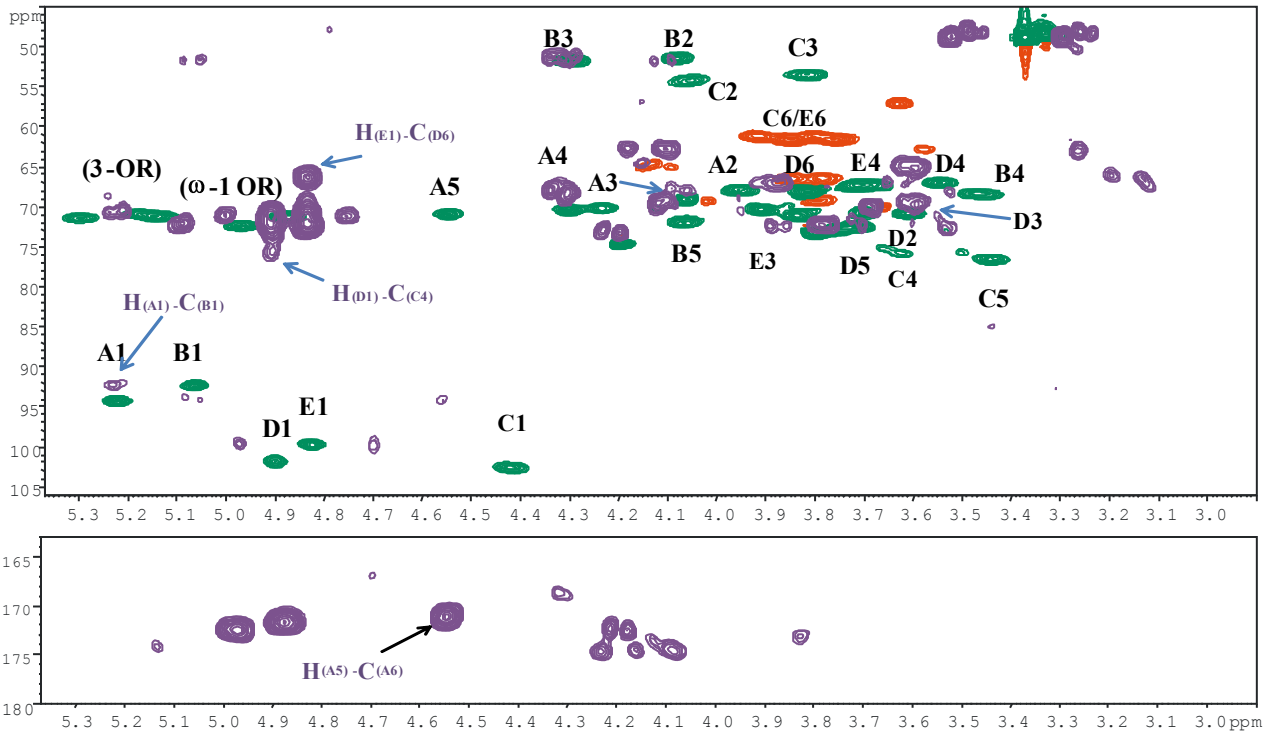


Fig 5.18. Overlapping of the ^1H , ^{13}C HSQC with HMBC spectrum of the lipid A fraction with all cross peaks assignments.

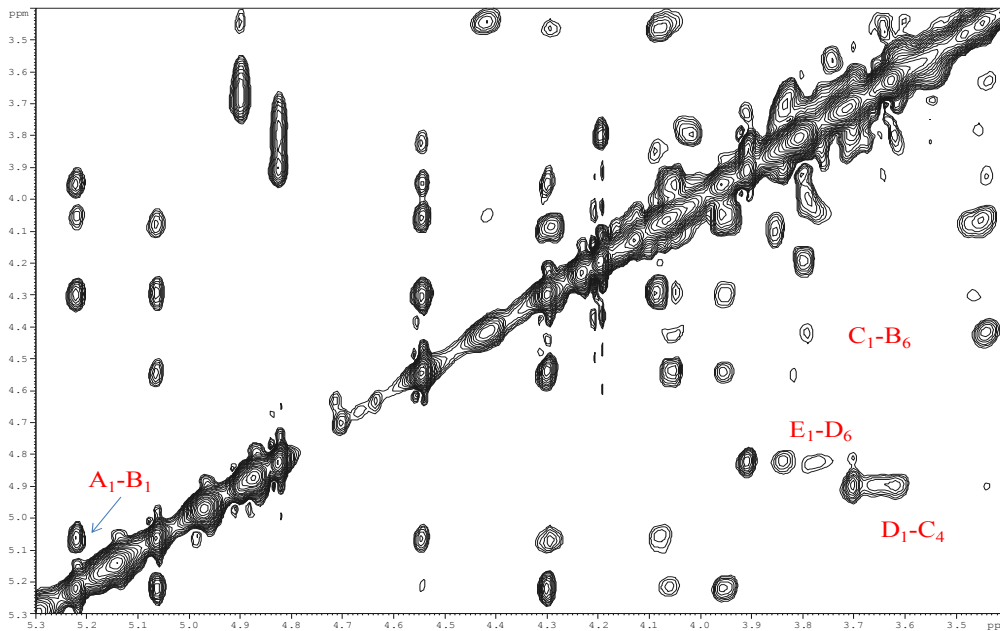


Fig 5.19. Zoom of the NOESY spectrum of the lipid A from *Bradyrhizobium* sp. BTAi1 and ORS278. Only *inter-glycosidic* NOE contacts are shown.

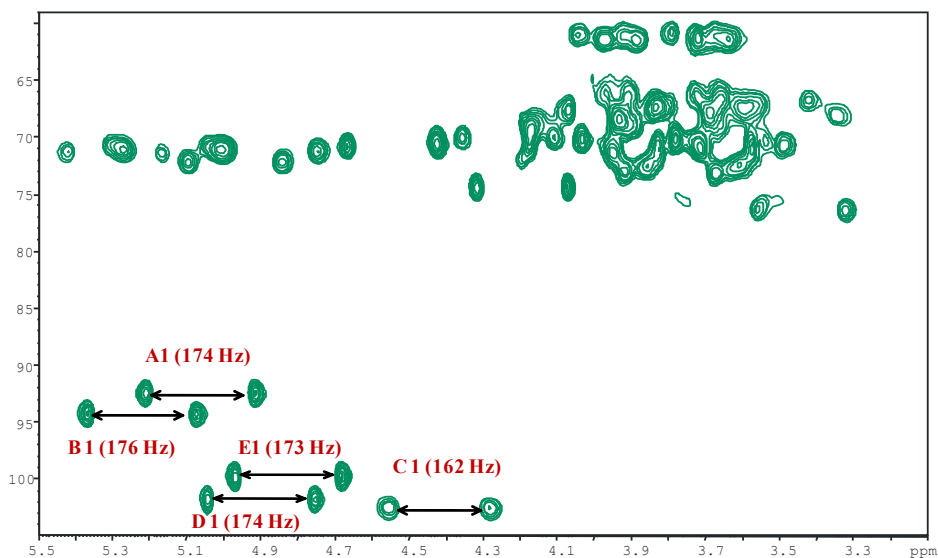


Fig 5.20. Zoom of the J -coupled ^1H , ^{13}C HSQC. $^1J_{\text{C,H}}$ (Hz) of anomeric positions are marked.

In summary, all NMR and MS data are in accordance with of the following lipid A from *Bradyrhizobium sp.* BTAi1 and ORS278:

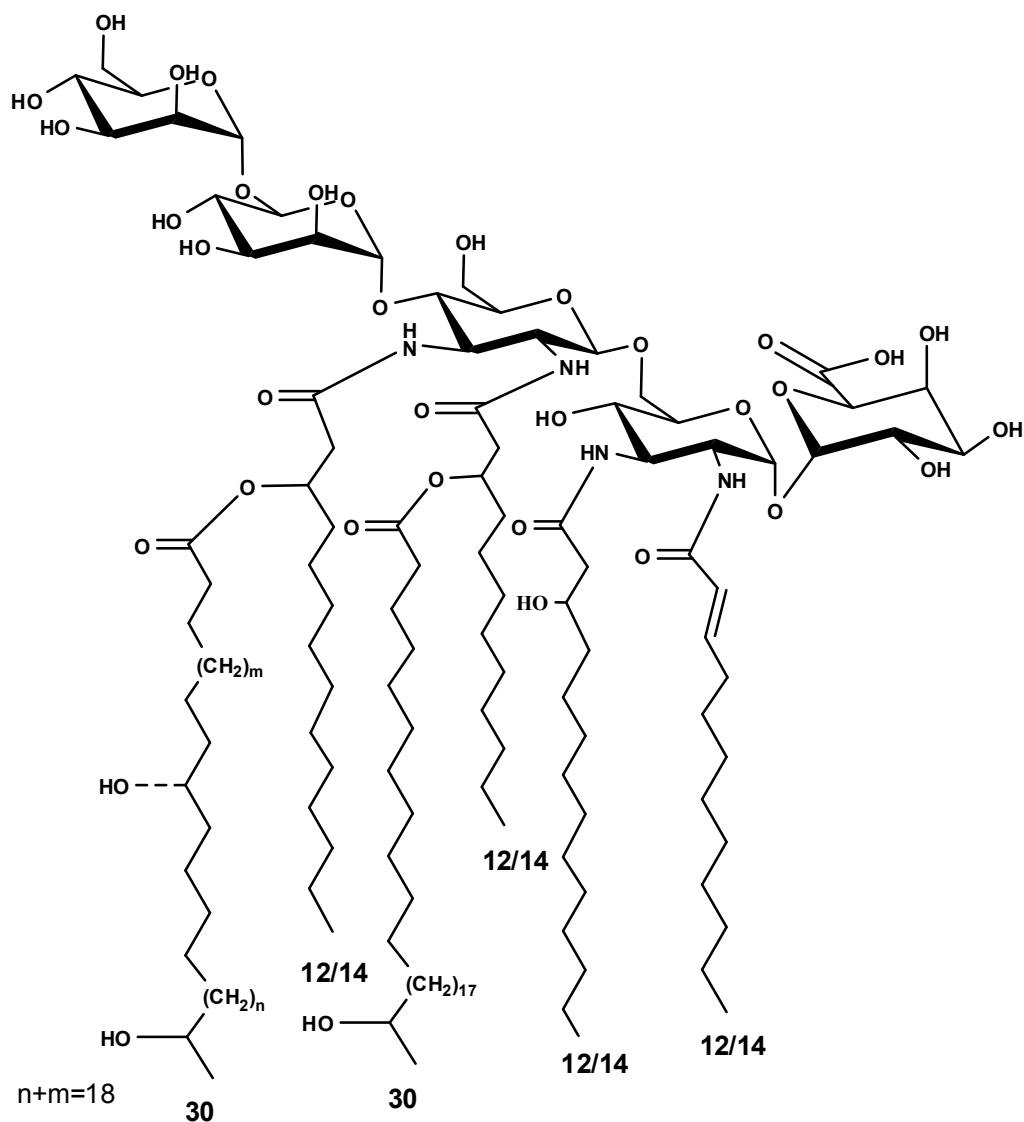


Fig.5.21 Lipid A structure of the ion species at m/z 2606 from *Bradyrhizobium sp.* BTAi1 and ORS278..

5.4 Biological assay on LPS from *Bradyrhizobium sp.* BTAi1 and ORS278

It was widely demonstrated that the LPS is a strong elicitor of immune system in plants. A number of reports details the effect of LPS on the induction of basal plant defences including the oxidative burst, NO production, calcium influx, the induction of PR gene expression and cell wall alteration that include deposition of callose and phenolics^[6]. Particularly, the callose polymer is a β -glucan produced in response to wounding and infection by pathogens.

In order to understand the activity of the LPS from *Bradyrhizobium sp.* BTAi1 and ORS278, the group of Prof. Newman of University of Copenhagen tested the formation of callose afterward the injection of LPS preparations in *Arabidopsis thaliana*. In the assay the positive control was constituted by the flagelline, a strong inducer of plant immune response, while treatment with water

and no-treatment were used as negative control. In Fig. 5.22 it has been shown callose deposits in *Arabidopsis* leaves after infiltration with *Bradyrhizobium* LPS preparations. The immune response owing to inoculation of LPS from both *Bradyrhizobium sp.* BTAi1 and ORS278 resulted to be very reduced respect to flagellin indicating that these LPSs are a very poor inducer of the immune system in plants.

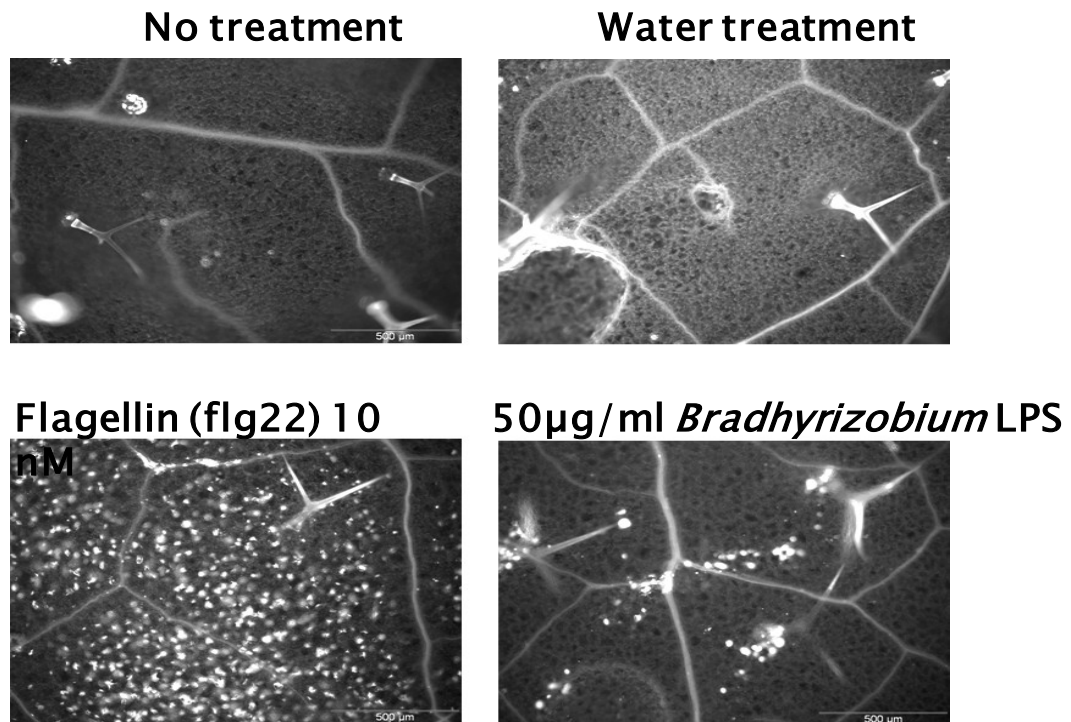
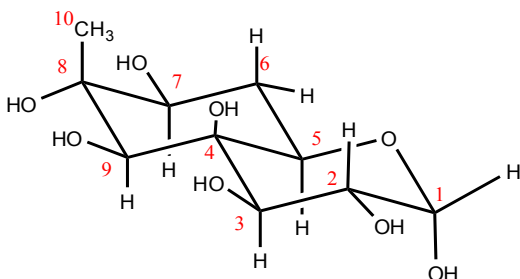


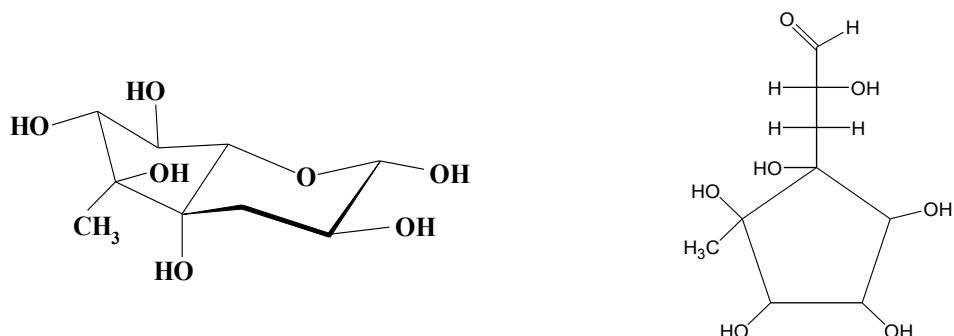
Fig.5.22. Callose deposits in *Arabidopsis* leaves after inoculation with *Bradyrhizobium* LPS preparations. Light zones reveal callose fluorescing after aniline blue staining.

Discussion

In this chapter we have reported the full chemical characterization of the LPS from two strains of *Bradyrhizobium sp.* BTAi1 and ORS278. The O-chain fraction from these LPSs is omopolymeric and characterized by the presence of a unique carbocyclic sugar that we named Bradyrhizose:



This sugar has been never found in nature and presents a characteristic structure with a trans-decaline junction. It constitutes the second example of carbocyclic sugar found so far in nature being the first one the caryose, isolated and characterized in our laboratories as component of homopolymeric O-chain polysaccharide from a phytopathogen *Burkholderia caryophilly* responsible of wilting of carnation [4,5].



The novel monosaccharide resulted to be linked in the polymer with α -(1 \rightarrow 7) linkage for *Bradyrhizobium sp.* BTAi1 O-chain, while the sugar fraction from *Bradyrhizobium sp.* ORS278 presented a mixture of polysaccharides constituted by α -(1 \rightarrow 7) and α -(1 \rightarrow 9) linked Bradyrhizose. The lipid A fraction from both strains of *Bradyrhizobium* resulted to have a very particular structure. The saccharide backbone was constituted by a pentasaccharide of Manp- α -(1 \rightarrow 6)-Manp- α -(1 \rightarrow 4)-GlcN-3Np- β -(1 \rightarrow 6)-GlcN-3Np- α -(1 \rightarrow 1)-GalAp in which the position 1 and 4' were not phosphorylated as very often occurring in the lipid A but substituted by Man and GalA residues; furthermore, the classical GlcNs were both substituted by two units of GlcN-3N. The fatty acid composition and their distribution on both GlcN-3N was performed with a combination of mass and NMR data. The lipid A resulted mainly composed of a mixture of hexa- and penta-acylated species with asymmetrical distribution of the acyl chains (arrangement 4+2, see Fig.5.21). Notable is the presence of lipid A species carrying an additional fatty acid ($\Delta m/z$ 512) not yet identified but likely present as tertiary fatty acid linked to the ω -1 position of the long fatty acids resulting in an unusual 5+2 arrangement of the acyl chains on the saccharide backbone. This lipid A structure is innovative since it is among the first *Bradyrhizobium* structures characterised so far. Komaniecka et al.^[7] recently published a lipid A structure from *Bradyrhizobium elkanii*. The lipid A backbone was constituted by a pentasaccharide of Manp- α -(1 \rightarrow 6)-Manp- α -(1 \rightarrow 4)-GlcN-3Np- β -(1 \rightarrow 6)-GlcN-3Np- α -(1 \rightarrow 1)-Manp mainly hexa-acylated.

In summary, we have identified a LPS from *Bradyrhizobium sp.* BTAi1 and ORS278, that present a relevant peculiarities from chemical and biological point of view. The peculiar chemical structures are probably correlated to a peculiar biological activity. Preliminary biological assays, performed

by the group of Prof. Newman of University of Copenhagen, demonstrated that the LPS from both strains of *Bradyrhizobium* showed a very reduced immune response (tested with callose formation) in *Arabidopsis thaliana*. The LPS does not trigger the plant immune response in order to permit the bacterial symbiotic infection and to establish a correct symbiosis with the host. Of course, these LPS will be also tested on their specific symbiont plants (*Aeschynomene sensitiva* or *indica*) in order to confirm the absence of immune response by the plant and also to clarify their role in the symbiotic process and in the nodule formation.

References

1. Ogutcu H, Adiguzel A, Gulluce M, Karadayi M, Sahin F. *Romanian Biotechnological Letters*, (2009) **14**: 4294-4300
2. Giraud, E. et al. *Science* (2007) **316**: 1307-1312
3. Harada N, Nakanishi K. Circular dichroic spectroscopy exciton coupling in organic chemistry. (1983).
4. Adinolfi M, Corsaro MM, De Castro C, Evidente A, Lanzetta R, Molinaro A, Parrilli M. *Carbohydrate Research* (1996) **284**: 111-118.
5. Adinolfi M, Corsaro MM, De Castro C, Evidente A, Lanzetta R, Molinaro A, Lavermicocca P, Parrilli M. *Carbohydrate Research* (1996) **284**: 119-133.
6. Dow MJ, Molinaro A, Cooper RM, Newman MA. *In Microbial Glycobiology Structures, Relevance and Applications*
7. Komaniecka I, Choma A, Lindner B, Holst O. *Chemistry*. (2010) **16**: 2922-9

Chapter 6
Experimental methods

6.1 Bacterial growth

6.1.1 *Burkholderia rhizoxinica* B1 (wt and *waaL* mut) and B4

Pure cultures of *B. rhizoxinica* were grown in Tryptic Soy Broth supplemented with 10 g L⁻¹ glycerol (TSB) or MGY medium (M9 minimal medium supplemented with 1.25 g L⁻¹ yeast extract and 10 g L⁻¹ glycerol) at 30 °C. For production of biomass, 18.5 L TSB media were inoculated with 1.5 L *B. rhizoxinica* pre-culture (OD600 = 1.4) and grown for 3 days under constant stirring (300 rpm) at 30 °C in a fermentor (final OD600 = 3.5). Biomass was harvested by centrifugation and washed twice with sucrose solution (300 mM) and lyophilized.

6.1.2 *Burkholderia cepacia* strain ASP B 2D

B. cepacia strain (ASP B 2D), isolated from *Asparagus officinalis*, and investigated as a potential biocontrol agent against *Fusarium oxysporum* (Coventry, unpublished), was supplied by the Plant Biotechnology Division, AECI Ltd, South Africa. The bacteria, being nonpathogenic to tobacco, had no adverse effect on the plants. The bacteria were cultivated in Nutrient Broth (BioLab) liquid medium, and were incubated at 25°C on a continuous rotary shaker for 8±10 days.

6.1.3 *Bradhirizobium* sp. BTAi1 and ORS278

Bradhirizobium sp. BTAi1 and ORS278 were grown in Arabinose-Gluconate [HM salts + 0.1% L-arabinose, 0.1% gluconate and 0,1% of yeast extract] medium [AGM]. The specific composition of medium expressed in g/l is reported in the following table.

Salt	g/L
<i>FeCl₃</i>	0,004 g
<i>CaCl₂</i>	0,010 g
<i>Na₂HPO₄</i>	0,125 g
<i>MgSO₄·7H₂O</i>	0,180 g
<i>Na₂SO₄</i>	0,250 g
<i>NH₄Cl</i>	0,320 g
<i>HEPES</i>	1.3 g
<i>MES</i>	1.1 g
<i>L-Arabinose</i>	1.0 g
<i>Na-Gluconate</i>	1.0 g
<i>Yeast extract</i>	1.0 g

The pH was adjusted to 6.6 with addition of NaOH 4M. The growth was performed in three days at 30 °C with shaking (100 rpm). The broth culture was centrifuged, the cells were washed with water, ethanol, acetone and ethyl ether and finally freeze-dried.

6.2 LPS and LOS extraction

Dried cells were extracted three times with a mixture of aqueous 90% phenol/chloroform/petroleum ether (2:5:8 v/v/v, 10 ml/g dry cells)^[1]. After removal of the organic solvents under vacuum, the LOS fraction was precipitated from phenol with water, washed first with aqueous 80% phenol, and then three times with cold acetone, each time centrifuged, and lyophilized.

LPS extraction was subsequently performed extracting the cells with a mixture of 90%phenol/water 1:1 at 68°C (20 ml/g dry cells), according to the conventional hot phenol-water procedure^[2]. The water and the diluted phenol phase were dialysed against water (12.000 kDa molecular weight cut-off). After dialysis, the extract was centrifuged and lyophilized.

The extracts were digested with DNase, RNase and Proteinase K, dialysed and freeze-dried again. Sodium dodecyl sulfate polyacrylamide gel electrophoresis (SDS-PAGE) was performed as described on all the fraction obtained. LPS and LOS are screened with a 13,5%-polyacrylamide gels were stained with silver nitrate according to the described procedure^[3].

6.3 Isolation of lipidA and oligo(OS)/polysaccharide(PO) fraction

6.3.1 Isolation of PO and OS from *Burkholderia rhizoxinica*

The O-polysaccharide chain from *B. rhizoxinica* wt (strain B1 and B4) LPS and core oligosaccharide fraction from Δ waaL::Kan^r mutant LOS were both obtained by SDS promoted acetate buffer hydrolysis (100 mM AcONa, pH 4.5, 0.1% SDS, 100°C, 4 h). After SDS removal treating sample with EtOH/HCl 2M, lipid A fraction was precipitated from aqueous solution centrifuging at 4 °C, 8500 g, 1 h. As for LPS, the supernatant (14 mg, 70% of LPS) was purified by gel-permeation chromatography on a Sephacryl S100-HR column (Pharmacia, 90 cm x 1.5 cm) using 0.05 M ammonium bicarbonate as eluent. As for LOS, the recovered supernatant containing oligosaccharide fractions, were purified by gel-permeation chromatography using a column (1.5 x 94 cm, total volume 166 mL) of Biogel P-6 in H₂O (flow: 13 mL h⁻¹) as described.^[4]

6.3.2 Isolation of polysaccharide and lipid A fractions from *Bradirhizobium sp.* BTAi1 and ORS278

In order to obtain polysaccharide fraction, aliquots of LPSs were dissolved in anhydrous hydrazine (1 ml/ 20 mg sample), stirred at 37°C for 90 min, cooled, poured into ice-cold acetone (10 ml/ml Hydrazine), and allowed to precipitate. The precipitate was then centrifuged (3000 × g, 30 min), washed twice with ice-cold acetone, dried, dissolved in water and lyophilized. This material was *N*-deacylated with 4 M KOH, 120 °C, 18h^[5]. Salts were removed using a Sephadex G-10 (Pharmacia) column.

Other aliquots of LPSs were hydrolyzed in 2% acetic acid (100°C, 5h) in order to obtain the lipid A fraction. It was purified according to Que and co-workers procedure^[6]. So, adequate amounts of chloroform and methanol were added to the hydrolysate to obtain chloroform/methanol/hydrolysate 2:2:1.8 (v/v/v), and the mixture was vigorously shaken, then centrifuged. The chloroform phase, containing the lipid A, was collected and washed twice with the water phase from a freshly prepared two-phase Bligh/Dyer mixture [chloroform/methanol/water, 2:2:1.8 (v/v/v)]. The organic phases were collected and dried.

6.4 Compositional analysis

Small amount of LPS, LOS and lipid A (200-500 µg) were utilized for sugar and fatty acid analysis. Monosaccharide analyses were realized by means of GC-MS of acetylated *O*-methyl glycosides derivatives, obtained after methanolysis (2M HCl/MeOH, 85°C, 18 h) and acetylation with acetic anhydride in pyridine (85°C, 30 min).

The absolute configuration of the monosaccharides was obtained according to the published method [7].

The ring size and the attachment points were determined by a methylation analysis. The sample was firstly methylated with CH₃I/NaOH in DMSO. After this treatment a chloroform/water extraction was performed, the organic phase was evaporated and hydrolysed with 4 M trifluoroacetic acid (100°C, 3h), carbonyl reduced with NaBD₄, acetylated with acetic anhydride: pyridine (1:1, v/v) and analysed by GC-MS.

For LOS oligosaccharides, methylation analysis of Kdo region was achieved by carboxy-methylation with methanolic HCl (0.1 M, 5 min) and then with diazomethane to improve LOS solubility in DMSO. Methylation was carried out as described above. LOS was hydrolyzed with 2

M trifluoroacetic acid (100°C, 1 h), carbonyl-reduced with NaBD₄, carboxy-methylated as described above, carboxyl-reduced with NaBD₄ (4°C, 18 h), acetylated and analyzed by GC-MS. Fatty Acids were revealed as their Methyl Esters derivatives. Total fatty acids content was determined after strong hydrolysis of Lipid A, first with 4 M HCl (100°C, 4 h) and subsequently with 5 M NaOH (100°C, 30 min). Fatty acids were then extracted with chloroform, methylated with diazomethane and analysed by GC-MS.

6.4.1 Absolute configuration of bradirizose.

LPS was hydrolysed with 2M HCl/MeOH, 85°C, 18 h and a mixture of α - β glycoside was obtained. The product was purified by gel-permeation chromatography using a column (1.5 x 94 cm, total volume 166 mL) of Biogel P-6 in H₂O (flow: 13 mL h⁻¹). The acid was evaporated and the residue was treated with dry pyridine (300 μ l) and p-bromobenzoyl chloride (stoichiometric quantity for derivatize four hydroxyl groups) at 30°C, following the reaction with MALDI experiments. The reaction was stopped when MALDI experiments revealed the presence of only three *O*-benzoyl derivate and the reaction was quenched by addition of MeOH, the solvent evaporated, and the residue purified by preparative TLC (20x20 cm Silica gel 60 TLC plates, Merck) with toluene/MeOH (8/2 v/v) as homogeneous solids. The spots are visualized by spraying the plate with 10% (v/v) ethanolic H₂SO₄ and charring. CD spectra were obtained in MeOH on a Jasco 710 instrument.

6.5 Mass spectrometry

6.5.1 *Burkholderia rhizoxinica waaL* mutant

MALDI mass spectra of native LOSs samples were performed in linear-mode on a Perspective (Framingham, MA, USA) Voyager STR instrument, equipped with delayed extraction technology. Ions formed by a pulsed laser beam (nitrogen laser, λ 337 nm) were accelerated by 24 kV and detected in negative-ion (LOSs) and in positive-ion polarity (Lipid A moieties). Sample preparation: the native LOSs required specific preparations as described in details^[8]. Briefly, a few aliquot of sample was first desalted with cation exchange beads (Dowex 50WX8, Sigma-Aldrich) in the ammonium form, prior to crystallization on the MALDI plate. A thin film composed of 2,4,6-trihydroxyacetophenone (THAP) and nitrocellulose (trans-blot membrane, BioRad) was used as matrix. MS analyses of Lipid A species were performed by dissolving the samples obtained after acetate buffer hydrolysis in CH₃Cl/CH₃OH (50:50). Such samples were finally mixed in a 1:1 (v/v)

ratio with the matrix solution [THAP, 75 mg mL⁻¹ in CH₃OH/trifluoroacetic acid/CH₃CN (7:2:1)], deposited onto the MALDI plate and left to crystallize at room temperature.

6.5.2 *Bradirhizobium sp.* BTAi1 and ORS278

Mass spectrometry of the native, the partially O-deacylated and the dephosphorylated lipid A was performed on a 4800 Proteomics analyzer MALDI time-of-flight/time-of-flight mass spectrometer (Applied Biosystems, Framingham, MA) in reflector mode, in positive polarity. Compounds were dissolved in CHCl₃/CH₃OH (50:50, v/v) at a concentration of 1mg/ml. Matrix solution was prepared by dissolving trihydroxyacetophenone (THAP) in CH₃OH/ 0.1% trifluoroacetic acid/CH₃CN (7:2:1, by volume) at a concentration of 75 mg/ml. One microliter of the sample/matrix solution (1:1, v/v) was deposited onto a Opti- TOFi 384 well plate and allowed to dry at room temperature. Mass spectra, resulting from the sum of 1250 laser shots, were obtained with a resolution higher than 10,000 (as the ratio between the mass of the peak and its full width at half maximum intensity) and with mass accuracy below 100 ppm.

6.6 NMR analysis

All NMR spectra were carried out using a Bruker DRX-600 equipped with a cryogenic probe. 1D and 2D ¹H-NMR spectra on oligo-/polysaccharides were recorded in D₂O, at 298K. Spectroscopic analyses on lipid A from *Bradirhizobium sp.* BTAi1 and ORS278 were carried out in a solution of MeOD:CDCl₃ (1:1, by vol.) at 298K. ROESY and NOESY spectra were measured using data sets (t₁ × t₂) of 4096 × 256 points with mixing times between 100 ms and 400 ms. Double quantum-filtered phase sensitive COSY experiments were performed using data sets of 4096 × 512 points; total correlation spectroscopy experiments (TOCSY) were performed with a spinlock time of 100 ms, using data sets (t₁ × t₂) of 4096 × 256 points. In all homonuclear experiments the data matrix was zero-filled in the F1 dimension to give a matrix of 4096 × 2048 points and was resolution enhanced in both dimensions by a cosine-bell function before Fourier transformation. Coupling constants were determined on a first-order basis from 2D phase sensitive double quantum filtered correlation spectroscopy (DQF-COSY) ^[9,10]. Heteronuclear single quantum coherence (HSQC) and heteronuclear multiple bond correlation (HMBC) experiments were measured in the ¹H-detected mode via single quantum coherence with proton decoupling in the ¹³C domain, using data sets of 2048 × 256 points. Experiments were carried out in the phase-sensitive mode according to the described method ^[11]. A 60 ms delay was used for the evolution of long-range connectivity in the HMBC experiment. In all heteronuclear experiments the data matrix was extended to 2048 × 1024 points using forward linear prediction extrapolation ^[11,12].

6.7 Biological assays

6.7.1 Testing of LPS mutants for defects in bacterial-fungal interaction

Bacterial cells were grown in MGY media without antibiotics until OD₆₀₀ = 1.5. Cell suspension (100 µL) was plated on one half of a nutrient agar plate (60 mm Ø). The second half of the plate was inoculated with endosymbiont-free (cured) *R. microsporus* ATCC62417. Ten plates of each wild-type and mutant strain were prepared in parallel. Plates were dried and incubated at 30 °C. In liquid culture, 800 µL of VK-media (1% corn starch, 0.5% glycerol, 1 % yeast extract, 1 % corn steep, 1 % CaCO₃, pH = 6.5) were inoculated with 0.1 cm³ of *R. microsporus* mycelia and 100 µL of *B. rhizoxinica* pre-culture (OD = 1.5). Sporulation of plates was examined by eye. Light microscopy and test for survival of bacteria was carried out after staining with LIVE/DEAD® BacLight™ fluorescent dyes (Invitrogen Corporation, Karlsruhe, Germany).

6.7.2 Callose deposition

LPS (50µg/mL), flagellin (flg22) (100nM) and water controls were infiltrated by needleless syringe into the abaxial surface of four leaves on three replicate plants. After 20h leaves were carefully cut from the plants, decolorized with 70% ethanol at 70°C for 20 min, then rinsed with 50% ethanol and finally with water. Leaves were then stained with Leuco aniline blue (Fluka,) (0.05% in 0.15M K₂HPO₄, pH 8.2) in the dark for 30 min. Stained leaves were mounted in 50% glycerol and examined by fluorescence microscopy (Olympus, BX60). Average numbers of callose depositions per field of view (0.79mm²) ± standard deviations. Scale bar: 200µM.

References

1. Galanos C, Lüderitz O, Westphal O. A new method for the extraction of R lipopolysaccharides. *Eur. J. Biochem.* (1969) **9**: 245-249
2. Westphal O, Jann K. Bacterial lipopolysaccharides. Extraction with phenol / water and further application of the procedure. *Meth. Carbohydr. Chem.* (1965) **5**: 83-91.
3. Kittelberger R, Hilbink F. Sensitive silver-staining detection of bacterial lipopolysaccharides in polyacrylamide gels. *J. Biochem. Biophys. Meth.* (1993).**26**: 81-86.
4. Silipo A, Molinaro A, Ieranò T, De Soyza A, Sturiale L, Garozzo D, Aldridge C, Corris PA, Khan CMA, Lanzetta R, Parrilli M, *Chemistry* (2007), **13**: 3501-3511.
5. Holst, O. 2000. In *Methods in Molecular Biology, Bacterial Toxins: Methods and Protocols* (Holst, O., ed). Humana Press Inc., Totowa, NJ. 345-353.
6. Que NLS, Lin S, Cotter RJ, Raetz CRH. *J. Biol. Chem.* (2000), **275**: 28006-28016.
7. Leontein K, Lönngren J, Determination of the absolute configuration of sugars by gas liquid chromatography of their acetylated 2-octyl glycosides. *Meth. Carbohydr. Chem.* (1978) **62**. 359- 362.
8. Sturiale L, Garozzo D, Silipo A, Lanzetta R, Parrilli M, Molinaro A. *Rapid. Commun. Mass Spectrom.* (2005). **19**: 1829-1834.
9. Piantini U, Sørensen OW, Ernst RR, Multiple quantum filters for elucidating NMR coupling networks. *J. Am. Chem. Soc.* (1982).**104**: 6800-6801.
10. States DJ, Haberkorn RA, Ruben DJ. A two dimensional nuclear overhauser experiment with pure absorption phase in four quadrants. *J. Magn. Res.* (1982),**48**. 286-292.
11. de Beer R, van Ormondt D. Analysis of NMR data using time domain fitting procedures. *NMR Basic Princ. Prog.* 1992. **26**: 201.
12. Hoch JC, Stern AS. In Hoch, J.C. and Stern, A.S. (Eds.) *NMR data processing*. Wiley Inc. New York. 1996 77-101.

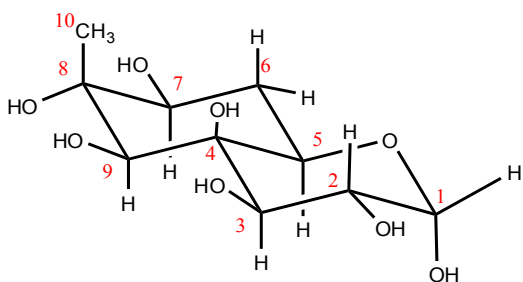
CONCLUSIONS

This project was entirely focused on increasing the knowledge on the structure/activity relationships of LPS in plant immune system and their roles in instauration of important biological process like symbiosis. In the first part of the work, chemical characterization of LPSs from different *Burkholderia* species was presented. Firstly, we have completely characterized the LPS and the LOS produced by the endosymbiont *Burkholderia rhizoxinica* strain B1 isolated from *Rhizopus microsporus* fungi responsible for causing rice seedling blight. The O-chain fraction from LPS was constituted by a peculiar homopolymer of $[2-\beta\text{-Gal}]_n$ that presented a particular biological activity. In fact, biological results demonstrated that bacteria were capable to biosynthesize polygalactofuranose O-antigen, a new structure if related to the O-chain from other known *Burkholderia* species. Since GalF conjugates are especially abundant in cell wall of filamentous fungi, the biosynthesis by *Burkholderia rhizoxinica* of this peculiar polysaccharide is a strategy used by bacteria to protect themselves against fungal defense mechanisms by mimicking the fungal cell wall components. This phenomenon is known as “molecular mimicry”, and can be found in other associations of bacteria with higher organisms. For example, beneficial bacteria inhabiting mammalian intestines decorate their surface with fucose, which is an abundant surface molecule of intestinal epithelial cells.

We have also reported the chemical characterization of the LPS from *Burkholderia rhizoxinica* strain B4 isolated from *Rhizopus microsporus* var. *microsporus*. The O-chain domain was constituted by a mixture of two polysaccharides with different primary structure and containing a large quantity of rhamnose. It is very typical in *Burkholderia* O-chain structure since rhamnose residues increase the hydrophobic character of the O-antigen moiety. The lipid A moiety possessed, in all analyzed *Burkholderia rhizoxinica* strains the typical carbohydrate backbone characterized by a $[P\rightarrow 4-\beta\text{-D-GlcpN-(1}\rightarrow 6)\text{-}\alpha\text{-D-GlcpN-1}\rightarrow P\rightarrow]$ sequence and revealed to be constituted by a mixture of penta and tetra acylated species carrying on the polar heads the non-stoichiometric presence of Ara4N, that constitute an expedient used by bacteria to avoid the attack from host-released cationic antimicrobial peptides and from different classes of antibiotic molecules. Similar data were founded also for lipid A isolated from *Burkholderia cepacia* strain ASP B 2D, an endophytic bacterium. In this case the lipid A has been found to possess a identical structure of lipid a from *Burkholderia rhizoxinica* but with higher amount of under-acylated species and a lower amount of phosphate. Probably, the presence of under-acylated/phosphorylated species and the presence of Ara-4N residues might allow *B. cepacia* strain ASP B 2D to survive as an endophyte in plant host by reducing the net charge. In addition to these data, new insights into the biochemical

action mechanism of *B. cepacia*-derived lipid A as a MAMP, a resistance elicitor and triggering agent of transcriptional changes during defense responses have been obtained. The results showed that the lipid A was perceived by *A. thaliana* leading to up-regulation of a large broad of genes, some of which are associated with defense responses and biotic and abiotic stresses, while others are associated with metabolic reprogramming of cellular activities in support of immunity and defense.

In the last part of the project, we have reported the full chemical characterization of the LPS from *Bradyrhizobium sp.* BTAi1 and ORS278, peculiar strains that do not possess a canonical genes for nod factors biosynthesis. The O-chain fraction from these LPSs is formed by a homopolymer with the presence of a unique carbocyclic sugar that we named Bradyrhizose:



The novel monosaccharide resulted to be linked in the polymer with α -(1 \rightarrow 7) linkage for *Bradyrhizobium sp.* BTAi1 O-chain, while the sugar fraction from *Bradyrhizobium sp.* ORS278 presented a mixture of polysaccharides constituted by α -(1 \rightarrow 7) and α -(1 \rightarrow 9) linked Bradyrhizose. Important structural results were found for what concerns the lipid A fraction from both strains of *Bradyrhizobium*. The saccharide backbone was constituted by a pentasaccharide of Manp- α (1 \rightarrow 6)-Manp- α -(1 \rightarrow 4)-GlcN-3Np- β -(1 \rightarrow 6)-GlcN-3Np- α -(1 \rightarrow 1)-GalAp in which position 1 and 4' were not phosphorylated but substituted by Man and GalA residues; furthermore, the classical GlcNs were both replaced by two units of diaminoglucose. The lipid A resulted manly composed of a mixture of hexa- and penta-acylated species with asymmetrical distribution of the acyl chains (arrangement 4+2, see Fig. 5.20) . Notable is the presence of lipid A species carrying an additional fatty acid ($\Delta m/z$ 512) not yet identified but likely present as terziary fatty acid linked to the ω -1 position of the long fatty acids and resulting in an unusual 5+2 arrangement of the acyl chains on the saccharide backbone. This lipid A structure is innovative since it among the first *Bradyrhizobium* structures characterized so far. Preliminary biological assays demonstrated that the LPS from both strains of *Bradyrhizobium* showed a very reduced immune response (tested with

callose formation) in *Arabidopsis thaliana*. The LPS does not trigger the plant immune response in order to permit the bacterial symbiotic infection and to establish a correct symbiosis with the host. The obtained results are a clear demonstration of the importance of LPSs in bacterial life and in its adaptation to the host environment. Moreover, structural and biological data obtained in this PhD thesis constitute a good start point to clarify, at molecular level, the role of LPS in both plant immune system and symbiotic process.

An Unusual Galactofuranose Lipopolysaccharide That Ensures the Intracellular Survival of Toxin-Producing Bacteria in Their Fungal Host**

Maria R. Leone, Gerald Lackner, Alba Silipo, Rosa Lanzetta, Antonio Molinaro,* and Christian Hertweck*

Bacteria are involved in a plethora of interactions with higher organisms; these interactions can be beneficial or detrimental to the host.^[1] Irrespective of the type of symbiosis, in all cases the fine-tuned communication between the organisms is mediated by biomolecules. Diffusible chemical signals allow for long-range communication,^[2] whereas carbohydrate structures (antigens) coating the cell surfaces enable cell–cell recognition.^[3] Such antigenic components are highly specific and particularly important when bacteria have direct physical contact with the host, or even invade eukaryotic cells.^[4,5] Among the most important and ubiquitously occurring surface determinants of Gram-negative bacteria are lipopolysaccharides (LPSs).^[3,5,6] LPSs share a common architecture featuring a hydrophilic heteropolysaccharide moiety that is typically composed of a core oligosaccharide and an O-specific polysaccharide. This complex carbohydrate is covalently linked to the third component, a lipophilic moiety termed lipid A, which is embedded in the outer leaflet of the membrane.^[3] The ability of a host organism to recognize LPSs and the consequences of this recognition in infection and symbiosis have been the subject of many ground-breaking studies and constitute a major research area.^[7] However, these studies have focused on LPSs in the context of bacteria–animal or bacteria–plant interactions.^[3–5]

There is an evident gap of knowledge on the role of LPSs in microbe–microbe interactions, such as bacterial–fungal encounters, which are crucial in the environment.^[8]

We have recently unveiled a unique symbiosis of the rice blight fungus *Rhizopus microsporus*, and intracellular bacteria (*Burkholderia rhizoxinica*)^[9], which serve their fungal host as toxin factories.^[10–12] The bacterial endosymbionts produce numerous antimetabolic macrolides of the rhizoxin complex that efficiently stall cell division in rice plants and most other eukaryotes.^[13] Notably, the fungal host itself has become resistant to the toxin as a result of a mutation in the tubulin sequence.^[14] Thus, it is likely that *Rhizopus–Burkholderia* symbiosis underwent a parasitism–mutualism shift during evolution.^[15] Still, it is a mystery how the endobacteria can survive within fungal host cells and how they interact with their host by means of chemical recognition and communication.^[12] Herein we disclose the complete structure of an unusual LPS from *B. rhizoxinica*, elaborate its molecular basis, and provide the first evidence that the O antigen is a critical molecular determinant for the stability of the symbiosis.

To elucidate the structure of the LPS of the endofungal bacteria and its role in the interaction, we used a combination of GLC–MS, MALDI MS, and a series of 2D NMR experiments. Following hydrolysis of the LPS in an acetate buffer, the fraction containing lipid A was recovered as a sediment by centrifugation. The pure O polysaccharide (OPS), present in the supernatant, was obtained by gel permeation chromatography. Lipid A fatty acid analysis revealed the presence of (*R*)-3-hydroxyhexadecanoic acid (16:0 (3-OH)) with an amide linkage, and (*R*)-3-hydroxytetradecanoic acid (14:0 (3-OH)) and tetradecanoic acid (14:0) with ester linkages. According to chemical analysis, MALDI MS, and NMR spectroscopic data, the *B. rhizoxinica* LPS lipid A substructure has a typical *Burkholderia* lipid A architecture with a β -1 \rightarrow 6 D-GlcN disaccharide and the nonstoichiometric presence of two L-Ara4N units (Scheme 1).^[16]

The OPS was also characterized by a combination of chemical analysis and 2D NMR spectroscopy, in particular COSY, TOCSY, NOESY, HSQC (see Figures S1–S3 in the Supporting Information), and F2-coupled HSQC. The ¹H NMR spectrum showed a single anomeric signal indicative of a single-spin system, which was fully assigned by homonuclear 2D NMR spectroscopy, whereas from HSQC spectra it was possible to assess the furanosidic nature and anomeric configuration of the monosaccharide. These data, in conjunction with chemical analysis, revealed that the OPS is a

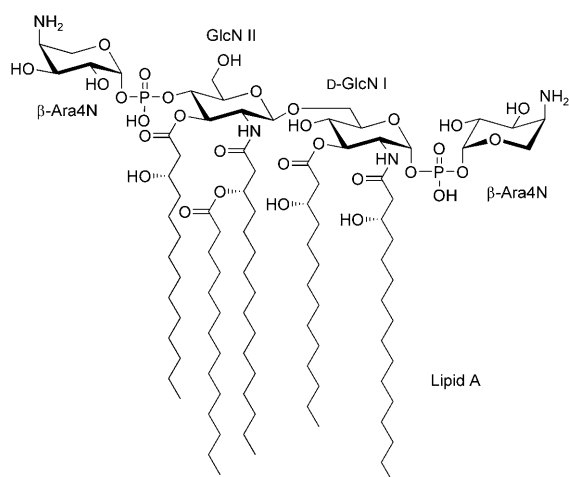
[*] Dipl.-Biochem. G. Lackner,^[†] Prof. Dr. C. Hertweck
Abteilung für Biomolekulare Chemie
Leibniz-Institut für Naturstoff-Forschung und Infektionsbiologie,
HKI, Beutenbergstrasse 11a, 07745 Jena (Germany)
Fax: (+49) 3641-532-0804
E-mail: christian.hertweck@hki-jena.de

Prof. Dr. C. Hertweck
Friedrich-Schiller-Universität, Jena (Germany)
Dr. M. R. Leone,^[†] Prof. Dr. A. Silipo, Prof. Dr. R. Lanzetta,
Prof. Dr. A. Molinaro
Dipartimento di Chimica Organica e Biochimica
Università di Napoli Federico II
via Cintia 4, 80126 Napoli (Italy)
E-mail: molinaro@unina.it

[†] These authors contributed equally.

[**] We thank the JCVI Annotation Service for providing us with automatic annotation data and the manual annotation tool Manatee, K. Graupner for PCR screening of mutants, L. Sturiale for MS spectra, and G.-M. Schwinger for fungal-strain maintenance. This research was supported by the graduate school of excellence ILRS/JSMC (C.H.) and by PRIN MIUR 2007/2008 (R.L. and A.M.).

Supporting information for this article is available on the WWW under <http://dx.doi.org/10.1002/anie.201003301>.



Scheme 1. Structure of lipid A of endosymbiotic *B. rhizoxinica*. Ara4N = 4-amino-4-deoxy-L-arabinose, GlcN = 2-amino-2-deoxy-D-glucose.

homopolymer of 2-substituted D-galactofuranose, $[\rightarrow 2)\text{-}\beta\text{-D-Galf-(1}\rightarrow)_n$. This unusual type of polysaccharide is fully unprecedented for *Burkholderia* spp. and related bacteria. Furthermore, the existence of $[\rightarrow 2)\text{-}\beta\text{-D-Galf-(1}\rightarrow)_n$ in nature has only been implicated once, on the basis of a limited data set.^[17] The discovery of an antigenic poly-D-galactofuranose chain in an endofungal bacterium is particularly intriguing, since Galf conjugates have been found to be especially

abundant in filamentous fungi.^[18,19] Furthermore, structurally related galactofuranan bioactive antigens have been identified in fungi.^[20,21] Thus, it is well conceivable that the O antigen mimics structural components of the host cell.

To test this hypothesis and gain insight into the molecular basis of LPS formation, we analyzed shotgun-sequence data of the *B. rhizoxinica* genome and searched for candidate genes for LPS biosynthesis. Automated annotation revealed a gene cluster comprising 29 open reading frames, 22 of which code for proteins similar to known enzymes involved in LPS biosynthesis (Figure 1 a; see also the Supporting Information). The majority of the genes in this locus code for the biosynthesis and transfer of outer-core and O-antigen building blocks, including the pathway for dTDP-L-rhamnose (*rmlA-F*; dTDP = deoxythymidine diphosphate). More importantly, the finding of genes that code for a UDP-galactopyranose mutase (Glf; UDP = uridine diphosphate)^[22] and a UDP-glucose-4-epimerase (GalE) is fully in line with the elucidated LPS O-antigen structure, since these enzymes are well known to be involved in the formation of UDP-D-galactofuranose (Figure 1 b).^[23] Furthermore, the gene cluster contains several glycosyl-transferase genes, and two genes (*wzm* and *wzt*) for an ABC transporter system that shuttles membrane-anchored O-antigen chains from the cytosol to the periplasm prior to ligation to the core oligosaccharide.^[24] Finally, we found a gene coding for an O-antigen ligase (WaaL). WaaL is essential for the transfer of the O antigen to the outer core to finish the LPS-assembly process.^[24,25] Consequently, mutants devoid of the O-antigen ligase gene

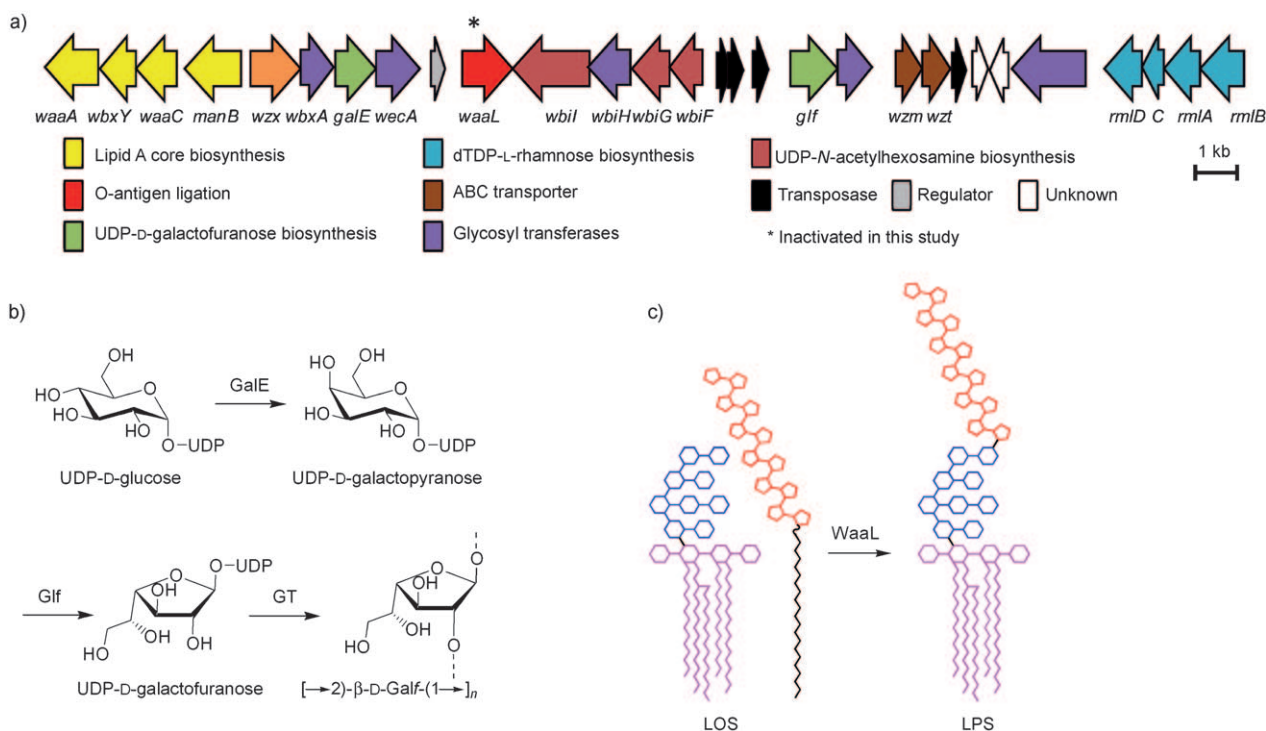
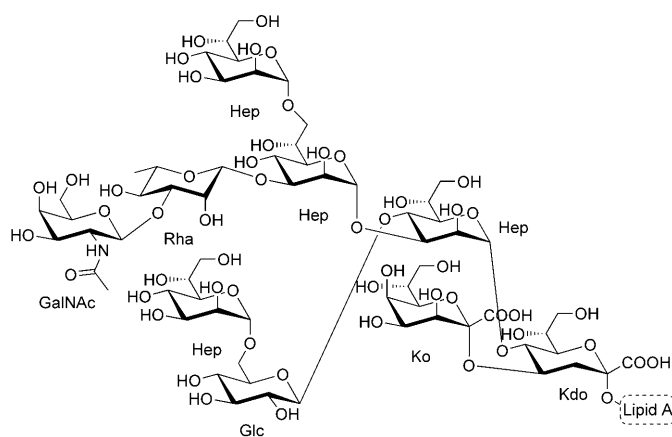


Figure 1. a) Schematic illustration of the LPS biosynthesis gene cluster of *B. rhizoxinica*. Protein-coding genes are indicated as arrows. Colors represent deduced functional categories of gene products. See Table S3 in the Supporting Information for details. b) Model for the biosynthesis of UDP-D-galactopyranose, the O-antigen building block of *B. rhizoxinica* (GT = glycosyl transferase). c) Attachment of the O antigen to the LOS by the ligase WaaL.

($\Delta waaL$ mutants) would lack the O-antigenic chain on the cell surface (rough phenotype). To study the role of the O antigen *in vivo*, we created an O-antigen ligase mutant by replacing the *waaL* gene with a kanamycin-resistance cassette ($\Delta waaL::Kan^r$). Thus, we created a suicide vector containing a counter-selectable marker: a mutated phenylalanyl-tRNA synthetase gene *pheS*.^[26] After various selection rounds, we succeeded in generating the desired mutant with a rough colony phenotype indicative of the presence of a lipooligosaccharide (LOS); that is, with the core oligosaccharide region attached to lipid A, but with no O antigen.

The full structure of the LOS core region of the mutant was deduced by a combination of chemical analysis, MALDI mass spectrometry, and 2D NMR spectroscopy. Seven anomeric signals were identified in the 1H NMR spectrum. Furthermore, the upfield-shifted signals were identified as the 3-H methylene hydrogen atoms of the 3-deoxy-D-manno-oct-2-ulosonic (Kdo) residue (see the Supporting Information). The proton resonances of all spin systems were identified from DQF-COSY and TOCSY spectra and were used to assign the carbon resonances in the HSQC spectrum. The anomeric configuration of each monosaccharide was assigned on the basis of the $^3J_{1-H,2-H}$ coupling constants observed by DQF-COSY and the intraresidual NOE contacts observed in the ROESY and NOESY spectra, whereas the values of the vicinal $^3J_{H,H}$ coupling constants enabled the determination of the relative configuration of each sugar residue. The absence of chemical-shift values above 80 ppm for ring carbon atoms confirmed that all monosaccharides were in the pyranose form. The relative intensities of the anomeric signals suggested the existence of a mixture of oligosaccharides with different carbohydrate-chain lengths owing to the presence of the Kdo reducing end as multiple ring isomers or as lactone forms. Once 1H and ^{13}C resonances had been attributed to each spin system, it was possible to assign the oligosaccharide-chain resonances from the interglycosidic contacts found in the NOESY and ROESY spectra (see Table S1 in the Supporting Information for complete structural assignment). The full structure was confirmed by mass spectrometry (see Table S2 and Figures S7 and S8 in the Supporting Information). The core of the LPS from *B. rhizoxinica* consists of a nonasaccharide backbone comprising four heptose (Hep) residues as well as a GalNAc, a Glc, a rhamnose (Rha), a 3-deoxy-D-manno-oct-2-ulosonic acid (Kdo), and a D-glycero-D-talo-oct-2-ulosonic acid (Ko) unit (Scheme 2). The core oligosaccharide structure of the *B. rhizoxinica* LOS resembles that of *B. multivorans*,^[27] especially in terms of the inner core and the presence of a further heptose residue attached to the β -Glc unit. The outer core is different from but still coherent with LOS structures from *Burkholderia* spp.^[16] Finally, the structure of the truncated LPS clearly showed that the mutant lacks the O antigen.

To test whether this mutant is capable of initiating a stable symbiosis with the host fungus, we mixed pure cultures of *B. rhizoxinica* (wild-type and mutant) with endosymbiont-free (cured) *R. microsporus* cultures. Usually, wild-type bacteria readily reinfest the fungus, reestablish the symbiosis, and elicit sporulation of the host. Cured fungi, however, are unable to sporulate.^[28] Consequently, we considered host



Scheme 2. Core oligosaccharide structure of the R-LPS (LOS) from the O-antigen-ligase mutant ($\Delta waaL::Kan^r$). GalNAc = 2-amino-2-deoxy-D-galactose, Glc = D-glucose, Hep = L-glycero-D-manno-heptose, Rha = L-rhamnose.

sporulation as an indicator for the reestablishment of symbiosis. Thus, we monitored sporulation behavior over time both on agar plates and in liquid culture by using 48-well plates. Cocultivation of the cured fungus with wild-type bacteria typically resulted in high levels of successful reinfection, which is mirrored by about 90% host sporulation. In stark contrast, the $\Delta waaL$ mutant showed significantly reduced reinfection/sporulation rates (Figure 2). In cases in which reinfection with $\Delta waaL::Kan^r$ mutants gave a positive response, the intensity of host sporulation was much lower than with the wild type. When the fungus was reinfected with $\Delta waaL::Kan^r$ mutants, intracellular bacteria could be detected by microscopic examination, albeit in greatly reduced number (< 10%) relative to the wild type. Furthermore, after the subcultivation of reinfected fungi, we observed persistently low host sporulation or even a complete lack of spore formation.

Our findings provide strong evidence that the O antigen plays a crucial role in the bacterial–fungal symbiosis. Since the carbohydrate coating supports the processes of host infection and triggering of sporulation, it seems to serve as a key determinant in chemical-recognition processes during infection and colonization of the host. Furthermore, it is a prerequisite for the long-term intracellular survival of the endosymbiont and for the formation of a stable bacterial–fungal association. A plausible explanation for these observations is given by a model in which the polygalactofuranose O antigen protects endobacteria against as yet unknown fungal defense mechanisms. Such strategies are only known from associations of bacteria with higher organisms. For example, beneficial bacteria inhabiting mammalian intestines decorate their surface with fucose, which is an abundant surface molecule of intestinal epithelial cells.^[29] It is also well-known that some other Gram-negative pathogens, such as *Neisseria* and *Helicobacter*, decorate their surface with blood-group antigens.^[30]

In summary, we have fully elucidated the first LPS structure of a bacterium living within a fungus and revealed

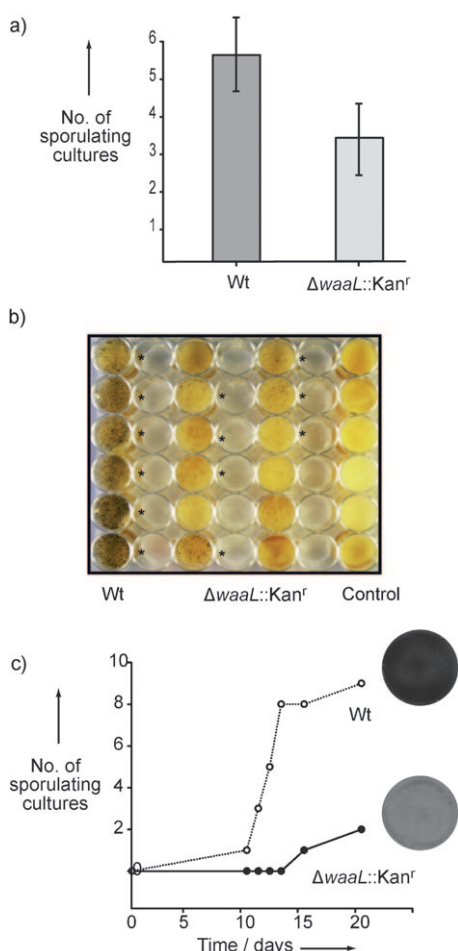


Figure 2. Testing of O-antigen mutants for defects in the symbiont–host interaction by the monitoring of reinfection/sporulation rates. a) Bar chart showing re-infection/sporulation rates in liquid cultures. Six cultures were observed in parallel, and each experiment was repeated four times. Mean values were calculated from the results of all experiments; error bars show the standard deviation. Wild-type (Wt) bacteria reinfected the host with significantly higher rates than those observed for O-antigen-ligase ($\Delta waaL::Kan^r$) mutants. b) Photograph of a completed re-infection/sporulation experiment (liquid culture); sporulating cultures are marked with an asterisk. Wild-type controls (left) showed strong sporulation; O-antigen mutants (middle) showed decreased sporulation; negative controls (endosymbiont-free *R. microsporus*) did not sporulate. c) Re-infection experiment on agar plates, as observed over time.

the presence of a unique 1,2- β -D-galactofuranose glycoconjugate. To gain insight into the biological function of the O antigen, we sequenced an LPS-biosynthesis gene locus, which fully supported the structure elucidation. Furthermore, we succeeded in generating a targeted O-antigen-ligase mutant, which was incapable of producing the polygalactofuranoside conjugate, and confirmed the absence of the O-antigenic chain by chemical analysis. A sporulation assay and microscopic investigation finally revealed that the intracellular survival of the mutant was critically impaired, and that the O antigen is a crucial component for stable bacterial–fungal symbiosis to be established and maintained. Since

galactofuranose units are particularly abundant in filamentous fungi, one may conclude that the galactofuranosyl O antigen serves as mimicry to put the bacterium into “stealth mode”. To our knowledge, this study is the first to shed light on the role of surface carbohydrates in an interaction between endobacteria and fungi. Our results disclose the role of a glycoconjugate in a novel biological context and thus fill an evident gap in the current knowledge on LPS-mediated communication.

Received: May 31, 2010

Published online: August 16, 2010

Keywords: bacteria · carbohydrates · cell recognition · lipopolysaccharides · O antigens

- [1] C. Dale, N. A. Moran, *Cell* **2006**, *126*, 453.
- [2] R. Dudler, L. Eberl, *Curr. Opin. Biotechnol.* **2006**, *17*, 268.
- [3] A. Silipo, C. De Castro, R. Lanzetta, M. Parrilli, A. Molinaro in *Prokaryotic Cell Wall Compounds—Structure and Biochemistry* (Eds.: H. König, H. Claus, A. Varma), Springer, Heidelberg, **2010**, p. 133.
- [4] I. Lerouge, J. Vanderleyden, *FEMS Microbiol. Rev.* **2002**, *26*, 17.
- [5] M. A. Newman, J. M. Dow, A. Molinaro, M. Parrilli, *J. Endotoxin Res.* **2007**, *13*, 69.
- [6] A. Silipo, G. Erbs, T. Shinya, J. M. Dow, M. Parrilli, R. Lanzetta, N. Shibuya, M. A. Newman, A. Molinaro, *Glycobiology* **2010**, *20*, 406.
- [7] C. E. Bryant, D. R. Spring, M. Gangloff, N. J. Gay, *Nat. Rev. Microbiol.* **2010**, *8*, 8.
- [8] M. T. Tarkka, A. Sarniguet, P. Frey-Klett, *Curr. Genet.* **2009**, *55*, 233.
- [9] L. P. Partida-Martinez, C. Hertweck, *Nature* **2005**, *437*, 884.
- [10] L. P. Partida-Martinez, C. Hertweck, *ChemBioChem* **2007**, *8*, 41.
- [11] B. Kusebauch, B. Busch, K. Scherlach, M. Roth, C. Hertweck, *Angew. Chem.* **2009**, *121*, 5101; *Angew. Chem. Int. Ed.* **2009**, *48*, 5001.
- [12] G. Lackner, L. P. Partida-Martinez, C. Hertweck, *Trends Microbiol.* **2009**, *17*, 570.
- [13] K. Scherlach, L. P. Partida-Martinez, H.-M. Dahse, C. Hertweck, *J. Am. Chem. Soc.* **2006**, *128*, 11529.
- [14] I. Schmitt, L. P. Partida-Martinez, R. Winkler, K. Voigt, A. Einax, J. Wöstemeyer, C. Hertweck, *ISME J.* **2008**, *2*, 632.
- [15] G. Lackner, N. Moebius, K. Scherlach, L. P. Partida-Martinez, R. Winkler, I. Schmitt, C. Hertweck, *Appl. Environ. Microbiol.* **2009**, *75*, 2982.
- [16] A. De Soya, A. Silipo, R. Lanzetta, J. R. Govan, A. Molinaro, *Innate Immun.* **2008**, *14*, 127.
- [17] M. B. Perry, *Biochem. Cell Biol.* **1990**, *68*, 808.
- [18] W. Morelle, M. Bernard, J. P. Debeauvais, M. Buitrago, M. Tabouret, J. P. Latgé, *Eukaryotic Cell* **2005**, *4*, 1308.
- [19] J. P. Latgé, *Med. Mycol.* **2009**, *47*, S104.
- [20] M. M. Corsaro, C. De Castro, A. Evidente, R. Lanzetta, A. Molinaro, L. Mugnai, M. Parrilli, G. Surico, *Carbohydr. Res.* **1998**, *308*, 349.
- [21] M. M. Corsaro, C. De Castro, A. Evidente, R. Lanzetta, A. Molinaro, M. Parrilli, L. Sparapano, *Carbohydr. Polym.* **1998**, *37*, 167.
- [22] R. Koplin, J. R. Brisson, C. Whitfield, *J. Biol. Chem.* **1997**, *272*, 4121.
- [23] L. L. Pedersen, S. J. Turco, *Cell. Mol. Life Sci.* **2003**, *60*, 259.
- [24] C. R. Raetz, C. Whitfield, *Annu. Rev. Biochem.* **2002**, *71*, 635.
- [25] P. D. Abeyrathne, C. Daniels, K. K. Poon, M. J. Matewish, J. S. Lam, *J. Bacteriol.* **2005**, *187*, 3002.

- [26] A. R. Barrett, Y. Kang, K. S. Inamasu, M. S. Son, J. M. Vukovich, T. T. Hoang, *Appl. Environ. Microbiol.* **2008**, *74*, 4498.
- [27] T. Ieranò, A. Silipo, L. Sturiale, D. Garozzo, H. Brookes, C. M. A. Khan, C. Bryant, F. F. Gould, P. A. Corris, R. Lanzetta, M. Parrilli, A. De Soya, A. Molinaro, *Glycobiology* **2008**, *18*, 871.
- [28] L. P. Partida-Martinez, S. Monajembashi, K. O. Greulich, C. Hertweck, *Curr. Biol.* **2007**, *17*, 773.
- [29] M. J. Coyne, B. Reinap, M. M. Lee, L. E. Comstock, *Science* **2005**, *307*, 1778.
- [30] A. Moran in *Microbial Glycobiology* (Eds.: A. Moran, O. Holst, P. J. Brennan, M. von Itzstein), Academic Press, London, **2010**, p. 847.
-

Deciphering the structural and biological properties of the lipid A moiety of lipopolysaccharides from *Burkholderia cepacia* strain ASP B 2D, in *Arabidopsis thaliana*

Ntakadzeni E. Madala¹, Maria R. Leone², Antonio Molinaro², Ian A. Dubery^{1*}

¹Department of Biochemistry, University of Johannesburg, Kingsway campus, Auckland Park, Johannesburg, South Africa and ²Dipartimento di Chimica Organica e Biochimica, Università di Napoli Federico II, via Cintia 4, I-80126, Napoli, Italy.

*¹To whom correspondence should be addressed:

Department of Biochemistry, University of Johannesburg, P.O. Box 524, Auckland Park, 2006, South Africa.

Tel: 27-011-5592401, Fax: 27-011-5592605, e-mail: idubery@uj.ac.za

Abstract

Lipopolysaccharides (LPSs) are major, indispensable cell surface components of Gram-negative bacteria that have diverse roles in bacterial pathogenesis of plants. Environmental strains of *Burkholderia cepacia* have been described as phytopathogens, growth promoters, biocontrol agents and bioremediation agents. We have previously shown that LPSs from *B. cepacia* can be recognized as microbe-associated molecular pattern (MAMP) molecules, to elicit defense responses in plants. Recent findings suggest that the lipid A moiety might be partially responsible for LPSs perception. These studies were extended by analysis of the structure and biological activity of the lipid A moiety of LPSs of *B. cepacia*. The full structure was determined by a combination of negative/positive-ion matrix assisted laser desorption ionization (MALDI) mass spectrometry on intact and partially degraded substrates. *B. cepacia* lipid A was found to contain a tetra- or penta-acylated, 1,4'-diphosphorylated, β -(1-6)-linked D-GlcN disaccharide and further substituted by L-Ara4N in position 4'. As primary fatty acids, *R*-configured 16:0(3-OH) (amide-linked in 2 and 2') and 14:0(3-OH) (ester-linked in 3, and 3', non-stoichiometric) were identified. A secondary 14:0 was located at position 2'. Its biological activity to elicit defense-related responses was subsequently investigated by monitoring the changes in the transcriptome of *A. thaliana* seedlings. Genes found to be up-regulated code for proteins involved in signal perception and transduction, transcriptional regulation, defense- and stress responses. Furthermore, genes encoding proteins involved in chaperoning, protein interactions and protein degradation were differentially expressed as part of the metabolic reprogramming of cellular activities in support of immunity and defense.

Key words: *Burkholderia cepacia*/Lipid A/Lipopolysaccharides/Plant basal resistance/Structure

Introduction

The plant immune system perceives the presence of pathogens by recognition of molecules known as microbe-associated molecular pattern molecules (MAMPs) or by sensing effector proteins that are secreted to the host during plant-pathogen interactions (Jones and Dangl, 2006; Dow *et al.*, 2009). MAMPs have several common characteristics, including highly conserved structures, indispensability to the microorganism and absence in the host organisms. Plants can specifically recognize MAMPs and can respond with appropriate defenses by activating a multi-component and multi-layered response (Jones and Dangl, 2006). The induction of defense responses is triggered by complex pathways that can involve Ca^{2+} influx, H^+/K^+ exchange, generation of reactive oxygen and nitrogen species (ROS, RNS) and the synthesis of jasmonic acid (JA), salicylic acid (SA) and ethylene (ET), that act in a multi-faceted cross-talk manner as signal molecules (Hammond-Kosack and Parker, 2003; McDowell and Dangl, 2000; Jalali *et al.*, 2006). The inducible plant defense responses are characterized by defense gene activation, activation of programmed hypersensitive / cell death responses and production of antimicrobial phytoalexins, strengthening of the cell wall and synthesis of pathogenesis-related (PR) proteins (Lamb, 1994; Hammond-Kosack and Jones, 1996; Lamb and Dixon, 1997; van Loon, 1997).

Several MAMPs from different microorganisms have been reported with potential to trigger plant defense responses. These include flagellin, chitin, cell wall derived glucans, peptidoglycan (PGN), elongation factor Tu (EfTu) and lipopolysaccharides (LPSs) (Jones and Dangl, 2006). The corresponding receptors for some of these MAMPs in plants have been identified and characterized as pattern-recognition receptors (PRRs) such as receptor-like kinases (RLKs) (Gomez-Gomez and Boller, 2002; Zipfel *et al.*, 2004; Altenbach and Robatzek, 2007; Robatzek, 2007; Zipfel, 2008). Compared to other MAMPs, little is known about the perception of LPSs by plant cells as no receptor(s) have been identified thus far.

LPSs are amphiphilic lipoglycans (Silipo *et al.*, 2010), composed of a hydrophilic heteropolysaccharide, (comprising the core oligosaccharide and O-specific polysaccharide or O-chain), that are covalently linked to a lipophilic moiety, lipid A, that anchors these macromolecules to the bacterial outer membrane (Dow *et al.*, 2000; Newman *et al.*, 2007; Molinaro *et al.*, 2009, Silipo *et al.*, 2010). LPSs can be directly recognized by plants to trigger defense responses (Dow *et al.*, 2000). As lipoglycan macromolecules, LPSs can potentially contain molecular pattern structures within the lipid A, core and O-chain moieties (Newman *et al.*, 2007; Molinaro *et al.*, 2009). The MAMP-active eliciting part(s) of LPSs have not yet been fully investigated. Lipid A has been suggested to be, at least partially, the inducing part of LPSs due to the overall chemical architecture of lipid A that is conserved in Gram-negative bacterial LPSs (Molinaro *et al.*, 2009; Silipo *et al.*, 2010). However there is little evidence

implicating the lipid A to be the sole MAMP or immuno-modulatory stimulant of LPSs in plants (Newman *et al.*, 2007; Silipo *et al.*, 2008).

Several structural features were previously identified to play a key role in biochemical pathophysiological activity of lipid A in animals. These include the number and location of acyl chains, the overall charge of the lipid A molecule, i.e. phosphorylation of the disaccharide backbone and presence of further polar heads (Schromm *et al.*, 2000; Alexander and Rietschel, 2001; Raetz and Whitfield, 2002; Raetz *et al.*, 2007). Different biological activities of LPSs are directly attributed to the molecular shape of lipid A, which in turn is dependent on the structural features of the molecule (Munford and Varley, 2006). The chemical composition, structure and conformation of lipid A are thus important determinants during bacterial pathogenesis. In addition, interest in lipid A stems from the observation that certain bacteria can manipulate the composition of their lipid A in response to environmental cues and thereby modulate or even antagonize the triggering of innate host responses (Scheidle *et al.*, 2004; Silipo *et al.*, 2005, 2010; Al-Qutub *et al.*, 2006). Some reports showed that lipid A is an agonist of plant defense responses while others report contrary, antagonist effects. For example, lipid A from *Xanthomonas campestris* has been shown to induce both PR 1 and 2 in *Arabidopsis thaliana* (Silipo *et al.*, 2008). On the other hand, lipid A from *Sinorhizobium meliloti* suppresses the oxidative burst in host plants (*Medicago sativa* and *M. truncatula*) and *Nicotiana tabacum* (Scheidle *et al.*, 2004; Silipo *et al.*, 2010). Due to the limited number of lipid A structures determined from plant-associated bacteria, no clear structure : activity relationship exists as for lipid A effects in animals.

Burkholderia species occupy a wide range of ecological habitats, being found in soil and water, in and on plants and roots, and associated with fungal mycelia. Some species are effective as plant growth promoters, biocontrol agents and bioremediation agents (Vandamme *et al.*, 2007). *B. cepacia* is a bacterium of low virulence and is a frequent colonizer rather than an infecting agent. Our ongoing research has shown that the LPS from a plant-derived endophytic strain (*B. cepacia*, strain ASP B 2D) exhibit activity as an inducer or modulator of plant defense-related responses. We have previously shown that LPS from *B. cepacia* can elicit enhanced defensive capacity in tobacco plants (Coventry and Dubery, 2001). These responses include influx of Ca^{2+} , an oxidative burst, an NO burst, extracellular alkalization (K^+/H^+ exchange), and changes in reversible protein phosphorylation, including MAP-kinase activation (Gerber *et al.*, 2004; Piater *et al.*, 2004; Zeidler *et al.*, 2004; Sanabria and Dubery, 2006; Gerber *et al.*, 2008). Here we report the complete structure of the lipid A from this strain of *B. cepacia*, attained by chemical analyses, mass spectrometry and nuclear magnetic resonance spectroscopy. The biological or immuno-modulatory activity of this lipid A molecule was further investigated by monitoring its ability to affect gene expression in *A. thaliana* on the transcriptome level with the aid of annealing

control primer (ACP)-based differential display reverse transcription polymerase chain reaction (DDRT-PCR) technique.

Results and Discussion

Chemical characterization of lipid A structure

LPS was isolated from dried *B. cepacia* cells with phenol/water extraction and it was identified in the water phase as confirmed by sodium dodecyl sulfate (SDS)–polyacrylamide gel electrophoresis (PAGE). Further purification was obtained by enzymatic treatment (DNase, Rnase and Proteinase-K) and gel permeation chromatography. The lipid A moiety was isolated from LPS by acetate buffer hydrolysis and the lipid fraction was recovered as sediment by ultracentrifugation. The results from chemical analysis revealed the presence of 6-substituted and terminal D-GlcpN, 4-amino-4-deoxy-arabinopyranose with L-configuration, and phosphate (this latter obtained by colorimetric assay). Fatty acid analyses, carried out by GLC-MS of methyl-ester derivatives, showed the presence of (*R*)-3-hydroxyhexadecanoic acid (16:0(3-OH)), (*R*)-3-hydroxytetradecanoic acid (14:0(3-OH)) and tetradecanoic acid (14:0) (Fig. S1, supplementary information). The fatty acids substitution corresponds with that previously reported for *B. caryophylli* and a clinical isolate of *B. cepacia* (Molinaro *et al.*, 2003; Silipo *et al.*, 2005). To determine the lipid A structure, a combination of NMR spectroscopy and negative/positive ion MALDI-TOF mass spectrometry on intact and partially degraded substances was used.

NMR spectroscopy of lipid A

A combination of homo- and heteronuclear NMR experiments were performed in DMSO on the *O*-deacylated lipid A aiming at the definition of the carbohydrate backbone. DQF-COSY, TOCSY, ROESY, ^{13}C - ^1H and ^{31}P - ^1H HSQC spectra were used to assign ^{13}C , ^1H and ^{31}P resonances. The NMR data revealed the presence of the typical [β -D-GlcpN-(1 \rightarrow 6)- α -D-GlcpN] disaccharide backbone with a variety of acyl chains that resulted in a heterogeneous mixture of species all sharing the *N*-acylation (Table SI, supporting information). The presence in non-stoichiometric amount of a β -L-Arap4N residue attached via phosphodiester bond at O-4 of GlcN II was demonstrated by ^{31}P - ^1H HSQC where a correlation between H-4 of GlcN II and the anomeric proton of Ara4N was evident (Fig. SII, supporting information). Conversely, the anomeric position of GlcN I was either present as a free reducing end or, when bound to phosphate, as an α -configured residue (Table SI, supporting information). All the other chemical shifts and correlations in the NMR spectra were similar to those previously obtained for a clinical isolate of *B. cepacia* (Silipo *et al.*, 2005; De Soya *et al.*, 2008), and are not discussed further.

MS analysis on intact and selectively degraded lipid A

The negative ion MALDI spectrum on intact lipid A (Fig. 1) showed the presence of a heterogeneous mixture of penta- and tetra-acylated species substituted in different fashion (Table I). The peak at m/z 1363.3 (species **1**) was deduced as tetra-acylated mono-phosphorylated lipid A, possessing one 14:0(3-OH) and one 14:0 residue and two 16:0(3-OH) residues. Species **3** (m/z 1493.8) corresponded to tetra-acylated lipid A, that carried an additional Ara4N residue with respect to species 1. Ara4N was identified in comparison with an authentic sample from *B. caryophylli* (Molinaro *et al.*, 2003). The peaks at m/z 1442.8 and 1573.9 (species **2** and **4**) were recognized as the corresponding *bis*-phosphorylated species. The ion at m/z 1668.6 (species **5**) was assigned to a *bis*-phosphorylated penta-acylated lipid A that carried two 14:0(3-OH), one 14:0 residues and two 16:0(3-OH) residues. The ion at m/z 1798.9 (species **7**) was identified as penta-acylated species with an additional Ara4N with respect to the species **5**. In the spectrum, traces of an ion at m/z 1719.7 were also present (species **6**) that was deduced as mono-phosphorylated penta-acyl lipid A, carrying two 14:0(3-OH), a 14:0 residue and two 16:0(3-OH) residues. The complete and precise distribution of all fatty acid has been carried out by negative and positive MALDI-TOF mass spectrometry on *O*-deacylated and dephosphorylated lipid A.

In order to accurately locate the fatty acids residues, lipid A underwent two parallel and complementary treatments: mild hydrolysis with ammonium hydroxide and total de-phosphorylation with 48% HF. The first procedure leaves the amide-linked acyloxyacyl groups unaffected and selectively removes ester-linked acyloxyacyl and acyl moieties (Leontein and Lönnegred, 1978). The negative ion MALDI mass spectrum of the obtained product (Fig. 2), showed two patterns of peaks corresponding to a mixture of tri-acylated lipid A. Hence, the ion at m/z 1138.0 was consistent with a mono-phosphorylated tri-acylated lipid A, possessing two primary fatty acids, 16:0(3-OH), in amide linkage and a secondary fatty acid, 14:0, in ester linkage. The peak at m/z 1268.8 possessed an additional Ara4N. Both species were present in a lower amount also as the *bis*-phosphorylated form. The positive ion mode MALDI mass spectrum (not shown) of the above product showed, beside the pseudomolecular ions in accordance with previous analysis, two oxonium ions, a major one at m/z 706.1 and a minor one at m/z 837.6. The former ion was inferred as a GlcN II oxonium ion carrying one 14:0 and one 16:0(3-OH) residues, i.e., an acyloxyacylamide moiety. The latter ion at m/z 837.6 carried an additional Ara4N. Thus, by the analysis of the ammonium treated lipid A fraction, it was evident that the secondary 14:0 fatty acid residue substitutes the amide bound 16:0(3-OH) residue on GlcN II and that Ara4N, when present, is very likely attached to GlcN II.

In analogy with a procedure previously adopted with another *Burkholderia* lipid A an aliquot of product was dephosphorylated with 48% HF and then analyzed by positive ion MALDI-TOF mass spectrometry (Silipo *et al.*, 2005). The mass spectrum showed pseudomolecular ions $[M+Na]^+$ in

accordance with ion peaks analysis of the previous analyses and in addition, two oxonium ions both arising from the glycosidic cleavage of the non-reducing unit and thus, indicative of the fatty acids distribution between the two GlcN residues (Silipo *et al.*, 2005). In particular, one ion m/z 933.8 could be ascribed to a tri-acylated GlcN II oxonium ion carrying one 14:0(3-OH), one 14:0 and a 16:0(3-OH) residue, whereas the ion at m/z 1064.8 carried an additional Ara4N (not shown) (Silipo *et al.*, 2005). In low amounts, two other ion peaks were found assignable to the two oxonium ions above that lacked the 14:0(3-OH) residue ($\Delta m/z = 228$) indicating that, in the native tetra-acylated lipid A species, the 14:0(3-OH) residue may also lack the GlcN II, even though this does not exclude that it may lack the GlcN I as well.

On the basis of the MS and NMR information on the selectively degraded lipid A, the ion peaks of the native lipid A in the MS spectrum could be assigned. The highest mass ion peak, species **7** at m/z 1798.9, is consistent with a bis-phosphorylated penta-acylated disaccharide backbone substituted by a further arabinosamine residue [β -L-Arap4N-1-P \rightarrow 4- β -D-GlcpN-(1 \rightarrow 6)- α -D-GlcpN-1 \rightarrow P], carrying in ester linkage two 14:0(3-OH) chains and in amide linkage, two 16:0(3-OH) chains, one of which, on the GlcN II, is further substituted by a secondary fatty acid, a 14:0 residue. With respect to species **7**, the species **6** (m/z 1719.7) differed by a phosphate residue missing at the anomeric position of GlcN I, while species **5** (m/z 1668.6) lacked the Ara4N but still carried both phosphate groups. Species **4** (m/z 1573.9) was endorsed as a tetra-acylated lipid A carrying in ester linkage one 14:0(3-OH) chain and in amide linkage, two 16:0(3-OH) chains; one of which, on the GlcN II, is further substituted by a secondary 14:0 fatty acid residue. The GlcN bearing the free hydroxyl group left unbound by the missing 14:0(3-OH), could be either the reducing or non-reducing one. The species **3** (m/z 1493.8) differed by a phosphate residue missing at anomeric position of GlcN I with respect to species **4**. Mono-phosphorylated species **1** and bis-phosphorylated species **2** were analogues to **3** and **4**, respectively, but lacked Ara4N.

In conclusion, all the above data were in agreement with the presence of a heterogeneous mixture of tetra- and penta-acylated lipid A species differing by phosphorylation pattern and substitution by Ara4N as illustrated in Fig. 3.

Effect of lipid A perception on gene expression in Arabidopsis thaliana

Despite its importance in plant defense, little is known about the molecular basis of LPS-triggered immunity and the responsible molecular determinants within the lipoglycan. Lipid derivatives have been described as potent MAMP elicitors, e.g. cholic acid, ergosterol, rhamnolipids and cerebroside (Varnier *et al.*, 2009). Lipid metabolites influence pathogenesis and resistance mechanisms associated with plant-microbe interactions and recent findings indicate that lipid signaling is essential for plant resistance to pathogens (Shah, 2005; Raffaele *et al.*, 2009). The best described lipid MAMPs are LPS and LOS (LPSs

not containing O-chains) (Silipo *et al.*, 2005; Newman *et al.*, 2007). LPSs from *B. cepacia* does not elicit hypersensitive cell death and is a weaker inducer of basal resistance compared to other non-lipid MAMPs and transcriptome analysis indicate that it induces a slower and more subtle pattern of gene expression (Livaja *et al.*, 2008).

The results obtained with the *B.cepacia* lipid A indicate activation of signal transduction cascade(s) that resulted in reprogramming of the transcriptome. Table II shows a partial list of the genes whose transcription was prominently up-regulated at 8 h after *A. thaliana* seedlings were challenged with 20 $\mu\text{g ml}^{-1}$ lipid A, compared to the water treated control seedlings (Supplementary information, Fig. S3). The genes are grouped into 11 functional categories based on described gene ontologies with regard to cellular component, molecular function and biological process. These include: transcriptional regulation, signal transduction, stress management, molecular chaperones, cell transporters, RNA binding proteins, protein degradation, cytoskeleton rearrangements, vesicle trafficking and secretion, cuticle and cell wall-related, hormone-related and metabolism and energy production. Together they provide a molecular signature of the lipid A-induced responses in *A. thaliana* seedlings which is not unlike that reported for other MAMPs like flagellin, Ef-Tu, PGN, LPS and harpin (Navarro *et al.*, 2004; Zeidler *et al.*, 2004; Gust *et al.*, 2007; Livaja *et al.*, 2008).

Transcriptional analysis of genes expressed in *A. thaliana* in response to elicitation by MAMPs such as flagellin (flg22), Ef-Tu and LPS, indicated that a considerable number of the up-regulated genes can be classified as being involved in signal perception and – transduction (Navarro *et al.*, 2004; Nuernberger, 2006). This is indicative of positive feedback regulation operating in innate immunity with activation of the components involved in the perception and signaling (Zipfel *et al.*, 2004; Altenbach and Robatzek, 2007), thereby enhancing the sensitivity of the plant to further stimuli. LPSs have been reported to trigger an enhanced defensive capacity in plants (Coventry and Dubery, 2001; Sanabria and Dubery, 2006; Mishina and Zeier, 2007) and to lead to a primed state (Newman *et al.*, 2007). The up-regulated expression of RLK genes presumably contributes to this enhanced sensitivity of the plant to sense the presence of invading microorganisms. Under the conditions of this study, lipid A was found to up-regulate the expression of typical perception-related genes such as At5g58150, a LRR transmembrane RLK that is also responsive to flg22 and PGN, hrpZ and benzothiadiazole, a chemical inducer of resistance (Navarro *et al.*, 2004; Gust *et al.*, 2007). LRR-RLKs are known to act as potential PRRs of pathogen-derived ligands and to trigger downstream signal transduction cascades involving mitogen-activated protein kinases (MAPKs) (Nuernberger and Kemmerling, 2006; Nicaise *et al.*, 2009). At1g10210, the gene encoding MAPK1, was recently reported to be associated with defense signaling and induced under different stress conditions such as wounding, abscisic acid, jasmonic acid and hydrogen peroxide (Ortiz-Masia *et al.*, 2007). Several other protein kinase genes were also found to be up-regulated

in the current study (Table II) but their involvement in signal transduction is not well documented. Lipid A from *B. cepacia* is thus able to trigger activation of genes involved in plant surveillance systems and defense-related signal perception and transduction.

The upregulation of the oxysterol-binding protein (OBP) gene, At4g08180, is of great interest. These proteins play roles as lipid sensors / transporters in signal transduction by controlling the extracellular signal-regulated (ERK/MAPK) pathways in mammalian cells (Wang *et al.*, 2007) and, in plants, were found to be rapidly up-regulated in potato in response to *Phytophthora infestans* and oligogalacturonides (Avrova *et al.*, 2004). In the context of lipid-based signaling, gene At4g12470, *azi-1*, encodes a lipid transfer protein (LTP) reported to be involved in priming of SA induction and systemic immunity triggered by pathogens or azelaic acid (Jung *et al.*, 2009) and to confer disease resistance when overexpressed (Chassot *et al.*, 2007). This gene was also found to be up-regulated by PGN treatment (Gust *et al.*, 2007). A related LTP gene, *dir1-1*, was reported to be involved in systemic resistance signaling in *A. thaliana* (Maldonado *et al.*, 2002).

Protein degradation is an important regulatory process that allows cells to respond rapidly to intracellular signals and changing environmental conditions by adjusting the levels of key proteins. Targeted protein degradation of repressor proteins and the involvement of the 26S proteasome pathway (At1g75990) in pathogen resistance and establishing the 'defensome' is known (Vierstra, 2003). Moreover, the induced turnover of resistance genes can be important for mounting appropriate plant defenses and targeting of selected proteins can aid in controlling the extent of cell death and overall resistance response at the site of infection (Boyes *et al.*, 1998). At1g21780 encodes a BTB domain-containing protein reported to associate with cullin proteins to form ubiquitin protein ligases that target substrates for proteolysis by the 26S proteasome (Figuerosa *et al.*, 2005; Dieterle *et al.*, 2004). In addition, the F-box containing proteins (subunits of E3 ubiquitin ligase complexes) such as the 'kelch repeat-containing F-box family protein' (At3g59940), are believed to be involved in a variety of cellular activities, from hormone responses to pathogen defense responses (Callis and Vierstra, 2000; Hellmann and Estelle, 2002). Interestingly, a similar finding was made with PGN as elicitor (Gust *et al.*, 2007).

Molecular chaperones like the 'heat shock protein (HSP) 70 interacting protein 1' (At4g22670), are involved in the folding of newly synthesised or damaged proteins as well as in the association of proteins in complexes, important in recognition and defense in plants. HSP 70 family proteins are known to be induced by nitric oxide and SA (Huang *et al.*, 2002), messengers involved in signal transduction and activation of genes involved in defense (Klessig *et al.*, 2000). These messengers are produced in *A. thaliana* as an induced response to LPS from *B. cepacia* (Zeidler *et al.*, 2004). Chaperones such as HSP 70 and 90 are believed to be essential components of hypersensitive - and non-host resistance responses, participating in multi-member complexes (Kanzaki *et al.*, 2003). Protein-protein interactions play an

important role in innate immunity in plants and the recognition of pathogen effectors (Cohn *et al.*, 2001). Here the up-regulation of At1g24300 (a ‘GYF domain containing protein’) and At4g03460 (an ankyrin-repeat containing protein) could support such interactions (Koffler *et al.*, 2004). Furthermore, thioredoxins (At1g08570) also play a role in protein folding by reducing thiol-disulphides of other proteins (Berndt *et al.*, 2008; Meyer *et al.*, 2008). Their involvement in plant defense/stress responses is known; CITRX thioredoxin interacts with the tomato resistance protein, Cf-9, and subsequently to regulate the plant defense response, thereby enhancing resistance (Rivas *et al.*, 2004).

It was also found that *B. cepacia* lipid A induced genes involved in oxidative stress related responses, such as glutathione S-transferase (At1g02920). This gene product was previously reported to be induced in *Arabidopsis* cell suspensions treated with fungal elicitor and also in plants challenged with pathogens or SA (Chivasa *et al.*, 2006; Wagner *et al.*, 2002). The senescence-associated responsive protein-21 (At4g02380), an oxidative stress and pathogen-inducible signature gene was also identified (Thilmony *et al.*, 2006).

Three genes encoding peroxidase-related proteins (At3g49120, At4g21960 and At5g64120) were also found to be up-regulated. Plants respond to pathogen attack in several ways, one being cell wall reinforcement in order to combat the pathogen by preventing further spreading to other unaffected parts of the plant (Lamb and Dixon, 1997; de Ascensao and Dubery, 2000). Induced peroxidases are involved in oxidative cross-linking of proteins and polymers in papillae and cell wall structures. Some peroxidases are now regarded as PR proteins, suggesting their involvement in pathogen-induced defense responses in plants (van Loon *et al.*, 2006).

Other induced genes involved in carbohydrate metabolism and cell wall activity include an UDP-glycosyl transferase family protein (At3g16520), pectinesterase (At2g45220) and the cell wall-plasma membrane linker protein (At3g22120).

Some types of priming like systemic acquired resistance (SAR) and induced systemic resistance (ISR) have been known to involve phytohormones that seem to be important during the establishment of the primed state (Korolev *et al.*, 2008). The phytohormone-related transcripts listed in Table II involving abscisic acid, gibberelin and auxin, may therefore be indicative of these dynamics. Plant hormone pathways influence each other strongly and the modulation of a single hormone pathway can greatly affect plant defenses (Robatzek and Saijo, 2009).

Transcriptional responses towards priming agents also include genes involved in metabolism (Table II), indicative of metabolic reprogramming where the normal metabolic flow in the host plant is altered in support of defense responses.

Conclusion

Lipid A structures from *Burkholderia* strains can vary with the strain and the environment from which the bacteria have been isolated (De Soyza *et al.*, 2008). As for the chemical structure of lipid A from *B. cepacia* ASP 2D, the transcriptional re-programming described above can have an explanation in terms of the acylation and phosphorylation patterns of the lipid A molecule. This lipid A has been found to possess either a consistent amount of under-acylated species such as tetracyl lipid A or a low amount of phosphate. Both these are important factors in the elicitation of innate immune response in animals (Munford and Varley, 2006) and an interesting parallel with basal resistance in plant can be drawn (Silipo *et al.*, 2006). Substitution of lipid A with L-Arap4N is associated with growth under stress conditions (Silipo *et al.*, 2005). The physico-chemical properties and substitution pattern of its lipid A might allow *B. cepacia* to survive as an endophyte in plant hosts by reducing the net charge and ionic attraction to cationic antimicrobial peptides. Being able to elicit an enhanced level of basal resistance against fungal pathogens would then explain the beneficial aspects of this interaction to the host. Following chemical characterization of its structure, new insights into the biochemical action mechanism of *B. cepacia*-derived lipid A as a MAMP, a resistance elicitor and triggering agent of transcriptional changes associated with defense responses have been obtained. It can be concluded that lipid A was perceived by the seedlings, leading to the induction of a broad range of genes; some known to be associated with defense responses and biotic and abiotic stresses, whilst others are associated with metabolic reprogramming of cellular activities in support of immunity and defense. Although it cannot be ruled out that, in addition to lipid A, other molecular patterns within LPSs can also be recognised to contribute to the overall set of LPS-induced responses; the obtained results support the paradigm that lipid A is perceived by plants as a determinant of microbial non-self (Sanabria *et al.*, 2010). The nature of the physical interaction between lipid A as a ligand and plant protein(s) that can act in its perception, are topics that warrants further investigation.

Materials and methods

Lipid A preparation

B. cepacia strain ASP B 2D was grown in Nutrient Broth liquid medium as previously described (Coventry and Dubery, 2001). LPS was prepared from freeze dried cells using the phenol-water method, extracted into the water phase and freeze dried. After enzymatic treatment with DNase, RNase and Proteinase-K, the LPS was dialyzed and subjected to gel permeation chromatography on a Sephacryl S-300 column (90 cm x 1.5 cm) with 0.05 M ammonium bicarbonate as eluent and monitored with a differential refractometer before freeze drying (Leone *et al.*, 2006). Free lipid A was obtained by

treatment of LPS (10 mg) with 0.1 M sodium acetate buffer (pH 4.4) containing 1% SDS (100°C, 3 h, until a precipitate was visible in the tube (Silipo *et al.*, 2005). The solution was then lyophilized, treated with 2 M HCl : EtOH (1:100, v/v) to remove the SDS, evaporated, dissolved in water and ultracentrifuged (100,000 g, 4°C, 90 min). The obtained precipitate (free lipid A) was washed with water (yield: 1.8 mg, 18 % of the LPS). Lipid A was partially *O*-deacylated by treatment with 12% NH₄OH at 25°C for 18 h (Silipo *et al.*, 2002). Lipid A was dephosphorylated by treatment with 48% aqueous HF (4°C, 48 h).

General and analytical procedures

Monosaccharides were identified as acetylated *O*-methyl glycosides derivatives. After methanolysis (2M HCl/MeOH, 85°C, 24 h) and acetylation with acetic anhydride in pyridine (85°C, 30 min) the sample was analyzed by GLC-MS (Supplementary information, Fig. S1). The absolute configuration of the monosaccharides was obtained according Leontein and Lönngren (1978). Total fatty acid content was obtained by acid hydrolysis of lipid A. Briefly, lipid A was first treated with 4M HCl (4 h, 100°C) and then with 5M NaOH (30 min, 100°C). Fatty acids were then extracted in CHCl₃, methylated with diazomethane and analyzed by GLC-MS. The ester bound fatty acids were selectively released by base-catalyzed hydrolysis with NaOH 0.5M/MeOH (1:1 v/v, 85°C, 2h), then the product was acidified, extracted in CHCl₃, methylated with diazomethane and analyzed by GLC-MS. The absolute configuration of fatty acids was determined as described (Rietschel, 1976).

All GLC analyses were performed on a Hewlett-Packard 5890 instrument, SPB-5 capillary column (0.25 mm x 30 m, Supelco), for sugar methylation analysis and *O*-methyl glycosides derivatives the temperature program was: 150°C for 2 min, then 2°C min⁻¹ to 200°C, then 10°C min⁻¹ to 260°C for 11 min, then 8°C min⁻¹ to 300°C for 20 min; for absolute configuration analysis it was: 150°C for 8 min, then 2°C min⁻¹ to 200°C, then 6°C min⁻¹ to 260°C for 5 min. For fatty acids analysis the temperature program was 80°C for 2 min, then 8°C min⁻¹ to 300°C for 15 min.

Mass spectrometry

Matrix-assisted laser desorption/ionization time-of-flight mass spectrometry (MALDI-TOF-MS) of native lipid A, partially de-*O*-acylated and dephosphorylated lipid A, was performed with a Voyager DE-PRO MALDI-TOF mass spectrometer (Applied Biosystems), in the positive and negative ion mode at an acceleration voltage of 24 kV. In general, compounds were dissolved in CHCl₃/MeOH (4:1 v/v) at a concentration of 1 µg µl⁻¹. One µl of the sample was then mixed (directly on the metallic sample surface) with 1 µl of a 20 mg ml⁻¹ solution of 2,5-dihydroxybenzoic acid (Sigma-Aldrich, Germany) in acetonitrile / 0.1 M trifluoroacetic acid (7:3 v/v). The mass spectra shown are the average of at least 50 single scans.

An external mass scale calibration was performed with lipid A from *E. coli* O:55 B:5 obtained from Sigma Aldrich, USA.

NMR spectroscopy

^1H , ^{13}C -NMR spectra of *O*-deacylated lipid A were recorded in DMSO at 343K aiming at the definition of the carbohydrate backbone on a Bruker DRX-600 spectrometer equipped with a cryogenic probe. ^{31}P -NMR spectra were recorded on a Bruker DRX 400 spectrometer equipped with a reverse probe. Aqueous 85% phosphoric acid was used as external reference (0.00 ppm) for ^{31}P -NMR spectroscopy. Rotating frame Overhauser enhancement spectroscopy (ROESY) was measured using data sets (t1 x t2) of 2048 x 1024 points, and 16 scans were acquired. A mixing time of 400 ms was employed. Double quantum-filtered phase-sensitive COSY (DQF-COSY) experiment was performed with 0.258 s acquisition time using data sets of 2048 x 512 points and 88 scans were acquired. The total correlation spectroscopy experiment (TOCSY) was performed with a spinlock time of 120 ms, using data sets (t1 x t2) of 4096 x 1024 points, and 16 scans were acquired. In all homonuclear experiments the data matrix was zero-filled in the F1 dimension to give a matrix of 4096 x 2048 points and was resolution enhanced in both dimensions by a shifted sine-bell function before Fourier transformation. Coupling constants were determined on a first order basis from DQF-COSY (States *et al.*, 1982). The heteronuclear single quantum coherence (HSQC) experiment spectrum was measured in the ^1H -detected mode via single quantum coherence with proton decoupling in the ^{13}C domain, using data sets of 2048 x 512 points, and 64 scans were acquired for each t1 value. The experiments were carried out in the phase-sensitive mode (Rance *et al.*, 1983).

Plant growth and elicitation

Surface sterilized *A. thaliana* seeds were grown in sterile half strength Murashige and Skoog (MS) medium, containing 2% glucose at pH 5.8. The seeds were allowed to grow on the orbital shaker at approximately 25 rpm at 24°C in a 9 h dark photoperiod (Zhang *et al.*, 2002). Ten days old seedlings were harvested and placed in newly prepared MS medium. Lipid A dissolved in MS medium was added to a final concentration of 20 $\mu\text{g ml}^{-1}$ and water was added to the control tube. Plant elicitation was allowed to take place for 8 h while the tubes were continuously shaken at 25 rpm.

RNA isolation and ACP-DDRT-PCR

Total RNA was isolated using the Trizol reagent method (Invitrogen, USA). RNA integrity and concentration were evaluated using denaturing RNA gel electrophoresis and NanoDrop spectrophotometer (NanoDrop Technologies, USA) analysis. Using 3 μg of RNA, mRNA differential

display was performed with the aid of the ACP-based DDRT-PCR technique using the GeneFishing kit (SeeGene, Korea). ACP technology is an improved method for identification of differentially expressed genes (DEGs) using a novel, patented annealing primer system. Because of high annealing specificity during PCR using the ACP system, the application for DEG discovery generates highly reproducible, authentic, and long PCR products. Furthermore, it generates no false positives (Hwang *et al.*, 2003; Kim *et al.*, 2004). Forty different ACP arbitrary primers with different universal sequences (Supplementary data, Table SII) were used. ACP-DDRT-PCR amplicons were evaluated on 1.5 % agarose gels stained with Gel Green stain (Biotium, USA). Bands representing up-regulated genes were identified and excised from the gel and kept at -80°C until further use. Using the Zymoclean Gel DNA Recovery kit (Zymo Research, USA), DNA was extracted from the gel slices. The recovered DNA was further PCR-reamplified using the GoTaq Flexi DNA polymerase kit (Promega, USA). Universal primers with sequences complementary to the 5' end of the ACP-primers were used: upstream primer, 5'-GTCTACCAGGCATTCGCTTCAT-3' and downstream primer, 5'-CTGTGAATGCTGCGACTCGAT-3'. The PCR components were 1X GoTaq Flexi buffer, 2.5 mM MgCl₂, PCR nucleotide mix (0.2 mM each), 1 μM upstream universal primer, 1 μM downstream primer, 1.25 U GoTaq DNA polymerase, 5 μl purified DNA, and nuclease free water. The PCR conditions were as follows: initial denaturation at 95°C for 2 min, denaturation at 95°C for 30 sec, annealing at 65°C for 30 sec, extension at 72°C for 1 min, and final extension at 72°C for 10 min, PCR number of cycles were limited to 35. Amplicons derived from the same treatment were combined in one pool (i.e. control in one tube and lipid A in another tube) and further cleaned up with the aid of QIAquick PCR purification kit (Qiagen, Germany) and quantified using NanoDrop spectrophotometry.

DNA sequencing and bioinformatics analysis

Purified DNA (12 μg) was sequenced using the GS-FLX sequencer (Inqaba Biotec, RSA) with the aid of 454 high throughput pyosequencing technology (Roche, Germany). Gene annotation or identification was done using the basic local alignment search tool (BLAST) programme from National Centre for Biotechnology Information (NCBI) and each EST independently annotated. Genes which code for proteins with similar functions were grouped into functional categories based on described gene ontologies with regard to cellular component, molecular function and biological process. To further understand the functions of the proteins encoded by the genes identified, web information tools, the InterPro database (<http://www.ebi.ac.uk/interpro/>) and Genevestigator Response Viewer (<http://www.genevestigator.com>) were used.

Acknowledgements

This work was supported by the South African National Research Foundation [Grant number 206492].

Abbreviations

ACP, Annealing control primer; BLAST, Basic local alignment search tool; BTB, Bric-a-brac, tramtrack, broad-complex; DDRT-PCR, Differential display reverse transcription- polymerase chain reaction; Eftu, Elongation factor Tu; ERK, extracellular signal regulated kinase; EST, Expressed sequence tags; ET, ethylene; Flg, flagellin; GLC, Gas liquid chromatography; HSP, Heat shock protein; HR, Hypersensitive response; ISR, Induced systemic resistance; JA, jasmonic acid; LOS, Lipooligosaccharide; LPS, Lipopolysaccharide; LRR, Leucine rich repeats; MAMP, Microbe-associated molecular pattern; MALDI, Matrix assisted laser desorption ionisation; MAPK, Mitogen-activated protein kinase; MS, Mass spectrometry; NCBI, National center for biotechnology information; PGN, Peptidoglycan; PR, Pathogenesis-related; PRR, Pattern-recognition receptors; RLK, Receptor like kinase; ROS, Reactive oxygen species; SA, Salicylic acid; SAR, Systemic acquired resistance; TOF, Time of flight.

References

- Alexander, C. and Rietschel, E.T. 2001. Bacterial lipopolysaccharides and innate immunity. *J Endotoxin Res* **7**, 167-202.
- Altenbach, D. and Robatzek, S. 2007. Pattern Recognition Receptors: From the cell surface to intracellular dynamics. *Mol Plant-Microbe Interact* **20**, 1031-1039.
- Al-Qutub, M.N., Braham, P.H., Karimi-Naser, L.M., Liu, X., Genco, C.A., and Darrveau, R.P. 2006. Hemin-dependent modulation of the lipid A structure of *Porphyromonas gingivalis* lipopolysaccharide. *Infect Immun* **74**, 4474-4485.
- Avrova, A.O., Taleb, N., Rokka, V-M., Heilbronn, J., Campbell, E., Hein, I., Gilroy, E.M., Cardle, L., Bradshaw, J.E., Stewart, H.E., Fakim, Y.J., Loake, G. and Birch, P.R.J. 2004. Potato oxysterol binding protein and cathepsin B are rapidly up-regulated in independent defence pathways that distinguish R gene-mediated and field resistances to *Phytophthora infestans*. *Mol Plant Pathol* **5**, 45-56.
- Berndt, C., Lillig, C.H. and Holmgren, A. 2008. Thioredoxins and glutaredoxins as facilitators of protein folding. *Biochim Biophys Acta* **1783**, 641-650.
- Boyes, D.C., Nam, J. and Dangl, J.L. 1998. The *Arabidopsis thaliana* RPM1 disease resistance gene product is a peripheral plasma membrane protein that is degraded coincident with the hypersensitive response. *Proc Natl Acad Sci U.S.A* **95**, 15849-15854.
- Callis, J. and Vierstra, R.D. 2000. Protein degradation in signalling. *Curr Opin Plant Biol* **3**, 381-386.
- Chassot, C., Nawrath, C. and Métraux J-P. 2007. Cuticular defects lead to full immunity to a major plant pathogen. *Plant J* **49**, 972-980.
- Chivasa, S., Hamilton, J.M., Pringle, R.S., Ndimba, B.K., Simon, W.J., Lindsey, K. and Slabas A.R. 2006. Proteomics analysis of differentially expressed proteins in fungal elicitor-treated *Arabidopsis* cell culture. *J Expl Bot* **57**, 1553-1562.
- Cohn, J., Sessa, G. and Martin, G.B. 2001. Innate immunity in plants. *Curr Opin Imm* **13**, 55-62.
- Coventry, H.S. and Dubery, I.A. 2001. Lipopolysaccharides from *Burkholderia cepacia* contribute to an enhanced defensive capacity and the induction of pathogenesis-related proteins in *Nicotiana tabacum*. *Physiol Mol Plant Pathol* **58**, 149-158.
- De Ascensao, A.R.D.C.F., and Dubery, I.A. 2000. Panama disease: Cell wall reinforcement in banana roots in response to elicitors from *Fusarium oxysporum* f. sp. *cubense* race four. *Phytopathology* **90**, 1173-1180.
- De Soyza, A., Silipo, A., Lanzetta, R., Govan, J.R. and Molinaro, A. 2008. Chemical and biological features of *Burkholderia cepacia* complex lipopolysaccharides. *Innate Immun* **14**, 127-144.
- Dieterle, M., Thomann, A., Renou, J-P., Parmentier, Y., Cognat, V., Lemonnier, G., Müller, R., Shen, W-H., Kretsch, T. and Genschik, P. 2004. Molecular and functional characterization of *Arabidopsis* Cullin 3A. *Plant J* **41**, 386-399.
- Dow, M. J., Newman, M.A. and Von Roepenack, E. 2000. The induction and modulation of plant defense responses by bacterial lipopolysaccharides. *Ann Rev Phytopathol* **38**, 241-261.
- Dow, M., Molinaro, A., Cooper, R.M. and Newman, M-A. 2009. Microbial glycosylated components in plant disease. In: Moran, A., Holst, O., Brennan, P., and von Itzstein, M. editors. *Microbial Glycobiology* Academic Press, p. 803-820.
- Figueroa, P., Gusmaroli, G., Serino, G., Habashi, J., Ma, L., Shen, Y., Feng, S., Bostick, M., Callis, J., Hellmann, H., and Deng, X.W. 2005. *Arabidopsis* has two redundant Cullin3 proteins that are essential for embryo development and that interact with RBX1 and BTB proteins to form multisubunit E3 ubiquitin ligase complexes *in vivo*. *Plant Cell* **17**, 1180-1195.
- Gerber, I.B., Laukens, K., Witters, E. and Dubery, I.A. 2004. Early perception responses of *Nicotiana tabacum* cells in response to lipopolysaccharides from *Burkholderia cepacia*. *Planta* **218**, 647-657.

- Gerber, I.B., Laukens, K., De Vijlder, T., Witters, E. and Dubery, I.A. 2008. Proteomic profiling of cellular targets of lipopolysaccharides-induced signalling in *Nicotiana tabacum* BY-2 cells. *Biochim Biophys Acta – Prot Proteom* **1784**, 1750-1762.
- Gomez-Gomez, L. and Boller, T. 2002. Flagellin perception: a paradigm for innate immunity. *Trends Plant Sci* **7**, 251-256.
- Gust, A.A., Biswa, R., Lenz, H.D., Rauhut, T., Ranf, S., Kemmerling, B., Götz, F., Glawischnig, E., Lee, J., Felix, G. and Nürnberger, T. 2007. Bacteria-derived peptidoglycans constitute pathogen-associated molecular patterns triggering innate immunity in *Arabidopsis*. *J Biol Chem* **282**, 32338-32348.
- Hammond-Kosack, K.E. and Jones, J.D. 1996. Resistance gene-dependant plant defense responses. *Plant Cell* **8**, 1773-1791.
- Hammond-Kosack, K.E. and Parker, J.E. 2003. Deciphering plant-pathogen communication: fresh perspectives for molecular resistance breeding. *Curr Opin Biotech* **14**, 177-193.
- Hellmann, H. and Estelle, M. 2002. Plant development: regulation by protein degradation. *Science* **297**, 793-797.
- Huang, X., Von Rad, U. and Durner, J. 2002. The ubiquitin/26S proteasome pathway, the complex last chapter in the life of many plant proteins. *Planta* **215**, 914-923.
- Hwang, I-T., Kim, Y-J., Kim, S-H., Kwak, C-I., Gu, Y-Y. and Chun, J-Y. 2003. Annealing Control Primer system for improving specificity of PCR amplification. *Biotechniques* **35**, 1-5.
- Jalali, B.L., Bhargava, S. and Kamble, A. 2006. Signal transduction and transcriptional regulation of plant defense responses. *J Phytopathol* **154**, 65-74.
- Jones, J.D. and Dangl, J.L. 2006. The plant immune system. *Nature* **444**, 323-329.
- Jung, H.W., Tschaplinski, T.J., Wang, L., Glazebrook, J. and Greenberg, J.T. 2009. Priming in systemic plant immunity. *Science* **324**, 89-91.
- Kanzaki, H., Saitoh, H., Ito, A., Fujisawa, S., Kamoun, S., Yoshioka, H. and Terauchi, R. 2003. Cytosolic HSP90 and HSP70 are essential components of INF1-mediated hypersensitive response and non-host resistance to *Pseudomonas cichorii* in *Nicotiana benthamiana*. *Mol Plant Pathol* **4**, 383-391.
- Kim, Y-J., Kwak, C-I., Gu, Y-Y., Hwang, I-T. and Chun, J-Y. 2004. Annealing Control System for identification of differentially expressed genes on agarose gels. *Biotechniques* **36**, 1-5.
- Klessig, D.F., Durner, J., Noad, R., Navarre, D.A., Wendehenne, D., Kumar, D., Zhou, J.M., Shah, J., Zhang, S., Kachroo, P., Trifa, Y., Pontier, D., Lam, E. and Silva, H. 2000. *Proc Natl Acad Sci. U.S.A* **97**, 8849-8855.
- Koffler, M., Heuer, K., Zech, T. and Freund, C. 2004. Recognition sequences for the GYF domain reveal a possible spliceosomal function of CD2BP2. *J Biol Chem* **279**, 28292-28297.
- Korolev, N., David, D.R. and Elad, Y. 2008. The role of phytohormones in basal resistance and *Trichoderma*-induced systemic resistance to *Botrytis cinerea* in *Arabidopsis thaliana*. *BioControl* **53**, 667-683.
- Lamb, C.J. 1994. Plant disease resistance genes in signal perception and transduction. *Cell* **76**, 419-422.
- Lamb, C.J. and Dixon, R.A. 1997. The oxidative burst in plant disease resistance. *Ann Rev Plant Physiol Plant Mol Biol* **48**, 251-275.
- Leontein, K. and Lönnngred, J. 1978. Determination of the absolute configuration of sugars by gas-liquid chromatography of their acetylated 2-octyl glycosides. *J Meth Carbohydr Chem* **62**, 359-362.
- Leone, S., Molinaro, A., Lanzetta, R., Gerber, I.B., Dubery, I.A. and Parilli, M. 2006. The O-chain structure of the LPS of the endophytic bacterium *Burkholderia cepacia* strain ASP B2D. *Carb Res* **341**, 2954-2958.
- Livaja, M., Zeidler, D., Von Rad, U. and Durner, J. 2008. Transcriptional responses of *Arabidopsis thaliana* to the bacteria-derived PAMPs harpin and lipopolysaccharide. *Immunobiology* **213**, 161-171.
- Maldonado, A.M., Doerner, P., Dixon, R., Lamb, C.J. and Cameron, R.K. 2002. A putative lipid transfer protein involved in systemic resistance signalling in *Arabidopsis*. *Nature* **419**, 399-403.
- McDowell, J.M. and Dangl, J.L. 2000. Signal transduction in the plant immune response. *Trends Biochem Sci* **25**, 79-82.

- Meyer, Y., Siala, W., Bashandy, T., Riondet, C., Vignols, F. and Reichheld, J.P. 2008. Glutaredoxins and thioredoxins in plants. *Biochim. Biophys Acta* **15**, 809-834.
- Mishina, T.E. and Zeier, J. 2007. Pathogen-associated molecular pattern recognition rather than development of tissue necrosis contributes to bacterial induction of systemic acquired resistance in *Arabidopsis*. *Plant J* **50**, 500-513.
- Molinaro, A., Newman, M.A., Lanzetta, R. and Parrilli, M. 2009. The structure of lipopolysaccharides from plant associated Gram-negative bacteria. *Eur J Org Chem* **34**, 5887-5896.
- Molinaro, A., Lindner, B., De Castro, C., Nolting, B., Silipo, A., Lanzetta, R., Parrilli, M. and Holst, O. 2003. The structure of the lipid A of the lipopolysaccharide from *Burkholderia caryophylli* possessing a 4-amino-4-deoxy-L-arabinopyranose-1-phosphate residue exclusively in glycosidic linkage. *Chem Eur J* **9**, 1542-1548.
- Munford, R.S. and Varley, A.W. 2006. Shield as signal: lipopolysaccharides and the evolution of immunity to Gram-negative bacteria. *Plos Pathogens* **2**, 467-471.
- Navarro, L., Zipfel, C., Rowland, O., Keller, I., Robatzek, S., Boller, T. and Jones, J.D.G. 2004. The transcriptional innate immune response to flg22: interplay and overlap with Avr gene-dependent defense responses and bacterial pathogenesis. *Plant Physiol* **135**, 113-128.
- Newman, M.A., Dow, M.J., Molinaro, A. and Parrilli, M. 2007. Priming, induction and modulation of plant defence responses by bacterial lipopolysaccharides. *J Endotoxin Res* **13**, 69-84.
- Nicaise, V., Roux, M. and Zipfel, C. 2009. Recent advances in plant-triggered immunity against bacteria: pattern recognition receptors (PRRs) watch over and raise the alarm. *Plant Physiol* **150**, 1638-1647.
- Nuernberger, T. 2006. TAIR accession expression set 100808727.
- Nuernberger, T. and Kemmerling, B. 2006. Receptor protein kinases – pattern recognition receptors in plant immunity. *Trends Plant Sci* **11**, 519-522.
- Ortiz-Masia, D., Perez-Amador, M.A., Carbonell, J. and Marcote, M.J. 2007. Diverse stress signals activate the C1 subgroup MAP kinases of *Arabidopsis*. *FEBS Lett* **581**, 834-1840.
- Piater, L., Nurnberger, T. and Dubery, I.A. 2004. Identification of a lipopolysaccharide responsive erk-like MAP kinase in tobacco leaf tissue. *Mol Plant Pathol* **5**, 331-341.
- Raetz, C.R. and Whitfield, C. 2002. Lipopolysaccharide endotoxins. *Annu Rev Biochem* **71**, 635-700.
- Raetz, C.R., Reynolds, C.M., Trent, M.S. and Bishop, R.E. 2007. Lipid A modification systems in Gram-negative bacteria. *Annu Rev Biochem* **76**, 295-329.
- Raffaale, S., Leger, A. and Roby, D. 2009. Very long chain fatty acid and lipid signaling in the response of plants to pathogens. *Plant Signal Behav* **4**, 94-99.
- Rance, M., Sørensen, O.W., Bodenhausen, G., Wagner, G., Ernst, R.R. and Wüthrich, K. 1983. Improved spectral resolution in COSY ¹H-NMR spectra of proteins via double quantum filtering. *Biochem Biophys Res Commun* **117**, 479-485.
- Rietschel, E.T. 1976. Absolute configuration of 3-hydroxy fatty acids present in lipopolysaccharides from various bacterial groups. *Eur J Biochem* **64**, 423-428.
- Rivas, S., Rougon-Cardoso, A., Smoker, M., Schausser, L., Yoshioka, H. and Jones, J.D.G. 2004. CITRX thioredoxin interacts with the tomato Cf-9 resistance protein and negatively regulates defense. *EMBO J* **23**, 2156-2165.
- Robatzek, S. 2007. Vesicle trafficking in plant immune response. *Cell Microbiol* **9**, 1-8.
- Robatzek, S. and Saijo, Y. 2009. Plant immunity from A to Z. *Genome Biol* **9**, 304-308.
- Sanabria, N.M., Huang, J-C. and Dubery, I.A. 2010. Self/non-self perception in plants in innate immunity and defense. *Self/Non-self Immun Regul* **1**, 1-15.
- Sanabria, N.M. and Dubery, I.A. 2006. Differential display profiling of the *Nicotiana* response to LPS reveals elements of plant basal resistance. *Biochem Biophys Res Comm* **344**, 1001-1007.
- Scheidle, H., Grob, A. and Niehaus, K. 2004. The lipid A substructure of the *Sinorhizobium meliloti* lipopolysaccharides is sufficient to suppress the oxidative burst in host plants. *New Phytol* **165**, 559-566.
- Schromm, A.B.E., Lien, E., Henneke, P., Chow, J.C., Yoshimura, A., Heiner, H., Latz, E., Monks, B.G., Schwartz, D.A., Miyake, L. and Golenbock, D.T. 2000. Molecular genetic analysis of an endotoxin

- non-responder mutant cell line: a point mutation in a conserved region of MD-2 abolishes endotoxin-induced signaling. *J Exp Med* **194**, 79-88.
- Shah, J. 2005. Lipids, lipases and lipid modifying enzymes in plant disease resistance. *Annu Rev Phytopathol* **43**, 229-260.
- Silipo, A., De Castro, C., Lanzetta, R., Parrilli, M. and Molinaro, A. 2010. Lipopolysaccharides. In: *Prokaryotic Cell Wall Compounds - Structure and Biochemistry*. König, H., Claus, H. and Varma, A. editors; Springer, Heidelberg, p. 133-154.
- Silipo, A., Molinaro, A., Sturiale, L., Dow, M.J., Erbs, G., Lanzetta, R. and Newman, M.A. 2005. The elicitation of plant innate immunity by lipooligosaccharide of *Xanthomonas campestris*. *J Biol Chem* **280**, 33660-33668.
- Silipo, A., Erbs, G., Shinya, T., Dow, J.M., Parrilli, M., Lanzetta, R., Shibuya, N., Newman, M-A. and Molinaro, A. 2010 Glyco-conjugates as elicitors or suppressors of plant innate immunity. *Glycobiology* **20**, 406-419.
- Silipo, A., Sturiale, L., Garozzo, D., Erbs, G., Jansen, T.T., Lanzetta, R., Dow, M.J., Parrilli, M., Newman, M.A. and Molinaro, A. 2008. The acylation and phosphorylation patterns of lipid A from *Xanthomonas campestris* strongly influence its ability to trigger the innate immune response in *Arabidopsis*. *ChemBioChem* **9**, 896-904.
- Silipo, A., Molinaro, A., Cescutti, P., Bedini, E., Rizzo, R., Parrilli, M. and Lanzetta, R. 2005. Complete structural characterization of the lipid A fraction of the clinical strain of *Burkholderia cepacia* genomovar I lipopolysaccharide. *Glycobiology* **15**, 561-570.
- Silipo, A., Lanzetta, R., Amoresano, A., Parrilli, M. and Molinaro, A. 2002. Ammonium hydroxide hydrolysis: a valuable support in the MALDI-TOF mass spectrometry analysis of lipid A fatty acid distribution. *J Lipid Res* **43**, 2188-2195.
- States, D.J., Haberkorn, R.A. and Ruben, D.J. 1982. A two-dimensional nuclear overhauser experiment with pure absorption phase in four quadrants. *J Magn Reson* **48**, 286-292.
- Thilmony, R., Underwood, W. and He, S.H. 2006. Genome-wide transcriptional analysis of the *Arabidopsis thaliana* interaction with the plant pathogen *Pseudomonas syringae* pv. *tomato* DC3000 and the human pathogen *Escherichia coli* O157:H7. *Plant J* **46**, 34-53.
- Varnier, A-L., Sanchez, L., Vatsa, P., Boudesocque, L., Garcia-Brugger, A., Rabenoelina, F., Sorokin, A., Renault, J-H., Kauffmann, S., Pugin, A., Clement, C., Baillieul, F. and Dorey, S. 2009. Bacterial rhamnolipids are novel MAMPs conferring resistance to *Botrytis cinerea* in grapevine. *Plant Cell Environ* **32**, 178-193.
- Vandamme, P., Opelt, K., Knöchel, N., Schonmann, S., De Brandt, E., Erberl, L., Falsen, E. and Berg, G. 2007. *Burkholderia bryophila* sp. nov. and *Burkholderia megapolitana* sp. nov., moss-associated species with antifungal and plant-growth-promoting properties. *Int J Syst Evol Micr* **57**, 2228-2235.
- Van Loon, L.C. 1997. Induced resistance in plants and the role of pathogenesis-related proteins. *Eur J Plant Pathol* **103**, 753-765.
- Van Loon, L.C., Rep, M. and Pieterse, C.M.J. 2006. Significance of inducible defense-related proteins in infected plants. *Annu Rev Phytopathol* **44**, 135-162.
- Vierstra, R.D. 2003. The ubiquitin/26S proteasome pathway, the complex last chapter in the life of many plant proteins. *Trends Plant Sci* **8**, 135-142.
- Wagner, U., Edwards, R., Dixon, D.P. and Mauch, F. 2002. Probing the diversity of the Arabidopsis glutathione S-transferase gene family. *Plant Mol Biol* **49**, 515-532.
- Wang, P-Y., Weng, J. and Anderson, R.G.W. 2007. OSBP is a cholesterol-regulated scaffolding protein in control of ERK1/2 activation. *Science* **307**, 1472-1476.
- Zeidler, D., Zahringer, U., Gerber, I.B., Dubery, I.A., Hartung, T., Bors, W., Hutzler, P. and Durner, J. 2004. Innate immunity in *Arabidopsis thaliana*: Lipopolysaccharides activate nitric oxide synthase (NOS) and induce defense genes. *Proc Natl Acad Sci U.S.A* **101**, 15611-15816.
- Zhang, B., Ramonell, K., Somerville, S. and Stacey, G. 2002. Characterization of early, chitin-induced gene expression in *Arabidopsis*. *Mol Plant-Microbe Interact* **15**, 963-970.
- Zipfel, C. 2008. Pattern recognition receptors in plant innate immunity. *Curr Opin Immunol* **20**, 10-16.

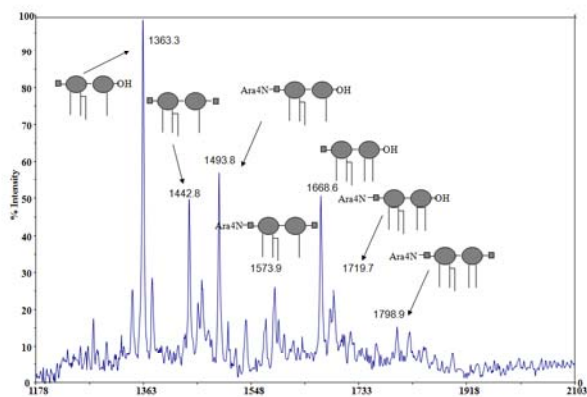
Zipfel, C., Robatzek, S., Navarro, L., Oakeley, E.J., Jones, J.D.G., Felix, G., and Boller, T. 2004. Bacterial disease resistance in *Arabidopsis* through flagellin perception. *Nature* **428**, 764-767.

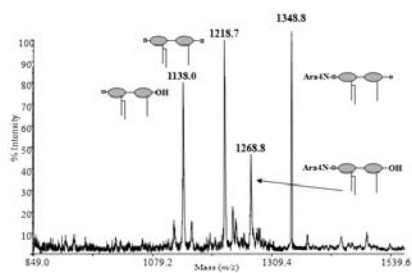
FIGURE LEGENDS

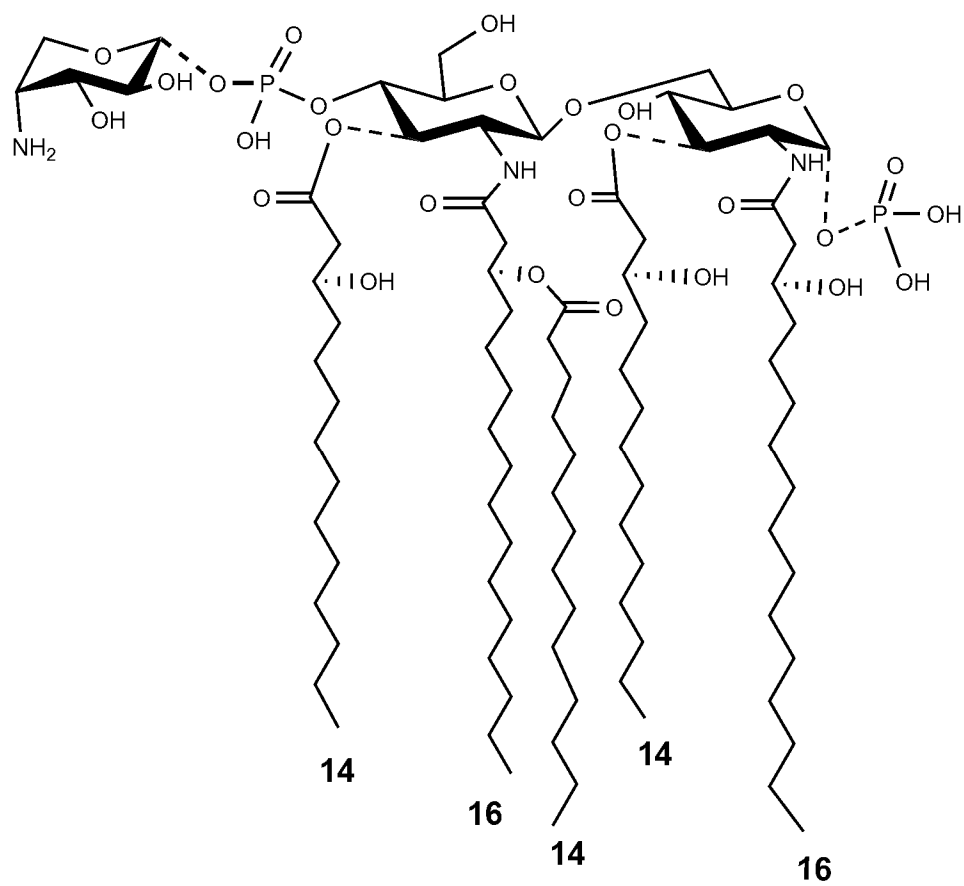
Figure 1. Negative ion MALDI mass spectrum of the lipid A fraction of LPS from *B. cepacia* ASP 2D. The relevant ion peaks are described in the text and in Table I. The non-specified ion peaks in the spectrum are sodium adducts of the main species ($\Delta m/z$ 22).

Figure 2. Negative ion MALDI mass spectrum of NH_4OH treated lipid A fraction of *B. cepacia* ASP 2D. The relevant ion peaks are described in the text.

Figure 3. The structure of the molecules present in the lipid A blend from the LPS of *B. cepacia* ASP B 2D sketched in a single formula. Dotted lines indicate non-stoichiometric bonds.







List of Tables

Table I. Main MALDI-MS negative ion peaks of Fig. 1 and proposed interpretation of the acyl, phosphate and carbohydrate substituents on the lipid A backbone of the LPS from *B. cepacia* ASP B 2D. Some high mass errors are due to the low abundance of the ion peaks in the spectrum.

Observed ion (<i>m/z</i>)	Predicted mass (<i>m/z</i>)	Species	Acyl substitution	Proposed fatty acid, phosphate and carbohydrate composition
1363.3	1363.95	1	Tetra-acyl	2 x 16:0(3-OH), 1 x 14:0(3-OH), 1 x 14:0, 1P
1442.8	1440.89	2	Tetra-acyl	2 x 16:0(3-OH), 1 x 14:0(3-OH), 1 x 14:0, 2P
1493.8	1495.01	3	Tetra-acyl	2 x 16:0(3-OH), 1 x 14:0(3-OH), 1 x 14:0, 1 x Ara4N, 1P
1573.9	1572.96	4	Tetra-acyl	2 x 16:0(3-OH), 1 x 14:0(3-OH), 1 x 14:0, 1 x Ara4N, 2P
1668.6	1667.09	5	Penta-acyl	2 x 16:0(3-OH), 2 x 14:0(3-OH), 1 x 14:0, 2P
1719.7	1721.2	6	Penta-acyl	2 x 16:0(3-OH), 2 x 14:0(3-OH), 1 x 14:0, 1 x Ara4N, 1P
1798.9	1799.15	7	Penta-acyl	2 x 16:0(3-OH), 2 x 14:0(3-OH), 1 x 14:0, 1 x Ara4N, 2P

Table II. Genes up-regulated in *A. thaliana* seedlings following an 8 h treatment with lipid A purified from LPS of *B. cepacia* cell walls.

Functional category	Gene number	Gene description
DNA binding proteins, transcription factors and transcriptional regulation.	At1g20340	DNA damage repair/toleration protein 112
	At1g21570	Zinc (CCH-type) family protein
	At1g24300	GYF domain-containing protein
	At1g80070	Abnormal suspensor 2
	At2g19430	Transducin family protein/WD-40 repeat family protein
	At2g32070	CCR4-NOT transcription complex protein
RNA binding proteins.	At1g18630	Glycine-rich RNA-binding protein 6
	At4g17390	60S ribosomal protein L15
	At4g27000	RNA binding
Signal transduction, protein kinases and - phosphatases.	At1g10210	Mitogen activated protein kinase 1
	At1g09870	Histidine acid phosphatase family protein
	At3g46280	Protein kinase-related protein
	At4g03460	Ankyrin repeat family protein
	At4g08180	Oxysterol-binding family protein
	At4g24740	FUS3-compl gene 1 (CLK/STY lammer-type protein kinase)
	At4g27280 #	Calcium binding EF hand family protein
	At5g58150	LRR transmembrane RLK
At5g60548	Geminivirus REP interacting kinase 2	
Stress-responsive and defense proteins.	At1g02920	Glutathione S-transferase
	At1g20440	Cold regulated 47
	At1g72610	Germin-like protein
	At2g05790	Glycosyl hydrolase family 17 protein, beta glucanase
	At2g32150 *	Haloacid dehalogenase-like hydrolase protein
	At2g44060	Late embryogenesis abundant family protein
	At3g49120	Peroxidase 34
	At3g53280	Cytochrome P450 71B5 monooxygenase
	At4g34180	Cyclase family protein
	At4g37930	Serine hydroxymethyltransferase 1
	At4g02380 #	Senescence-associated responsive protein 21
	At4g12470	Lipid transfer protein
	At4g21960 #	Peroxidase 42
	At5g64120	Peroxidase
Molecular chaperones.	At1g08570	Thioredoxin family protein (disulfide reductase)
	At1g13690	ATPase E1 / peptidyl-prolyl cis-trans isomerase
	At4g22670	Hsp 70 interacting protein
Cell transporters and ion homeostasis.	At1g11260 #	Sugar transporter 1
	At2g26900	Bile acid: sodium symporter family protein
	At2g34250	Protein transport protein Sec 61, putative protein
	At5g25050	Integral membrane transporter family protein

Protein degradation, ubiquitin and proteasome function.	At1g21780	BTB/POZ domain-containing protein
	At1g75990	26S proteasome regulatory subunit S3
	At3g12700	Aspartyl protease family protein
	At3g19390	Cysteine proteinase
	At3g59940	Kelch repeat-containing F-box family protein
	At5g48430	Aspartic-type endopeptidase/ pepsinA
Cytoskeletal re-arrangement and vesicle trafficking.	At1g64720 *	Membrane related protein, CP5
	At3g18780	Actin 2
	At5g53400	Nuclear movement family protein
Cuticle and cell wall-related.	At1g68530	Cuticular 1 acyltransferase
	At2g45220 *	Pectinesterase
	At3g16520 *	UDP-glycosyl transferase family protein
	At3g22120	Cell wall-plasma membrane linker protein
Hormone-related.	At1g67080 *	Abscisic acid deficient 4
	At2g21210 *	Auxin-responsive protein
	At2g36270	Abscisic insensitive 5
	At5g14920	Gibberelin-regulated family protein
Metabolism and energy.	At1g03090	3-Methylcrotonyl-CoA carboxylase 1
	At1g04420	Aldo/keto reductase family protein
	At1g13245	Rotundifolia like 15
	At1g68010	Hydroxypyruvate reductase
	At2g20830	Folic acid-binding/transferase
	At2g26560	Phospholipase A 2A
	At2g41530	S-Formylglutathione hydrolase
	At3g03070	NADH-ubiquinone oxidoreductase-related
	At3g04120	Glyceraldehyde-3-phosphate dehydrogenase C subunit
	At3g05020	Acyl carrier protein
	At3g06850	Dihydrolipoamide branched chain transferase
	At3g06850	Dark inducible 3
	At3g14100	Oligouridylate-binding protein
	At3g17810	Dihydroorotate dehydrogenase family protein
	At3g51620	Hypothetical protein (nucleotidyltransferase)
	At3g55970	Oxidoreductase, 20G-Fe (II) oxygenase family protein
At5g58560	Phosphatidate cytidyltransferase family protein	
Unknown	At1g19380 #	Hypothetical protein

Genes also identified in a microarray study of LPS-induced responses are indicated as * (Nuernberger, 2006) and # (Zeidler et al. 2004; Livaja et al. 2008). These conditions of elicitation differ significantly with regard to timepoints, tissue and concentrations, and are not readily comparable.